To be returned to the
ACADEMIC REGISTRAR,
UNIVERSITY OF LONDON,
SENATE HOUSE, W.C.1.
with the Examiners Report

ELECTRONIC IMPURITY STATES

AND

SCREENING IN METALS AND SEMICONDUCTORS

by

John Bethell

Thesis submitted for the Degree of Doctor of Philosophy of the University of London.

Department of Physics
Imperial College
London SW7

December, 1974

ABSTRACT

Problems concerned with the inter-relationship of electronic screening and the formation of localized electronic states associated with impurities are discussed in two types of physical system. The mathematical technique employed in each type of system involves the use of a separable potential.

For free-electron-like metals, a self-consistent non-linear scheme is presented for the calculation of screening charge densities associated with impurities. The scheme takes explicit account of bound state formation. The impurity potential is split into two parts: the separable form of the first part permits the summation of an important part of the perturbation series for the screening charge density, whilst the second part is weak and is treated in linear screening theory. Numerical calculations are carried out using model impurity potentials of the Heine-Abarenkov form and by employing a result of Singwi et al. to describe exchange and correlation within the electron gas. Corrections to the corresponding linear theory are appreciable in both the screening charge density and the screened potential. Compared with linear theory, an accumulation of charge of a realistic magnitude is found within the impurity core, whilst the total screening charge within the impurity cell is decreased from its value in linear theory.

Symmetry-induced gapless semiconductors are considered, and numerical computations of the temperature-dependent static interband dielectric function of such systems are presented.

A separable model of a screened impurity potential is introduced, and it is used to calculate a density of states associated with an impurity, and hence to discuss the possible formation of resonant donor and acceptor states. No well-defined donor states exist for any realisable set of physical parameters, whilst acceptor binding energies and resonant widths are strongly dependent on the details of the band structure and the screening process and also on the temperature.

ACKNOWLEDGEMENTS

I acknowledge with thanks the receipt of a Science Research Council Studentship during the course of the work described in this thesis. Special thanks are due to Dr. Roy Jacobs and Dr. David Sherrington who shared the supervision of my work and who respectively suggested the investigations into metals and semiconductors. I should also like to express my gratitude to the whole of the Solid State Theory Group of the Physics Department, Imperial College, who have contributed much good advice and moral support.

--- oOo ---

Se non è vero, è molto ben trovato.

CONTENTS

	Page No.
ABSTRACT	ii
ACKNOWLEDGEMENTS	iv
INTRODUCTION - Screened Potentials and Impurity States	1
CHAPTER 1 SCREENING THEORY: AN INTRODUCTION	2
1.1 Linear Screening Theory	4
(a) Perturbative Methods	5
(b) Self-Consistent Field Methods	7
1.2 Non-Linear Screening	9
(a) Perturbative Methods	9
(b) Non-perturbative Methods	11
1.3 Theories Non-Linear in the External Potential	14
CHAPTER 2 IMPURITY SCREENING IN SIMPLE METALS	20
2.1 The Non-Linear Problem	20
2.2 The Separable Potential	21
2.3 Construction of Charge Densities	26
2.4 Discussion of Charge Densities	34
2.5 A Self-Consistent Scheme	42
CHAPTER 3 COMPUTATIONS	44
3.1 The Model System	44
3.2 The Numerical Scheme	48
3.3 Numerical Behaviour	55

Page No.

CHAPTER 4 RESULTS AND FURTHER DEVELOPMENTS 61

4.1 Screening Charge 61

4.2 Charge Transfer 67

4.3 Screened Potentials and Bound States 68

4.4 Diagrammatic Arguments 76

4.5 Other Potentials 80

4.6 Summary 83

CHAPTER 5 ZERO-GAP SEMICONDUCTORS 84

5.1 Introduction 84

5.2 The Band Structure 86

5.3 Dielectric Behaviour 91

CHAPTER 6 IMPURITY STATES IN ZERO-GAP SEMICONDUCTORS 100

6.1 Introduction 100

6.2 The Model Potential 103

6.3 The Density of States 105

6.4 Impurity Levels: Activation Energies and Widths 112

6.4.1 Coulomb Potential 112

6.4.2 Zero-Gap Screening 115

6.4.3 Metallic Screening 118

6.5 Conclusions 124

APPENDIX 126

REFERENCES 127

INTRODUCTION

SCREENED POTENTIALS AND IMPURITY STATES

The problem of a potential perturbing a gas of interacting electrons has been a central one in the development of many-body theory. An important concept to emerge from the problem is that of a screened potential, arising from the many-body renormalization of the bare perturbing potential. The general problem has been subject to intense investigation and has a huge literature[1]. In this thesis, a few specialised instances of the problem will be discussed, and the results of sophisticated general calculations performed by others will be used whenever possible.

One situation where the details of the screening of a potential are particularly important is where an impurity is introduced substitutionally into a pure crystal, and the impurity and host differ in valence. The screened potential associated with the impurity may be strong enough to bind valence electrons or holes into localized states. In a typical semiconductor, such as Ge or Si, screening is rather ineffective and the binding energies of the donor and acceptor states are well-understood[2]. Furthermore, these states are close to the Fermi energy and exert an appreciable influence on the transport and optical properties of the semiconductor.

In a metal, on the other hand, the screening process is more difficult to understand, because of the much higher density of screening electrons. No general reliable scheme

exists for calculating the binding energies of localized states, or indeed for determining the existence of such states. This difficulty is compounded by the experimental inaccessibility of these states, as they may be far removed from the Fermi level. Nevertheless, this single-impurity problem has far-reaching consequences in its extension to the electronic structure of concentrated metallic alloys where localization of charge and charge transfer are controversial topics[3]. The first four chapters of this thesis are therefore devoted to a better understanding of the screening of a strong attractive impurity potential in a metal: particular attention is focussed on possible formation of localized electronic states.

In chapters 5 and 6, semiconductors are considered, but the discussion centres on the special case of zero-gap semiconductors[4]. In these systems, the formation of donor and acceptor states depends critically on the band structure and on the distinctive screening behaviour, and the states are only quasi-localized.

Thus, the inter-relationship of bound states and screening is a recurrent theme in this thesis. Bound states are treated throughout via singular t-matrices and separable potentials are used to evaluate these t-matrices.

CHAPTER 1

SCREENING THEORY: An Introduction

Since this thesis makes wide use of results from screening theory, it is useful to begin by outlining some of the techniques in screening theory which will be referred to.

It has already been noted that this thesis is concerned with the many-body problem of a potential perturbing a gas of N interacting electrons, that is the problem of a system described by the Hamiltonian

$$H = \sum_{i=1}^{N} [T_i + V_i] + \sum_{\substack{i<j \\ j}}^{N} v_{ij} \qquad (1.1)$$

where T_i is the kinetic energy of the ith electron, V_i is the perturbing potential experienced by that electron, and v_{ij} is the potential of interaction between the ith and jth electrons. (The units employed are described in the Appendix.) The classical approach to this problem is to transform the Hamiltonian into the form

$$H = \sum_{i}^{N^{(1)}} H_i^{(1)} + \sum_{i}^{N^{(2)}} H_i^{(2)} + \cdots \qquad (1.2)$$

Where $\{H_i^{(n)};\ i=1, \ldots N^{(n)}\}$ is a set of one-particle Hamiltonians describing non-interacting quasi-particles (quasi-electrons, plasmons etc.)[5]. For many purposes, however, the behaviour of collective excitations such as plasmons is

not required, the effects of these modes being present in the quasi-electron part of H. The simplified Hamiltonian

$$H = \sum_{i=1}^{N} \left[T_i + V_i^s \right] \qquad (1.3)$$

may then be used. That is, the electrons respond to a simple one-body potential, the screened potential V^s.

In practice the canonical transformation to (1.2) is not particularly useful and two other techniques have been widely used to obtain V^s: perturbation theory and self-consistent field methods. Ingredients from both techniques are used in this thesis, and both techniques are outlined in this chapter.

§1.1 Linear Screening Theory

The calculation of V^s is most simple when the applied potential $V(\underline{r},t)$ is weak and V^s is a simple linear response to it. V^s can then be described completely in terms of a single response function, the dynamic dielectric function $\varepsilon(\underline{k},\omega)$:

$$V^s(\underline{k},\omega) = V(\underline{k},\omega)\,\varepsilon^{-1}(\underline{k},\omega) \qquad (1.4)$$

where

$$V(\underline{k},\omega) = \int d^3r \int dt\, e^{i(\underline{k}\cdot\underline{r}+\omega t)} V(\underline{r},t).$$

The greater part of this thesis concerns situations where $V(\underline{r},t)$ is strong and (1.4) does not apply, but it is a useful point of departure.

(a) Perturbative Methods

Perturbative methods of describing screening rely on extensive use of Feynman diagrams[6]. The Hamiltonian (1.1) is written in second-quantized notation and causal Green's functions G and G_o set up for both this Hamiltonian and the unperturbed Hamiltonian

$$H_o = \sum_i T_i \qquad (1.5)$$

The diagrammatic perturbation series for G is written out and from it is extracted those diagrams corresponding to V^s (see Fig. 1.1): that is those diagrams containing at least one V, no external G_o, and which cannot be split by cutting a single G_o line.

Now in order for V^s to take the form (1.4), it is necessary for all diagrams in which V appears more than once to be negligible. (It is these diagrams which will interest us in later chapters.) The remaining diagrams have a divergent $\underline{k} = 0$ Fourier component. The procedure adopted is to now retain only the most divergent terms in each order of perturbation theory. This approximation is equivalent to the Random Phase Approximation (RPA) of Bohm and Pines[7]. The remaining terms, illustrated in Fig. 1.2, constitute an infinite series whose exact sum may be evaluated, and which is not divergent. Thus, the RPA dielectric function $\varepsilon_{RPA}(k,\omega)$ is obtained. At finite temperatures T, this takes the form

Figure 1.1 Some terms in the perturbation series for the screened potential.

The diagrammatic representation

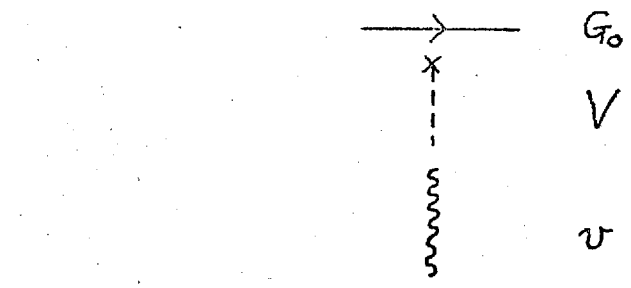

is used.

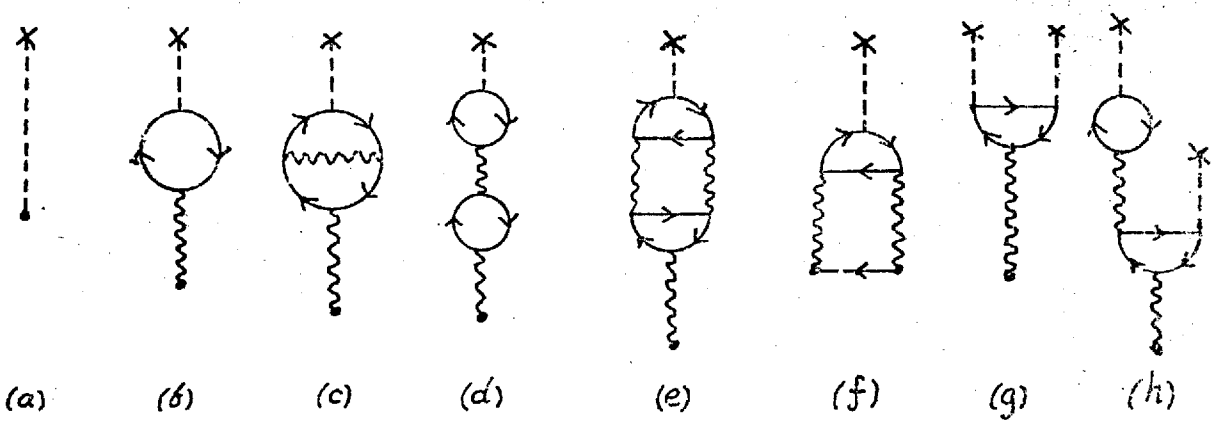

Figure 1.2 The RPA series for the screened potential.

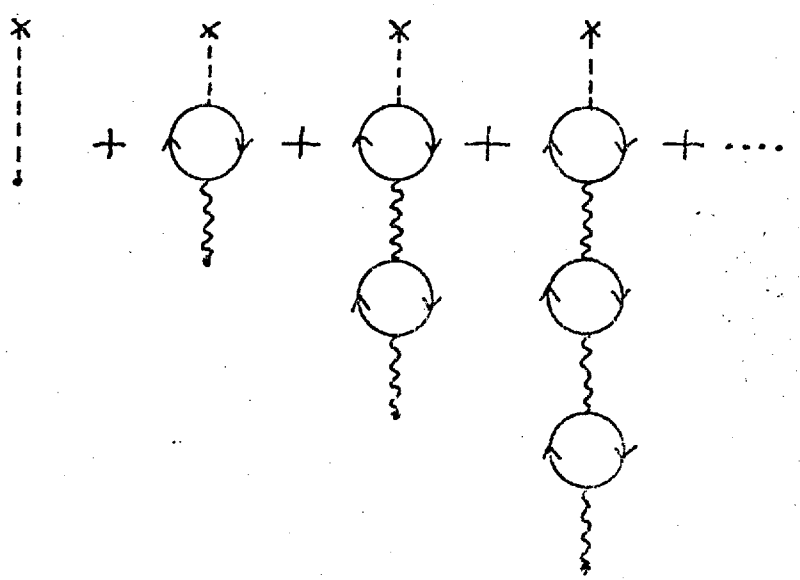

$$\varepsilon_{RPA}(\underline{k},\omega) = 1 - \lim_{\alpha \to 0+} \frac{8\pi}{\Omega k^2} \sum_{\underline{q}} \frac{f(\varepsilon_{\underline{k}+\underline{q}}) - f(\varepsilon_{\underline{k}})}{\varepsilon_{\underline{k}+\underline{q}} - \varepsilon_{\underline{k}} - \omega - i\alpha}$$

$$= 1 - v(k)\chi_0(\underline{k},\omega). \qquad (1.6)$$

Here Ω is the volume of the system, $\varepsilon_{\underline{k}}$ is the energy of an electron of momentum $\underline{k}$, f(E) is the Fermi function

$$f(E) = \left[1 + \exp\left(\frac{E - E_F}{k_B T}\right)\right]^{-1} \qquad (1.7)$$

and k_B is Boltzmann's constant. χ_0 is the free-electron susceptibility which Lindhard[8] has computed.

The screened potential calculated in this approximation is only partially successful; although the problem of divergent terms in perturbation theory has been circumvented, the pair correlation function of the electrons can take negative values. This is unphysical. The methods of overcoming this difficulty will be described in §1.2, but first the other approach to calculating the dielectric function will be described for comparison.

(b) Self-Consistent Field Methods

Under this heading, we collect all theories of screening which do not involve summing a perturbation series. They inevitably involve the decoupling of equations of motion and, although any given decoupling is in principle equivalent to a particular partial sum of a perturbation series[9], this is not always easy to do. The original Self-Consistent Field method[10], however, which is in all respects a linear theory,

is exactly equivalent to the RPA.

The Self-Consistent Field (SCF) method begins with the one-electron screened potential $V^s(\underline{r},t)$ and the one-electron Hamiltonian

$$H = H_o + V^s(\underline{r},t) . \tag{1.8}$$

The equation of motion for the operator ρ of the one-electron density matrix is then set up:

$$i \frac{\partial}{\partial t} \rho = [H, \rho] . \tag{1.9}$$

A plane-wave representation using the states $|\underline{k}\rangle$ is used and the density matrix written

$$\langle \underline{k}|\rho|\underline{k}+\underline{q}\rangle = \langle \underline{k}|\rho^{(0)}|\underline{k}+\underline{q}\rangle + \langle \underline{k}|\rho^{(1)}|\underline{k}+\underline{q}\rangle + \cdots \tag{1.10}$$

Here $\langle \underline{k}|\rho^{(0)}|\underline{k}+\underline{q}\rangle$ is the density matrix of the unperturbed electron gas and $\langle \underline{k}|\rho^{(1)}|\underline{k}+\underline{q}\rangle$ is the linear response of the density matrix to the potential $\langle k|V^s|\underline{k}+\underline{q}\rangle$. The equation of motion is now linearized retaining only these two terms. The solution is now made self-consistent by calculating V^s from $\rho^{(1)}$ using Poisson's equation:

$$\nabla^2 (V^s - V) = -8\pi n \tag{1.11}$$

where V is the applied potential and n the charge density due to $\rho^{(1)}$. This step constitutes a second linearization of the problem: in practice V^s will have an exchange contribution

which is non-linear in n. The SCF method is thus a linearized Hartree theory. The SCF dielectric function is readily deduced and is the same as the dielectric function of the RPA.

§1.2 Non-Linear Screening

It is clear from the previous section that two types of restriction apply to the simplest quantum mechanical screening theories. First, these theories refer to weak applied potentials V, which may be treated in linear-response theory. Second, they neglect exchange and correlation effects within the electron gas. Whilst the first restriction is not severe, since a weak V may often be chosen, the second restriction is not satisfactory at metallic densities of the electron gas. Considerable effort has been expended in correcting this shortcoming via both perturbative and non-perturbative methods.

(a) Perturbative Methods

One of the most notable sophistications of linear screening theory was due to Hubbard[11]. He noted that a certain class of diagram excluded from the RPA series was simply related to the diagrams of the RPA series. He termed pairs of diagrams related in this way "exchange conjugate" diagrams because they represent direct and exchange components of the electron-electron interaction: such diagrams are generated from each other by crossing pairs of G_o lines. Thus, in Fig. 1.1, (c) and (d) are exchange conjugate diagrams.

Hubbard was able to make an approximate sum of these diagrams and the effect on RPA was to replace χ_o as follows:

$$\chi_o(\underline{k},\omega) \longrightarrow \frac{\chi_o(\underline{k},\omega)}{1+v(k)\chi_o(\underline{k},\omega)f(k)} \qquad (1.12)$$

where

$$f(k) = \frac{1}{2}\,\frac{k^2}{k^2+k_F^2}$$

and k_F is the Fermi momentum. It should be noted, however, that diagram (f) of Fig. 1.1 is still excluded.

Although this calculation may be improved, non-perturbative treatments of the electron gas have been more successful. Recently, however, Fishlock and Pendry[12] have shown that the results of non-perturbative calculations can also be obtained perturbatively, if at a greater expense of effort. In their comparison with non-perturbative calculations of g(r), the electron pair distribution function, they have only been able to compute g(o). Nevertheless, this calculation indicates a future for perturbative methods of treating the electron gas, and indeed a similar technique to theirs is employed in Chapter 2. The essence of the technique is to split the short range part of the electron-electron interaction into two parts,

$$v = v_1 + v_2 \qquad (1.13)$$

such that v_2 is weak and v_1 is a separable, non-local

potential. In their computations they have used, for example,

$$V_1(\underline{r},\underline{r}') = \frac{V(\underline{r})\,V(\underline{r}')}{\int d^3r''\,V(\underline{r}'')} \qquad (1.14)$$

Since V_2 is weak, V_1 is chiefly responsible for the exchange and correlation effects which RPA neglects; the separable form of (1.14) makes calculations of these effects possible. In terms of diagrams, Fishlock and Pendry include, in addition to the exchange terms of Hubbard, terms like (e) of Fig. 1.1.

(b) Non-Perturbative Methods

Non-perturbative methods of treating the non-linearities in the screening of a weak potential in an electron gas here received extensive study, notably by Singwi and others[13]. The basic ideas of such methods will now be described.

As in the SCF method, we begin with the equation of motion of the density matrix (1.9). Now, however, we use the components

$$\rho_{\underline{k}} = \sum_i e^{i\underline{k}\cdot\underline{r}_i} \qquad (1.15)$$

of the density matrix, $\{\underline{r}_i\}$ being the positions of the electrons, and employ the full, many-body Hamiltonian (1.1). Furthermore, no linearisation is carried out: instead, the case where the external potential V vanishes is considered. Then,

$$\frac{\partial^2}{\partial t^2}\rho_{\underline{k}} = -\sum_i (2\underline{k}\cdot\underline{p}_i + k^2)\, e^{-i\underline{k}\cdot\underline{x}_i} - \sum_{\underline{q}}{}' v(q)\, 2\underline{k}\cdot\underline{q}\, \rho_{\underline{k}-\underline{q}}\, \rho_{\underline{q}} \qquad (1.16)$$

where $\underline{p}_i$ is the momentum operator for the ith electron. In the final summation of (1.16), the $\underline{k} = \underline{q}$ term is treated separately. If the $\underline{k} \neq \underline{q}$ terms are omitted, the RPA or SCF result will ultimately be recovered: these terms are now included by making a static approximation. They are re-written as

$$2\sum_{\underline{q}\neq\underline{k}} \underline{k}\cdot\underline{q}\, v(q) \sum_i e^{i\underline{k}\cdot\underline{x}_i} \sum_j e^{i(\underline{q}-\underline{k})\cdot(\underline{x}_i - \underline{x}_j)} \qquad (1.17)$$

and the sum over j is replaced by its ensemble average, a static quantity

$$\left\langle \sum_j e^{i(\underline{q}-\underline{k})\cdot(\underline{x}_i - \underline{x}_j)} \right\rangle . \qquad (1.18)$$

(1.18) is just the well known static structure factor $S(\underline{q}-\underline{k})$ of the electron gas[1] which is related to the dielectric function by

$$\mathrm{Im}\, \varepsilon(\underline{k},\omega)^{-1} = v(k)\left[S(\underline{k},-\omega) - S(\underline{k},\omega)\right] . \qquad (1.19)$$

Consequently, the equation of motion (1.16) becomes identical with the SCF equation of motion, with the replacement

$$v(k) \longrightarrow v(k)[1 - G(k)], \tag{1.20}$$

where

$$G(k) = \frac{-\rho_0^{-1}}{(2\pi)^3} \int d^3q \, \frac{\underline{k}\cdot\underline{q}}{q^2} \left[S(\underline{k}-\underline{q}) - 1 \right]. \tag{1.21}$$

The dielectric function becomes

$$\varepsilon(k,\omega) = 1 - \frac{v(k)\,\chi_0(k,\omega)}{1 + v(k)\chi_0(k,\omega)G(k)}, \tag{1.22}$$

and (1.19), (1.21) and (1.22) can be solved self-consistently to obtain G(k) or $\varepsilon(\underline{k},\omega)$. Although this scheme gives good results for large k, some modification is necessary for small k. Fortunately, the G(k) obtained in the two regimes of k may be fitted most satisfactorily to the function

$$G(k) = A\left[1 - \exp\left\{-B(k/k_F)^2\right\}\right], \tag{1.23}$$

where the parameters A and B depend on the density of the electron gas. This simple parameterization of electron correlations will be employed in Chapter 3.

The self-consistent scheme which has just been described has been extended by Sjölander and Stott[14] to take

account of mixed systems, such as positrons, protons and impurities interacting with the electron gas. They accomplish this by the introduction of partial static structure factors. Their approach is particularly successful for describing positron annihilation rates in solids and yet predicts unphysical electron densities around positively charged impurities. They attribute this failure to the formation of bound states.

We remark that the static approximation (1.18) is equivalent to neglecting the variation with electron energy of electron-electron correlations. For the repulsive electron-electron interaction this is a satisfactory procedure. However, when we introduce the attractive potential due to an impurity, we shall see that the energy dependence of electron-impurity correlations is vital: indeed, the t-matrix for electron-impurity scattering is singular as a function of energy if the impurity potential is strong enough for a bound state to be formed. It is for this reason that in Chapter 2 we incorporate into our self-consistent scheme a perturbative, energy-dependent treatment of electron-impurity scattering: in this way we hope to avoid the unphysical results of Sjölander and Stott.

§1.3 Theories Non-Linear in the External Potential

When a strong potential, for example an impurity potential, is screened by an electron gas, we have seen that a theory which treats the potential in non-linear way is required.

However, before describing such theories, it is instructive to see how such treatments may be avoided in many circumstances.

When a crystalline array of ions is embedded in an electron gas it is well known that the effective ionic potentials are weak and can be treated successfully by linear screening theory. This phenomenon may be explained by the introduction of a pseudopotential[15] to replace the complicated ionic potential. The pseudopotential is constructed so as to represent the repulsive effect of the core electrons of the ions in a simple way, which will describe the behaviour of states outside the core, whilst giving no information about the potential experienced by the core states themselves.

The most fundamental method of constructing such a pseudopotential is to project the nuclear potential on to a set of states which are orthogonal to the states of the ionic core. For many purposes, though, it is algebraically simpler and more physically appealing to use to model potential of Heine and Abarenkov[16]. In its simplest form it is

$$V_L^{HA}(r,E) = \begin{cases} A_L(E) & r \leq R_M \\ -\frac{2Z}{r} & r > R_M \end{cases} \qquad (1.24)$$

Here $A_L(E)$ is a constant depending on the energy E and on the orbital quantum numbers $L \equiv \{\ell,m\}$ of the electronic state on which it operates, Z is the total charge on the ion and R_M is the model core radius. The constants $A_L(E)$ are deter-

mined by fitting to spectroscopic data the asymptotic form as $r \to \infty$ of the wavefunctions $\psi_L(\underline{r},E)$ which are solutions, finite at the origin, of

$$\left[H_0 + V_L^{HA}(\underline{r},E)\right]\psi_L(\underline{r},E) = E\,\psi_L(\underline{r},E) \tag{1.25}$$

where H_0 is the kinetic energy operator of an electron.

In many situations, the repulsion represented by $A_L(E)$ is appreciable and the pseudopotential is weak. In pure free-electron-like metals, alkali metals for example, the ionic pseudopotentials have little effect on the valence electrons. In Chapter 3, the impurity system which we introduce has a free-electron-like metal as a host, and we ignore scattering from the host ions in that situation. If a substitutional impurity is introduced into the crystal, the pseudopotential on the impurity site is changed and the valence electrons scatter from this change in potential. Now, if the host and impurity ions are of similar size and have the same valence, this scattering will be weak and linear screening theory may be adequate.

However, if the impurity ion has a higher valence than the host, it is conceivable that the change in potential will be sufficiently strong for a bound state to be formed, even if the potential is screened linearly. Linear screening theory would then be most inappropriate. Such a potential can nevertheless be treated by what is essentially an extension of the pseudopotential method: the auxiliary neutral atom

model. In this method, which follows a suggestion by Ziman[17], and which has been exploited by Dagens[18], the scattering centre is made electrically neutral by the introduction of an arbitrary distribution of electronic charge. The resulting weak potential is treated in a linear, self-consistent way, thus avoiding the problem of screening a strong attractive potential. Unfortunately, this scheme takes no account of the nature of the states in the screening cloud, in particular whether they are localized states or not. To gain a proper understanding of the screening process, the full non-linear problem must be tackled directly and not avoided.

To clarify the ways in which a strong external potential affects screening theory, we write down a schematic self-consistent procedure by which a screened potential V^s and a screening charge density ρ^s determine each other.

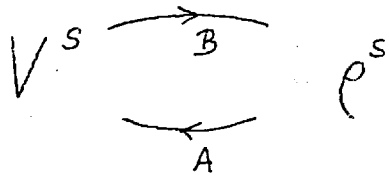

(1.26)

Calculation A has received most attention: the only non-linearities associated with it arise from the electron-electron interaction. The exchange and correlation effects which these non-linearities represent are handled in a similar way to the corresponding non-linearities in the presence of only a weak perturbing potential.

Calculation B, on the other hand, is one which has

almost invariably been linearized. This linear response theory is clearly inadequate when V^s become strong enough for a bound state to be formed: in such circumstances ρ^s will vary discontinuously as V is varied. Such discontinuous behaviour cannot arise merely from treating calculation A in a non-linear way.

The non-linear calculations of type A have been described by Dagens[18] and by other workers[19]. Typically, they involve including in V^s terms of the form

$$\mu_{XC}[\rho_0 + n'] - \mu_{XC}[\rho_0], \qquad (1.27)$$

where ρ_0 is the unperturbed charge density and n' the induced change in ρ_0. Various schemes[20] exist for choosing an appropriate functional μ_{XC} probably the simplest being due to Kohn and Sham[21]

$$\mu_{KS}[\rho] = -\frac{2}{\pi}[3\pi^2 n(\underline{r})]^{1/3}. \qquad (1.28)$$

The non-linearities of calculation B have received some treatment by March and Murray[22]. They have provided explicit expressions to the Hartree screening charge produced by a potential V to all finite orders in V.

$$\rho_0 = \frac{k_F^3}{3\pi^2} \qquad (1.29)$$

$$\rho_1(\underline{r}) = \frac{k_F^2}{2\pi^3} \int d^3s \, V(s) \frac{j_1(2k_F|\underline{r}-\underline{s}|)}{|\underline{r}-\underline{s}|^2}$$

$$\rho_2(\underline{r}) = \text{etc.}$$

The explicit expressions (1.29) have recently been used by Alfred[23] to obtain corrections to linear-response theory. However, such a procedure can only go a little way beyond linear-response theory and can never include bound states unless terms to all orders in V are included.

Finally, it must be mentioned that within the Fermi-Thomas approximation an exact numerical solution to the full non-linear impurity screening problem has been given by Murray and March[24]. Their approach involves solving the differential equation

$$-\nabla^2 V^s = \text{const} \times \left[(E_F - V^s)^{3/2} - E_F^{3/2} \right] \tag{1.30}$$

for the screened potential V^s. This method of approaching the problem is of a different character to the others which have been described, and it is difficult to relate the results of the method to those of other methods because of the imperspicuity of the Fermi-Thomas approximation.

CHAPTER 2

IMPURITY SCREENING IN SIMPLE METALS

§2.1 The Non-Linear Problem

In this and the next two chapters, we shall be concerned with the problem of a single substitutional impurity in a free-electron-like metal. We have seen in Chapter 1 that this situation is well represented by a potential embedded in an electron gas, and that linear screening theory is inadequate when this impurity potential is strong and attractive, because of possible bound state formation. We therefore set up a self-consistent scheme of the form (1.26). The calculation A is treated in a formal way for the present, but calculation B is studied in detail using a non-linear procedure based on perturbation theory. Certain approximations are needed to make this perturbative calculation, but all orders of perturbation theory are included so as to incorporate the possibility of bound states. To achieve this, the impurity potential is split into two parts. The first part has a separable form which permits the t-matrix of this part to be evaluated easily. The remaining part is weak, and linear screening theory (1st order perturbation theory) is employed to treat it. In this way a charge density is calculated, ignoring, for the moment, the electron-electron interaction. This charge density contains a term representing two electrons in a bound state, a term represent-

ing the charge density in linear screening theory and other terms which are expressed as integrals over momenta. These final terms are examined in detail and put into a form suitable for numerical evaluation. The scheme is finally made self-consistent and the electron-electron interaction is re-introduced by inclusion of calculation A.

We begin by introducing the separable potential which is to be used.

§2.2 The Separable Potential

We shall need to discuss two types of potential in what follows: the bare impurity potential and the impurity potential screened in a self-consistent way. The bare potential U takes the form

$$U(r) = -\frac{2Z^{excess}}{r} \qquad (2.1)$$

as $r \to \infty$ where Z^{excess} is the excess charge on the impurity ion. Charge neutrality implies that, when U is self-consistently screened to give V^s, then, for sufficiently large r, V^s is essentially zero. Now, it is quite possible that if U is strong enough, both U and V^s are strong enough to have bound electronic states. We mention both (2.1) and the possibility of bound states because we wish to emphasise how these two properties are retained and distinctly displayed in the analysis which follows.

We consider an impurity potential V, screened or unscreened, strong enough to bind at least one electron in an

s-state $|\psi\rangle$ of eigenenergy E_0. Writing H_0 as the Hamiltonian of a free electron, we have

$$(H_0 + \mathcal{V})|\psi\rangle = E_0|\psi\rangle \tag{2.2}$$

We separate $\mathcal{V}$ into two terms, each of which is non-local:

$$\mathcal{V} = \mathcal{V}_1 + \mathcal{V}_2 \tag{2.3}$$

where the constituent parts are defined by

$$\mathcal{V}_1 = \frac{\mathcal{V}|\psi\rangle\langle\psi|\mathcal{V}}{\langle\psi|\mathcal{V}|\psi\rangle}, \tag{2.4a}$$

$$\mathcal{V}_2 = \mathcal{V} - \mathcal{V}_1 . \tag{2.4b}$$

$\mathcal{V}_1$ is of a particularly simple form which we shall describe as separable. By this we mean that its matrix element between any two states $|\psi_1\rangle$ and $|\psi_2\rangle$ can be written as a simple product of a functional of $|\psi_1\rangle$ and a functional of $|\psi_2\rangle$. The choice (2.4a) will enable us to sum an important part of the perturbation series for the charge density in §2.3.

Separations like (2.3), (2.4) have been studied by Weinberg[25] and applied by Fishlock and Pendry[12] (c.f. (1.13-(1.14)) to the problem of electron correlations in the unperturbed electron gas of a metal. The separation (2.3) is, however, more transparent than that used by Fishlock and Pendry, because the state $|\psi\rangle$ used in the separation has a

clear physical interpretation via equation (2.2) and is not merely a mathematical construction.

We now note some important properties of the separation (2.3). First, $\mathcal{V}_1$ gives rise to the same bound state $|\psi\rangle$ as $\mathcal{V}$:

$$(H_o + \mathcal{V}_1)|\psi\rangle = (H_o + \mathcal{V})|\psi\rangle = E_o|\psi\rangle. \qquad (2.5)$$

We may therefore consider $\mathcal{V}_1$ to be a pseudopotential corresponding to the potential $\mathcal{V}$ and appropriate to the energy E_o and orbital angular momentum $\ell = 0$. Naturally, any other eigenstates to which $\mathcal{V}_1$ gives rise do not correspond to the eigenstates of the potential $\mathcal{V}$: in particular, this is true of the states of positive energy. However, the important point is that the bound state property of $\mathcal{V}$ is present exclusively in the part $\mathcal{V}_1$ and that this property can be easily dealt with by virtue of the separable form (2.4a).

We now turn our attention to $\mathcal{V}_2$. As a corollary of (2.5), we have

$$\mathcal{V}_2|\psi\rangle = 0. \qquad (2.6)$$

Thus, for energies close to E_o, $\mathcal{V}_2$ constitutes a weak potential. For positive energies $\mathcal{V}_2$ may not behave as a weak potential. This is anticipated by the analysis of Pendry[26] and confirmed by the numerical calculations in Chapter 3. Nevertheless, in what follows, $\mathcal{V}_2$ is assumed to be weak enough for its effects to be treated by linear perturbation

theory. This will clearly not be a good assumption if V_2 is strong enough to have bound states. Unfortunately, the non-local nature of V_2 prevents us from establishing rigorously whether or not V_2 has bound states. Certainly, if the range in real space of V is sufficiently short, V_2 has no bound state: putting

$$V(r) = - U_0 \delta(\underline{r}) \tag{2.7}$$

where U_0 is positive and $\delta(\underline{r})$ is the three-dimensional Dirac δ-function, we obtain in the Schrödinger representation

$$\begin{aligned} \langle \underline{r} | V_2 | \underline{r}' \rangle &= - U_0 \delta(\underline{r}-\underline{r}') \delta(\underline{r}') \\ &\quad + U_0 \delta(\underline{r}) \delta(\underline{r}') \\ &= 0 \end{aligned} \tag{2.8}$$

A second feature of V_2 arises when V is the unscreened potential of an impurity carrying an excess charge. Since $|\psi\rangle$ has a finite range, V_1 has a finite range, so that V_2 becomes local at long range and retains the behaviour (2.7)

$$V_2 \sim - \frac{2Z^{excess}}{r} \tag{2.9}$$

Thus, the charge on the impurity is manifested only in the part V_2 of the potential: each of the features of the potentials described in the first paragraph of this section are separately displayed in V_1 and V_2. We note that, although V_2 may be weak enough for linear perturbation

theory to be used, it is still responsible for inducing, by virtue of (2.7), the total of Z^{excess} units of screening charge. $\mathcal{V}_1$ can only lead to a redistribution of this screening charge.

Finally, we indicate how stronger potentials, having many bound states, may be separated to facilitate perturbative calculations. Suppose that a potential has a set $\{|\psi_n\rangle;\ n=1,\ldots N\}$ of bound states, orthogonal to each other, then we may write:

$$\mathcal{V} = \sum_{n=1}^{N} \mathcal{V}_n + \mathcal{V}'$$
$$\mathcal{V}_n = \mathcal{V}|\psi_n\rangle\langle\psi_n|$$
$$\mathcal{V}' = \mathcal{V} - \sum_{n=1}^{N} \mathcal{V}_n \qquad (2.10)$$

The constituent potentials $\mathcal{V}_n$ have the property

$$\mathcal{V}_n|\psi_m\rangle = \begin{cases} \mathcal{V}|\psi_n\rangle & m=n \\ 0 & m\neq n \end{cases}$$
$$\mathcal{V}'|\psi_n\rangle = 0 \qquad n=1,2\ldots N \qquad (2.11)$$

The potentials $\mathcal{V}_n$ are non-Hermitian, but this is not a serious difficulty because of the property (2.11) which ensures that all negative eigenenergies arising from the $\mathcal{V}_n$ are real. It is now a straightforward matter to treat the $\mathcal{V}_n$ by infinite order perturbation and $\mathcal{V}'$ by linear perturbation theory. Unfortunately, the terms of the perturbation

series involving different v_n have to be included, and this is not easy.

We shall see in later chapters that the effect of applying non-linear perturbation theory to v_1 of (2.3) is most significant for the greatest binding energyis $|E_o|$. We therefore conclude that the essential non-linear behaviour srising out of (2.10) is contained in the v_n representing the deepest bound state of v. Consequently, the simpler separation (2.3) should be adequate to describe the essential non-linear behaviour, provided that the deepest bound state is much deeper than any other bound states of the potential. This approximation is a good one when the potential in question is a Coulomb potential and we assume it to be satisfactory for the potentials which we study.

§2.3 Construction of Charge Densities

In this section, we calculate the screening charge density induced when an unscreened potential U is introduced into an electron gas. We suppose that U is sufficiently attractive for a separation of the form (2.3) to be performed and ignore interactions between the electrons for the present. The system is then described by the one electron Hamiltonian

$$H = H_0 + \mathcal{U}_1 + \mathcal{U}_2 . \qquad (2.12)$$

We also define Green's operators by

$$G(E) = (E - H)^{-1} \qquad (2.13)$$

$$G_0(E) = (E - H_0)^{-1} . \qquad (2.14)$$

Next we write down the perturbation series for G, and in line with the remarks following (2.6), truncate the series by excluding all terms in which U_2 appears to orders higher than one.

$$G = G_0 + G_0 T_1 G_0 + G_0 U_2 G_0 + G_0 \delta T G_0. \tag{2.15}$$

Here, T_1 is the t-matrix of U_1 satisfying

$$T_1(E) = U_1 + U_1 G_0(E) T_1(E), \tag{2.16}$$

and δT contains those terms in which both U_1 and U_2 appear, so that

$$\delta T = T_1 G_0 U_2 + T_1 G_0 U_2 G_0 T_1 + U_2 G_0 T_1. \tag{2.17}$$

Our next step will be to calculate the charge density arising from (2.15). Because of (2.9), the third term of (2.15) must lead to the entire total screening charge, the second and fourth terms representing redistribution of this charge. We now compare these two redistribution terms, and argue that the term in T_1 will dominate over the term in δT, provided that U_2 is much weaker than U_1. We have seen (2.8) that U_2 is weak when U is short-ranged, and consequently the term in T_1 will dominate most strongly when U is a screened potential. Since we shall calculate charge densities induced by a self-consistently screened potential, we make the approximation of dropping the δT term from (2.15). Combining T_1

and δT, we obtain terms of (2.15) of the form

$$(G_o + G_o U G_o) T_1 G_o \qquad (2.18)$$

Thus, the effect of the δT term is to modify the flux of electrons scattered by T_1 from that represented by G_o to that represented by $G_o + G_o U_2 G_o$. The approximation of dropping the term in δT is therefore most satisfactory when the density of the electron gas is greatest and $G_o U_2 G_o$ introduces only a small fractional change in the flux. The approximation is also necessitated by the complexity of the terms in δT: whilst the charge density associated with these terms may be written down formally as easily as that associated with T_1, numerical analysis of such terms would be prohibitively difficult. In summary, our approximation of neglecting δT is most satisfactory for

(a) small Z^{excess}

(b) short screening lengths

(c) small r_s

We now utilise the separable form (2.4a) of U_1 in equation (2.16) to obtain

$$T_1 = \frac{U|\psi\rangle\langle\psi|U}{\langle\psi|U|\psi\rangle} + \frac{U|\psi\rangle\langle\psi|UG_oU|\psi\rangle\langle\psi|U}{|\langle\psi|U|\psi\rangle|^2} + \cdots$$

$$= \frac{U|\psi\rangle\langle\psi|U}{[\langle\psi|U|\psi\rangle - \langle\psi|UG_oU|\psi\rangle]} \qquad (2.19)$$

The identity

$$U|\psi\rangle = (E_0 - E)|\psi\rangle + (E - H_0)|\psi\rangle \tag{2.20}$$

which follows from (2.2), together with the definition (2.14), enables (2.19) to be written

$$T_1(E) = \frac{U|\psi\rangle\langle\psi|U}{(E-E_0)\langle\psi|UG_0|\psi\rangle} \tag{2.21}$$

Because of the form (2.4a) of U_1, the singularity at $E = E_c$ is the only singularity of $T_1(E)$ and we can proceed to calculate the charge density associated with the Green's function (2.15).

We call the charge density of our system $\rho(\underline{r})$ and define its Fourier transform $\rho(\underline{q})$ by

$$\rho(\underline{q}) = \int d^3\underline{r}\, e^{i\underline{q}\cdot\underline{r}}\rho(\underline{r}) \tag{2.22}$$

We use this definition, along with the well-known expression for the charge density $\rho(\underline{r},E)$ of electrons of energy E

$$\rho(\underline{r},E) = \lim_{\delta\to 0+} \int d^3\underline{r}'\, \mathrm{Im}\langle\underline{r}'|G(E-i\delta)|\underline{r}'+\underline{r}\rangle \tag{2.23}$$

to obtain an expression for $\rho(\underline{q})$ which includes all occupied states at zero temperature:

$$\rho(\underline{q}) = \lim_{\delta \to 0+} \frac{1}{\Omega} \frac{2}{\pi} \int_{-\infty}^{E_F} dE \sum_{\underline{k}} \mathrm{Im} \langle \underline{k} | G_0(E - i\delta) | \underline{k}+\underline{q} \rangle \qquad (2.24)$$

We recall the notation of Chapter 1 which is used here:

$$H_0 | \underline{k} \rangle = k^2 | \underline{k} \rangle = \mathcal{E}_{\underline{k}} | \underline{k} \rangle \qquad (2.25)$$

is the eigenvalue equation for free-electrons, and $|\underline{k}\rangle$ is normalized according to

$$\langle \underline{r} | \underline{k} \rangle = \Omega^{-1/2} e^{i \underline{k} \cdot \underline{r}} \qquad (2.26)$$

We now write

$$\rho(\underline{q}) = \rho_0(\underline{q}) + \rho_1(\underline{q}) + \rho_2(\underline{q}) \qquad (2.27)$$

in which ρ_0, ρ_1 and ρ_2 derive respectively from the first three terms of (2.15). We consider the three terms of (2.27) separately.

ρ_0 is simply the charge density of the unperturbed electron gas,

$$\rho_0(\underline{q}) = \lim_{\delta \to 0} \frac{2}{\pi} \frac{1}{\Omega} \int_{-\infty}^{E_F} dE \sum_{\underline{k}} \mathrm{Im} (E - \mathcal{E}_{\underline{k}} - i\delta)^{-1} \delta_{\underline{k}, \underline{k}+\underline{q}}$$

$$= \frac{2}{\pi} \frac{1}{\Omega} \sum_{\underline{k}} \pi f(E - \mathcal{E}_k) \delta_{q,0}$$

$$= 2 \frac{N}{\Omega} \delta_{q,0} \qquad (2.28)$$

Here N is the number of occupied $\underline{k}$-states in the volume Ω, f(E) is the Fermi function in the zero temperature limit, and $\delta_{\underline{k},\underline{k}'}$ is the three-dimensional Kronecker delta

$$\delta_{\underline{k},\underline{k}'} = \begin{cases} 1 & \underline{k} = \underline{k}' \\ 0 & \underline{k} \neq \underline{k}' \end{cases} \tag{2.29}$$

The factor of 2 arises, of course, from spin degeneracy $\rho_o(\underline{q})$ therefore has only a $\underline{q} = 0$ component, and will be written simply as ρ_o from now on.

We now turn our attention to the multiple-scattering term $\rho_1(\underline{q})$:

$$\rho_1(q) = \lim_{\delta \to 0} \frac{1}{\Omega} \frac{2}{\pi} \int_{-\infty}^{E_F} dE \sum_{\underline{k}} \mathrm{Im} \frac{\langle \underline{k} | T_1(E - i\delta) | \underline{k}+\underline{q} \rangle}{(E - \varepsilon_{\underline{k}} - i\delta)(E - \varepsilon_{\underline{k}+\underline{q}} - i\delta)} . \tag{2.30}$$

(2.2), (2.25) and (2.14) are now used to establish the identities

$$\langle \underline{k} | U | \psi \rangle = (E_o - \varepsilon_{\underline{k}}) \langle \underline{k} | \psi \rangle \tag{2.31}$$

$$\langle \psi | U G_o(E - i\delta) | \psi \rangle = \tilde{D}(E - i\delta)$$

$$= \frac{1}{\Omega} \sum_{\underline{k}} |\langle \psi | \underline{k} \rangle|^2 \frac{E_o - \varepsilon_{\underline{k}}}{E - \varepsilon_{\underline{k}} - i\delta} , \tag{2.32}$$

and the real functions $\tilde{D}_r(E)$, $\tilde{D}_i(E)$, $D_r(E)$ and $D_i(E)$ are defined by

$$\lim_{\delta\to 0} \tilde{D}(E-i\delta) = \tilde{D}_+(E) + i\tilde{D}_i(E), \qquad (2.33)$$

$$\lim_{\delta\to 0} \left[\tilde{D}(E-i\delta)\right]^{-1} = D_+(E) + i D_i(E). \qquad (2.34)$$

(2.31), (2.32), (2.34) enable us to write

$$\lim_{\delta\to 0} \langle \underline{k}| T_1(E-i\delta)|\underline{k}+\underline{q}\rangle = \left[D_+(E) + i D_i(E)\right]$$

$$\lim_{\delta\to 0} \frac{1}{E-E_0-i\delta} \langle \underline{k}|\psi\rangle\langle\psi|\underline{k}+\underline{q}\rangle (E_0-\varepsilon_{\underline{k}})(E_0-\varepsilon_{\underline{k}+\underline{q}}) \qquad (2.35)$$

Furthermore, since $\langle\psi|\underline{r}\rangle$ is spherically symmetric, $\langle\psi|\underline{k}\rangle$ is a real function of k only. Thus, the real and imaginary parts of (2.35) are easily separated. We insert (2.35) into (2.30), pick out the imaginary part using the identity

$$\frac{1}{x-x_0-i\delta} = \mathcal{P}\frac{1}{x-x_0} + i\pi\delta(x-x_0) \qquad (2.36)$$

and perform the integral over energy. The δ-function terms lead to Fermi functions, and we obtain

$$\rho_1(q) = \frac{2}{\Omega}\mathcal{P}\sum_{\underline{k}} \langle \underline{k}|\psi\rangle\langle\psi|\underline{k}+\underline{q}\rangle (E_0-\varepsilon_{\underline{k}})(E_0-\varepsilon_{\underline{k}+\underline{q}})$$

$$\left\{ D_+(E_0) f(E_0)(E_0-\varepsilon_{\underline{k}})^{-1}(E_0-\varepsilon_{\underline{k}+\underline{q}})^{-1} \right.$$

$$\left. + D_+(\varepsilon_{\underline{k}}) f(\varepsilon_{\underline{k}})(\varepsilon_{\underline{k}}-E_0)^{-1}(\varepsilon_{\underline{k}}-\varepsilon_{\underline{k}+\underline{q}})^{-1} + \right.$$

$$+ D_\uparrow(\varepsilon_{\underline{k}+\underline{q}}) f(\varepsilon_{\underline{k}+\underline{q}})(\varepsilon_{\underline{k}+\underline{q}} - E_o)^{-1}(\varepsilon_{\underline{k}+\underline{q}} - \varepsilon_{\underline{k}})^{-1}$$

$$+ \frac{1}{\pi}\int_{-\infty}^{E_F} dE\, D_\downarrow(E)(E-E_o)^{-1}(E-\varepsilon_{\underline{k}})^{-1}(E-\varepsilon_{\underline{k}+\underline{q}})^{-1} \Big\} \qquad (2.37)$$

Finally we turn to $\rho_2(\underline{q})$. We recall the definition (2.4b) of U_2, and write ρ_2 as the difference in charge densities induced by U and U_1 in 1st order perturbation theory.

$$\rho_2(q) = \rho_2'(q) - \rho_2''(q). \qquad (2.38)$$

$\rho_2'(\underline{q})$ is the charge density associated with U and in RPA, for example,

$$\rho_2'(q) = \chi_o(q)\, U(q) \qquad (2.39)$$

where $\chi_o(q)$ the static limit of the function defined in (1.6) and U(q) is the Fourier transform of U(r), defined as in (2.22).

$\rho_2''(\underline{q})$ is the screening charge density associated with the non-local potential U_1 in linear screening theory. The screening of a non-local potential has been studied in detail by Animalu[27], but here a completely analogous result to his is obtained by the same type of analysis as led to (2.37).

$$\rho_2''(\underline{q}) = \frac{2}{\Omega}\mathcal{P}\sum_{\underline{k}} \frac{\langle \underline{k}|\psi\rangle\langle\psi|\underline{k}+\underline{q}\rangle}{\langle\psi|\mathcal{U}|\psi\rangle} \cdot (E_o-\mathcal{E}_{\underline{k}})(E_o-\mathcal{E}_{\underline{k}+\underline{q}})\,\frac{f(\mathcal{E}_{\underline{k}})-f(\mathcal{E}_{\underline{k}+\underline{q}})}{\mathcal{E}_{\underline{k}}-\mathcal{E}_{\underline{k}+\underline{q}}} \tag{2.40}$$

§2.4 Discussion of Charge Densities

We now study the expressions (2.37) and (2.40) for $\rho_1(\underline{q})$ and $\rho_2''(\underline{q})$: we shall first obtain a physical understanding of them and then cast them into a form which will permit them to be evaluated numerically.

We begin by examining the general form of $\tilde{D}(E)$ defined in (2.32). (2.33) and (2.36) enable us to write

$$\tilde{D}_i(E) = \frac{\pi}{\Omega}\sum_{\underline{k}} |\langle\psi|\underline{k}\rangle|^2 (E_o-\mathcal{E}_{\underline{k}})\,\delta(E-\mathcal{E}_{\underline{k}}). \tag{2.41}$$

Consequently, $D_i(E)$ is non-zero only for energies $E > 0$. Furthermore, (2.41) approaches zero for large E by virtue of the finite $\underline{k}$-space range of $\langle\psi|\underline{k}\rangle$. $\tilde{D}_r(E)$ may be written in terms of $\tilde{D}_i(E)$ in the dispersion relation

$$\tilde{D}_r(E) = \frac{1}{\pi}\mathcal{P}\int_{-\infty}^{\infty} dE'\,\frac{\tilde{D}_i(E')}{E-E'} \tag{2.42}$$

It follows that $\tilde{D}(E)$ is real and positive for $E < 0$. The

general forms of $\tilde{D}_r(E)$ and $\tilde{D}_i(E)$ are sketched in Fig. 2.1. In particular, we may obtain directly from (2.32)

$$\tilde{D}(E_0) = \frac{1}{\Omega} \sum_{\underline{k}} |\langle \psi | \underline{k} \rangle|^2 = 1 \qquad (2.43)$$

using the fact that $\langle \psi | k \rangle$ is normalized.

We are now in a position to understand the expression (2.37) for $\rho_1(\underline{q})$. Since $f(E_0) = 1$, the first term in the early braces reduces to

$$\frac{2}{\Omega} \sum_{\underline{k}} \langle \underline{k} | \psi \rangle \langle \psi | \underline{k}+\underline{q} \rangle = 2 \int d^3r \, e^{i\underline{q}\cdot\underline{r}} n_0(r),$$

$$n_0(r) = |\langle \underline{r} | \psi \rangle|^2. \qquad (2.44)$$

It consequently represents a pair of electrons (with opposite spins) bound in the state $|\psi\rangle$. The remaining terms of (2.37) all arise from states in the band region ($0 \leq E \leq E_p$). This is because the second and third terms both originate from poles of the form $(E - \epsilon_{\underline{k}})^{-1}$, whilst the fourth term contains the factor $D_i(E)$ which vanishes for $E < 0$. Furthermore, it is easy to establish that the sum of the second, third and fourth terms of (2.37) vanishes in the limit $E_F \to 0$.

We may obtain some idea of the effect of the second and third terms of (2.37) by writing them in the $q \to 0$ limit:

$$2 |\langle \psi | k_F \rangle|^2 (E_0 - E_F)^2 D_+(E_F) \lim_{q \to 0} \chi_0(q) \qquad (2.45)$$

It is well known that the $q \to 0$ limit of $\chi_0(q)$ is negative,

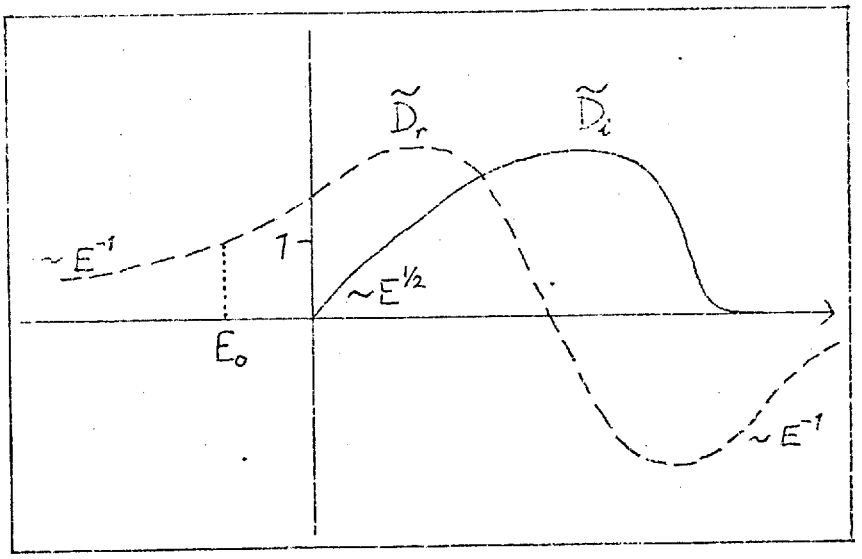

Figure 2.1 The functions $\tilde{D}_r(E)$ and $\tilde{D}_i(E)$.

and it turns out that the numerical values of $D_r(E_F)$ in the systems we have studied are positive. Thus, these terms give a negative contribution to $\rho_1(\underline{q})$, i.e. they represent a repulsion of electronic charge. This repulsive effect of the attractive potential U_1 is a significant physical effect which linear perturbation theory does not anticipate. We also remark that the limit (2.46) affords a useful check on numerical computations. No such easy check exists for the final term of (2.37), but, in practice, it also represents charge repulsion.

It is not yet clear how (2.37) may be evaluated in practice for non-zero q. In particular, the various poles of the integrand prevent direct numerical integration. However, (2.37) may be put into a form in which direct numerical integration is possible. To show this, we begin by writing the second and third terms as

$$\frac{1}{\pi^2} \mathcal{P} \int_0^{k_F} dk \int_{-1}^{1} d\mu \; I(k,\mu) \left(\mu + \frac{q}{2k}\right)^{-1} \tag{2.46}$$

where

$$I(k,\mu) = -\frac{k}{2q} \langle \underline{k} | \psi \rangle \langle \psi | \underline{k}+\underline{q} \rangle (E_{\underline{k}} - E_0) D_r(E_{\underline{k}}) \tag{2.47}$$

and μ is the cosine of the angle between $\underline{k}$ and $\underline{q}$. This is possible because the summation in (2.37) is over all $\underline{k}$ and because $\langle \psi | \underline{k} \rangle$ and $\varepsilon_{\underline{k}}$ are functions of $|\underline{k}|$ only. Our aim

is now to write (2.4b) as a sum of integrals, each of which is finite and can either be evaluated analytically or has no poles in its integrand. If this is possible, then (2.46) can be evaluated by a simple numerical technique.

We consider the identity

$$\int \alpha(x)\beta(x-x_0)\,dx = \int [\alpha(x)-\alpha(x_0)]\beta(x-x_0)\,dx + \alpha(x_0)\int \beta(x-x_0)\,dx \qquad (2.48)$$

If we suppose that

(a) $\beta(x-x_0)$ has a pole of some sort at $x = x_0$;

(b) $\int \beta(x-x_0)\,dx$ can be performed analytically and is finite; and

(c) $\{\alpha(x) - \alpha(x_0)\}\beta(x-x_0)$ is non-singular,

then (2.48) constitutes a method of writing an integral with a singular integrand as a sum of integrals which can either be evaluated analytically or by direct numerical integration.

A transformation like (2.48) is just what we require to re-write (2.46), and, after several transformations of this type, we obtain

$$\frac{1}{\pi^2}\left\{ \int_0^{k_F} dk \left[\left(\int_{-1}^{1} d\mu \, \frac{I(k,\mu) - I(k,-\frac{q}{2k})}{\mu + q/2k} \right) + \left(I(k,-\frac{q}{2k}) - I(\tfrac{q}{2},-1) \right) \ln\left| \frac{q+2k}{q-2k} \right| \right] \right.$$

+

$$+ I(\quad - 1)\left[\frac{}{}k_F \ln\left|\frac{q+2k_F}{q-2k_F}\right| + \frac{q}{2}\ln\left|\frac{q^2/4 - E_F}{q^2/4}\right|\right]\Bigg\}$$

(2.49)

The final term of (2.37) is a little harder to deal with. We split the integrand into partial fractions and introduce the function

$$\zeta(\epsilon) = \mathcal{P}\int_0^{E_F} dE\, \frac{D_i(E)}{E-\epsilon}\, dE \tag{2.50}$$

which enables us to write

$$\int_{-\infty}^{E_F} dE\, D_i(E)\,(E-E_0)^{-1}(E-\varepsilon_{\underline{k}})^{-1}(E-\varepsilon_{\underline{k}+\underline{q}})^{-1}$$

$$= (E_0-\varepsilon_{\underline{k}})^{-1}(\varepsilon_{\underline{k}}-\varepsilon_{\underline{k}+\underline{q}})^{-1}(\varepsilon_{\underline{k}+\underline{q}}-E_0)^{-1}$$

$$\Big\{(\varepsilon_{\underline{k}+\underline{q}}-\varepsilon_{\underline{k}})\zeta(E_0) + (E_0-\varepsilon_{\underline{k}+\underline{q}})\zeta(\varepsilon_{\underline{k}})$$

$$+(\varepsilon_{\underline{k}}-E_0)\zeta(\varepsilon_{\underline{k}+\underline{q}})\Big\} \tag{2.51}$$

Now, $\zeta(\varepsilon)$ has the important properties

$$\sum_{\underline{k}} \zeta(k^2) = 0 \tag{2.52}$$

and

$$\zeta(\epsilon) \propto \ln|\epsilon - E_F| \tag{2.53}$$

for ε close to E_F. Thus the fourth term of (2.37) splits up into three terms, one with a non-singular integrand, and the others with a simple pole and a logarithmic singularity

in each integrand. The additional logarithmic singularity complicates the procedure of removing singularities, and it has not proved possible to obtain an entirely satisfactory expression. Nevertheless, it is possible to write the fourth term of (2.37) as a sum of integrals, each of which is finite, apart from two integrals which each have a logarithmic singularity at $q = 2k_F$. Since the original expression had no such singularity, the two singular components must cancel. It turns out that, in the numerical calculations, satisfactory cancellation is obtained over all but a very narrow range of q. This restriction is not severe for present purposes, but if one wished to compute Friedel-like oscillations in the charge density within this scheme, the details of the behaviour close to $q = 2k_F$ would have to be computed more precisely.

We eventually obtain for the fourth term of (2.37), by applying identities like (2.48), and by using (2.52),

$$\frac{\mathcal{J}(E_0)}{\pi^3}\int_0^\infty dk \int_{-1}^{1} d\mu \;\tfrac{1}{2}k^2 \langle \underline{k}|\psi\rangle\langle\psi|\underline{k}+\underline{q}_F\rangle$$

$$+\frac{1}{\pi^3}\int_0^\infty dk \int_{-1}^{1} d\mu \left[\left\{H(k,\mu)-H(k,-q/2k)\right\}\frac{1}{\mu+\frac{q}{2k}}\right.$$

$$\left.-\left\{H(k_F,\mu)-H(k_F,-\frac{q}{2k_F})\right\}\frac{1}{\mu+\frac{q}{2k_F}}\right]\mathcal{J}(k^2)$$

$$+\frac{1}{\pi^3}\int_0^\infty dk\left[\left\{H(k)-H(q/2)\right\}\ln\left|\frac{q+2k}{q-2k}\right|\right.$$

$$+\left\{H(k_F)-H(q/2)\right\}\ln\left|\frac{q+2k_F}{q-2k_F}\right|\Big]\,\mathcal{J}(k^2)$$

$$+\frac{1}{\pi^3}H(q/2)\int_0^\infty dk\left[\mathcal{J}(k^2)-\mathcal{J}(q^2/4)\,\Theta(k-q/2)\right]$$

$$\times\left[\ln\left|\frac{q+2k}{q-2k}\right|-\ln\left|\frac{q+2k_F}{q-2k_F}\right|\right]$$

$$-\frac{1}{\pi^3}H(q/2)\,\mathcal{J}(q^2/4)\,q\left[\tfrac{3}{2}\ln 3-\ln\left|\frac{q+2k_F}{q-2k_F}\right|\right] \qquad (2.54)$$

Here,

$$H(k,\mu)=-\frac{k}{2q}\left(\mathcal{E}_{\underline{k}+\underline{q}}-E_0\right)\langle\underline{k}|\psi\rangle\langle\psi|\underline{k}+\underline{q}\rangle,$$

$$H(k)\equiv H(k,-q/2k)=-\frac{k}{2q}\left(\mathcal{E}_{\underline{k}}-E_0\right)|\langle\underline{k}|\psi\rangle|^2,$$

$$H(k_F,\mu)=-\frac{k_F}{2q}\left(\mathcal{E}_{k_F'}-E_0\right)\langle k_F|\psi\rangle\langle\psi|k_F'\rangle,$$

$$k_F'=\left(k_F^2+q^2+2k_Fq\mu\right)^{1/2},$$

$$H(k_F)\equiv H(k_F,-q/2k_F)=-\frac{k_F}{2q}\left(E_F-E_0\right)|\langle k_F|\psi\rangle|^2,$$

$$H(q/2)=-\frac{1}{4}\left(\mathcal{E}_{q/2}-E_0\right)|\langle q/2|\psi\rangle|^2.$$

and we have introduced the step function

$$\Theta(k-q/2)=\begin{cases}1 & k\geq q/2\\ 0 & k<q/2\end{cases}$$

The expression (2.40) for ρ_2'' is susceptible to the same treatment as the second and third terms of (2.37). In particular, there is a simple check on the q = 0 limit.

For arbitrary q, we obtain an expression identical to (2.49) with the replacement

$$I(k,\mu) \longrightarrow J(k,\mu) \tag{2.55}$$

$$J(k,\mu) = -\frac{k}{2q}\,\frac{\langle k|\psi\rangle\langle\psi|k+q\rangle}{\langle\psi|U|\psi\rangle}\,(E_0-\varepsilon_k)(E_0-\varepsilon_{k+q}).$$

§2.5 A Self-Consistent Scheme

Now that we have calculated the charge density induced by U, we are in a position to introduce the electron-electron interaction $v(q)$ and make the solution self-consistent. We write the total screened potential V^s, corresponding to bare potential U, as follows:

$$V^s(q) = U(q) + v(q)\left[\rho_1(q)+\rho_2'(q)-\rho_2''(q)\right] + F\left[\rho_1(q)+\rho_2'(q)-\rho_2''(q)\right] \tag{2.56}$$

The second term on the right hand side of (2.56) is just the Hartree potential of the screening charge; and the third term $F[\rho]$ is a non-linear functional of the screening charge density representing the exchange potential of the screening charge. This potential V^s becomes self-consistent if the charge densities are calculated in the field of V^s rather than U. Then, using (2.39), we may obtain

$$V^S(q) = \mathcal{U}(q)\,\mathcal{E}^{-1}_{RPA}(q) + v(q)\,\mathcal{E}^{-1}_{RPA}(q)\left[\rho_1(q) - \rho_2''(q)\right] + \mathcal{E}^{-1}_{RPA}(q)\,F\left[\rho_1(q) + \rho_2'(q) - \rho_2''(q)\right] \tag{2.57}$$

Schematically,

$$V^S = \mathcal{U}\,\mathcal{E}^{-1}_{RPA} + \gamma\left[V^S\right] \tag{2.58}$$

where γ is a non-linear functional of V^S. Provided that the correction $\gamma(V^S)$ to V^S is small, then an iterative solution to (2.58) is a straightforward proposition. A disadvantage of (2.58) is that the non-linear effects of the electron-electron and electron-impurity interactions are inseparable. When we go on to study numerically a scheme like (2.58), we shall use an approximation which distinguishes these two non-linear effects more clearly.

CHAPTER 3

COMPUTATIONS

In this chapter, we describe how the self-consistent scheme of Chapter 2 may be applied to a particular model impurity potential and a particular model of a metallic electron gas. The necessary numerical analysis is indicated and the general numerical behaviour of the seheme is presented.

§3.1 The Model System

We consider a free-electron-like metal of valence Z^o into which a single impurity ion of valence Z^i has been introduced substitutionally. We ignore deformation of the lattice and scattering from the ions of the host, and represent the situation by a single one-electron potential U embedded in an electron gas of suitable density. U takes the form

$$U = U^i - U^o \tag{3.1}$$

where U^i is the one-electron potential due to the isolated impurity ion and U^o the potential due to an isolated ion of the host. We use for U^i and U^o model potentials of the Heine-Abarenkov form (1.24) appropriate to the deepest bound s-states of the free ions. Whilst this choice is not particularly suitable for discussing band electrons, it yields, for $Z^o - Z^o \geq 1$ and alkali metal or alkaline earth hosts, a potential U with a bound state. Thus, this choice yields a

potential U with a feature which is essential to our scheme. The details of the core region of the potential are not important, beyond the fact that bound states are possible, because it is the effect of valence rather than core electrons on impurity screening which we wish to discuss. U therefore has the form

$$U = \begin{cases} A_o & r \leq R_M \\ -2\,\dfrac{Z^i - Z^o}{r} & r > R_M \end{cases} \qquad (3.2)$$

A_o is a constant for any particular system and we choose to study alloy systems compounded from elements of the same row of the periodic table so that the same model core radius R_M is suitable for both U^o and U^i.

We now turn to the electron gas. Since we are chiefly interested in the non-linear effects of the electron-impurity interaction, we satisfy ourselves with a linearized treatment of exchange and correlation in the electron gas; i.e. a treatment where the screened potential depends only linearly on the density of screening charge. Such a linearized treatment has been studied extensively by Singwi et al.[13] who find that correlation and exchange may be introduced into a Hartree screening theory by the replacement (1.20). We assume that this treatment, employing the function G(k) (1.23) gives the essential ingredients of correlation and exchange within our model, even though U is not a weak potential and some of the electrons with which we are concerned are in localized rather than free states.

Instead of (2.57), we have the self-consistent scheme

$$V^s(q) = \mathcal{U}(q)\mathcal{E}^{-1}(q) + [1 - G(q)]v(q)\mathcal{E}^{-1}(q)[\rho_1(q) - \rho_2''(q)] \tag{3.3}$$

where $$\mathcal{E}(q) = 1 - (1 - G(q))v(q)\chi_0(q) \tag{3.4}$$

((3.4) is not the dielectric function in the terminology of Singwi et al.)

Schematically,

$$V^s = \mathcal{U}\mathcal{E}^{-1} + \beta[V^s] \tag{3.5}$$

where β represents a non-linear functional. (3.5) may be solved for V^s by determining the limit $V_\infty = V^s$ of the sequence V_1, V_2 .... of functions generated from the trial function V_o by

$$V_n = \mathcal{U}\mathcal{E}^{-1} + \beta[V_{n-1}] \tag{3.6}$$

V_o must be chosen to obtain rapid convergence of the iterative scheme (3.6).

$$V_o = \mathcal{U}\mathcal{E}^{-1} \tag{3.7}$$

proves to be a most satisfactory choice, but

$$V_o = \mathcal{U} \tag{3.8}$$

also gives rapid convergence.

It is convenient to define some of the quantities which we shall calculate within this model. We define a charge density ρ_{lin}, arising in the corresponding screening theory, which is linear in the electron-impurity interaction, by

$$\rho_{lin}(q) = U(q)\,\chi_0(q)\,\varepsilon^{-1}(q) \tag{3.9}$$

The correction to ρ_{lin} in our non-linear scheme is then

$$\rho_{nl}(q) = \left[\rho_1(q) - \rho_2''(q)\right]\varepsilon^{-1}(q) \tag{3.10}$$

and the potential to which (3.10) gives rise is

$$V_{nl}(q) = \rho_{nl}(q)\left[1 - G(q)\right]v(q). \tag{3.11}$$

Thus

$$V^s(q) = U(q) + \rho_{lin}(q)\left[1-G(q)\right]v(q) + V_{nl}(q) \tag{3.12}$$

We also examine the $q \to 0$ limits of these charge densities: these represent the total screening charge present in the system. Now, since U(q) represents a charged object,

$$U(q) \to -(Z^i - Z^0)v(q) \quad (q \to 0) \tag{3.13}$$

Consequently,

$$\lim_{q\to 0} \rho_{lin}(q) = Z^i - Z^0 \tag{3.14}$$

On the other hand, the finite range of V^o implies that

$$\lim_{q \to 0} \left[\rho_1(q) - \rho_2''(q) \right] = \text{constant} \qquad (3.15)$$

so that

$$\lim_{q \to 0} \rho_{n\ell}(q) = 0 . \qquad (3.16)$$

Thus, the correction $\rho_{n\ell}(q)$ explicitly preserves overall charge neutrality: it represents a redistribution of the $Z^i - Z^o$ electrons represented by $\rho_{\ell in}(q)$.

§3.2 The Numerical Scheme

We now describe some of the numerical techniques which have been employed to carry out the self-consistent calculations described in Chapter 2 and §3.1. A block diagram showing the more important stages in the computational scheme appears in Fig. 3.1.

We begin by remarking on some of the general features of the scheme. All of the functions which it uses (by virtue of the spherical symmetry of the problem) are essentially functions of a single variable. Consequently, no storage problems arise on the computer. Most of the functions are smooth: they may be tabulated at suitable intervals and linear interpolation may be used to obtain intermediate values. No original techniques are involved in the scheme: the principal difficulties arise from the complexity with which simple techniques are assembled. We shall therefore outline these

simple techniques and then indicate some of the problems involved in assembling them.

The only numerical procedure, apart from integration and interpolation, which has been used, is the solution of the radial Schrödinger equation to obtain $\langle r|\psi\rangle$ and E_o. The technique which has been used, has been adapted from a method which has been widely employed for calculating logarithmic derivatives for use in the augmented plane wave method[28]. An energy is chosen, and, with this energy, the Schrödinger equation is integrated radically outwards on a logarithmic mesh, using first a Runge-Kutta and then a Milne method, for about two interatomic distances. This calculation is repeated at different energies, and an energy E_o, at which the wavefunction $\langle r|\psi\rangle$ is that of a bound state, is located.

Now, in general, the analytic form of the wavefunction as $r \to \infty$ for a finite ranged potential is

$$\psi(r,E) \sim A(E)\,\frac{e^{-Kr}}{r} + B(E)\,\frac{e^{Kr}}{r} \qquad (3.17)$$

where $K^2 = -E$. $A(E)$ and $B(E)$ are functions of energy only, and at a bound state energy, $E = E_o$

$$B(E_o) = 0 \qquad (3.18)$$

In practice, we are certain not to choose an energy exactly equal to a bound state energy: $B(E)$ remains finite and we obtain the wavefunction

$$\psi(r,E) \propto \frac{e^{Kr}}{r} \qquad (3.19)$$

Figure 3.1 Block Diagram of Numerical Procedure.

Key:

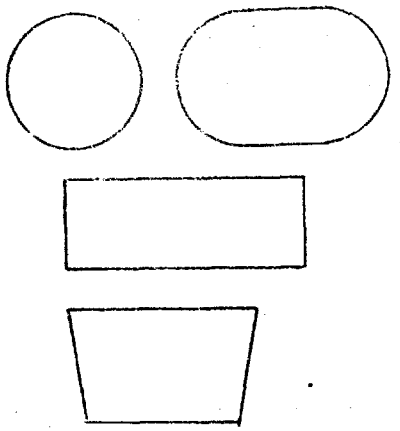

Parameters and functions

Numerical process

(FT = Fourier Transform)

Decision

Details of "INTEGRATION" Block (see next page):

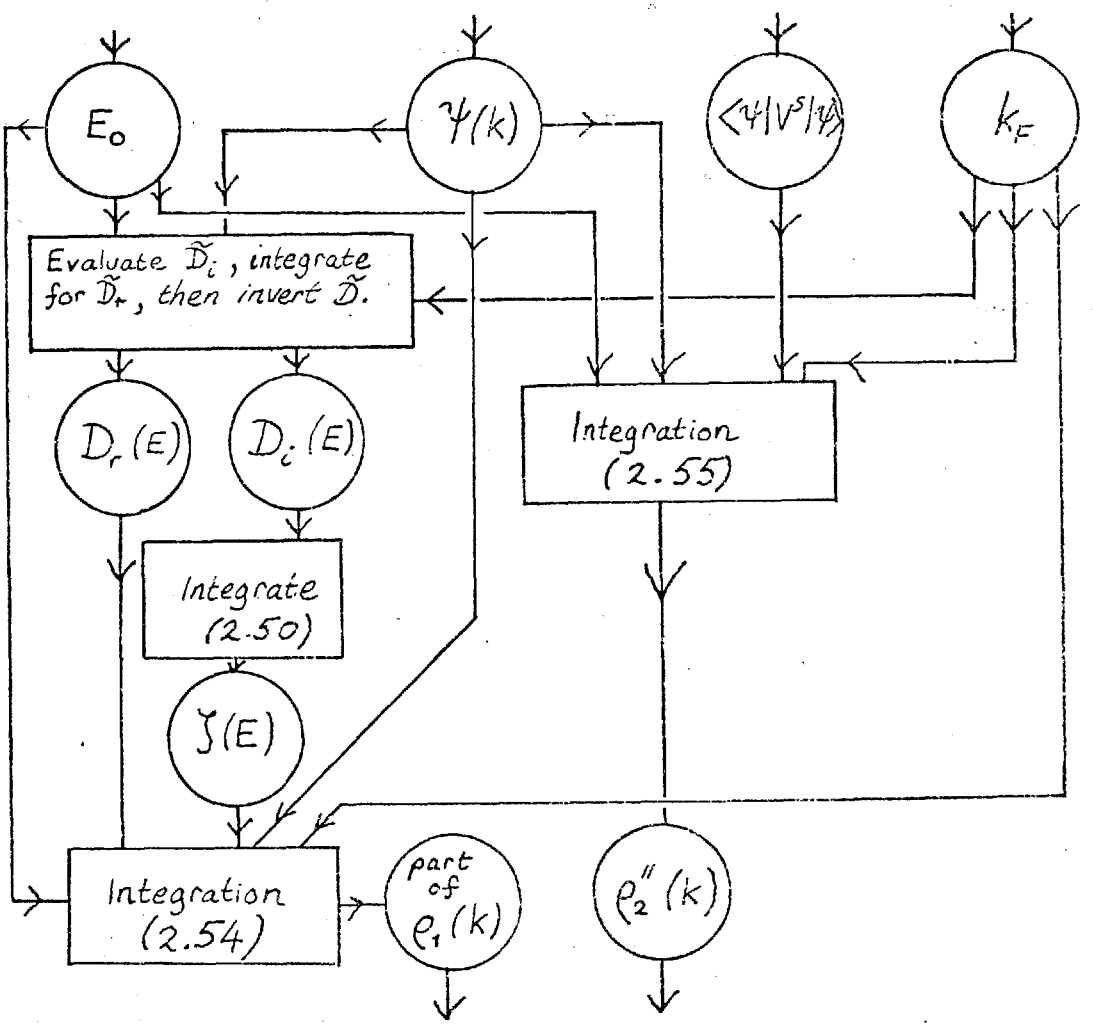

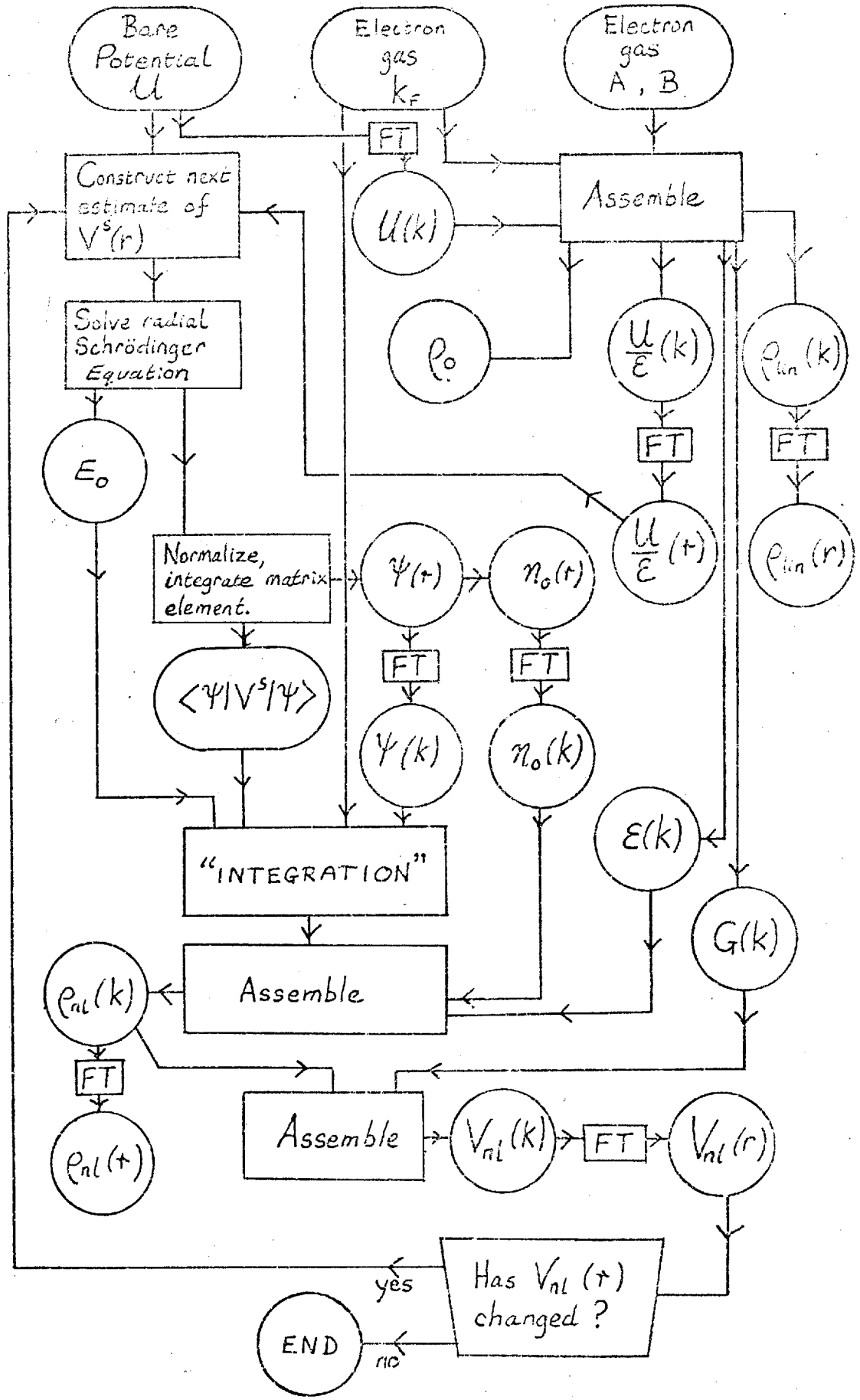

Figure 3.1 (continued)

which diverges for large r. Nevertheless, provided E is sufficiently close to a bound state energy, there exists a range of r over which $A(E)e^{-Kr}/r$ is small by virtue of the exponential and $B(E)e^{Kr}/r$ is small by virtue of B(E) being small. $\psi(r,E)$ is flat and small in this region, and the existence of such a flat region in the numerically integrated wavefunction is taken as evidence that E is close to E_o. In practice, it is found that once such a flat region has been obtained, further improvement of the chosen value of E leads to negligible change in the short range part of $\psi(r,E)$.

In a number of the simple integrals which have been performed (including Fourier transforms), the integrands have an infinite range. The range of integration is divided into two parts in those cases: Simpson's Rule or the trapezium rule is used for the short range part of the integral, and the asymptotic form of the integrand at long range enables an approximate long range contribution to be evaluated analytically.

A particular case of such an infinite ranged integrand arises in the Fourier transformation of the linearly screened $U(k)\varepsilon^{-1}(k)$. The long range oscillations in this function arise from the discontinuity at $r = R_M$ of our model potential, and since this discontinuity is not removed by screening, it is essential to reproduce it accurately in the screened potential. We proceed as follows:

We evaluate U(k) analytically and obtain

$$U(k) = 4\pi R_M^3 \left[A_0 \left\{ \frac{\sin c}{c^3} - \frac{\cos c}{c^2} \right\} - 2(Z^i - Z^o) \frac{\cos c}{c^2} \right],$$

$$c = k R_M. \tag{3.20}$$

$\varepsilon(k)$ is calculated from (3.4), so that $U(k)\varepsilon^{-1}(k)$ is known. The integral which gives the Fourier transform of $U(k)\varepsilon^{-1}(k)$ is spit into two. For $0 < k < K_M$, the integral is performed numerically. K_M is chosen so that

$$\mathcal{E}(k) \approx 1 \qquad (k > K_M) \tag{3.21}$$

and consequently the contribution to the integral for $k > K_M$ is approximately

$$\frac{A_0}{\pi} \left\{ \frac{2 \sin K_M R_M \sin K_M r}{K_M r} - \left[Si' K_M(r + R_M) + Si' K_M (R_M - r) \right] \right\}$$

$$- \frac{2(Z^i - Z^o)}{\pi r} \left[Si' K(R_M - r) - Si' K_M (R_M + r) \right] \tag{3.22}$$

The function Si'(x) is related to the sine integral function

$$Si(x) = \int_0^x \frac{\sin t}{t} dt - \frac{\pi}{2} \tag{3.23}$$

by

$$Si'(x) = \operatorname{sign} x \; Si(|x|) \tag{3.24}$$

and therefore has a discontinuity of π at $x = 0$. Thus (3.22) has a discontinuity of

$$-\frac{2(Z^{i}-Z^{o})}{r} - A_o \qquad (3.25)$$

exactly like the unscreened potential U(r). For the purposes of these calculations si(x) was calculated from

$$Si(x) = \sum_{n=0}^{\infty} \frac{(-1)^n x^{2n+1}}{(2n+1)(2n+1)!} - \frac{\pi}{2} \qquad (3.26)$$

for small x, and from the asymptotic from

$$si(x) \sim -\frac{\cos x}{x} \qquad (3.27)$$

for large x[29].

Next, we make some remarks about the numerical Fourier transforms. If we have a function f(r) tabulated at a set of points $\{r_i\}$ at constant intervals h, the simplest procedure to evaluate the Fourier transform f(k) involves using the trapezium rule for numerical integration. However, this technique gives rise to components f(k) which are finite for all k such that

$$kh = 2n\pi \qquad n = 1,2,3...$$

Thus, oscillations in f(k) for large k are produced by this technique. Such oscillations cannot be completely removed by any numerical technique, but we have adopted a procedure which reduces these oscillations to an acceptable magnitude. The function f(r) is assumed to vary linearly with r within each step of length h and the contribution to the Fourier transform from each of these steps is evaluated analytically.

These contributions are then summed on the computer.

Lastly, we describe some of the difficulties involved in assembling this conglomeration of numerical analysis. These revolve around choosing appropriate ranges and intervals over which to evaluate the intermediate functions appearing in Fig. 3.1. Since these functions are usually integrated in three dimensions to obtain further functions, their long range parts are heavily weighted. Considerable care has to be taken that spurious oscillations arising from the numerical Fourier transforms do not produce appreciable effects after subsequent integration: appropriate tabulations of all the functions used are vital.

§3.3 Numerical Behaviour

We begin by remarking on the form of some of the functions we have calculated in q-space.

As we have already mentioned, $\rho_1(q)$ contains a term representing a bound state and a term representing repelled band electrons, whilst $\rho_2''(q)$ represents screening electrons in linear screening theory. These function typically take the form shown in Fig. 3.2. As U is made stronger, $\rho_2''(q = 0)$ is increased, whilst the repelled charge term in $\rho_1(q = 0)$ is also augmented. Consequently, the difference $\rho_1(q = 0) - \rho_2''(q = 0)$, which is always negative in our model calculations, becomes most negative for the strongest impurity potentials.

For larger q, the difference $\rho_1 - \rho_2''$ becomes positive. As U is increased and $\langle r|\psi\rangle$ made more short-ranged, the main

effect is an increase in the range of $\rho_1(q)$ leading to an increased positive region in $\rho_1 - \rho_2''$. This positive region gives rise to an enhanced charge density on the impurity ($\rho_{n\ell}$ (r = 0) positive) whilst the negative region gives rise to transfer of charge out of the impurity cell. Broadly speaking, we find that the enhancement and transfer have the following trends at U and r_s are varied:

	Enhancement	Transfer
Increasing U	increase	increase
Increasing r_s	decrease	decrease

Examples of these trends may be seen in the results of Chapter 4.

The potential $V_{n\ell}$ which we calculate from the charge densities is cut off at large q by the function $\left(1-G(q)\right)$. Consequently, the positive region of $\rho_1 - \rho_2''$ gives rise only to a very weak potential. This fact is reflected in real space where $V_{n\ell}$ is attractive throughout the impurity cell in the systems we have studied.

The computational scheme defined by (3.6) and (3.7) is found to give most rapid convergence: about 5 iterations are typically required to establish V^s accurately. The scheme (3.6) and (3.8) is less satisfactory because V^s is closer to U/ε than to U.

We are now in a position to understand the behaviour of the functions $V_{n\ell}$ and $\rho_{n\ell}$ as the iterative calculation proceeds. Typical behaviour is given in Fig. 3.3. As the $V_{n\ell}$

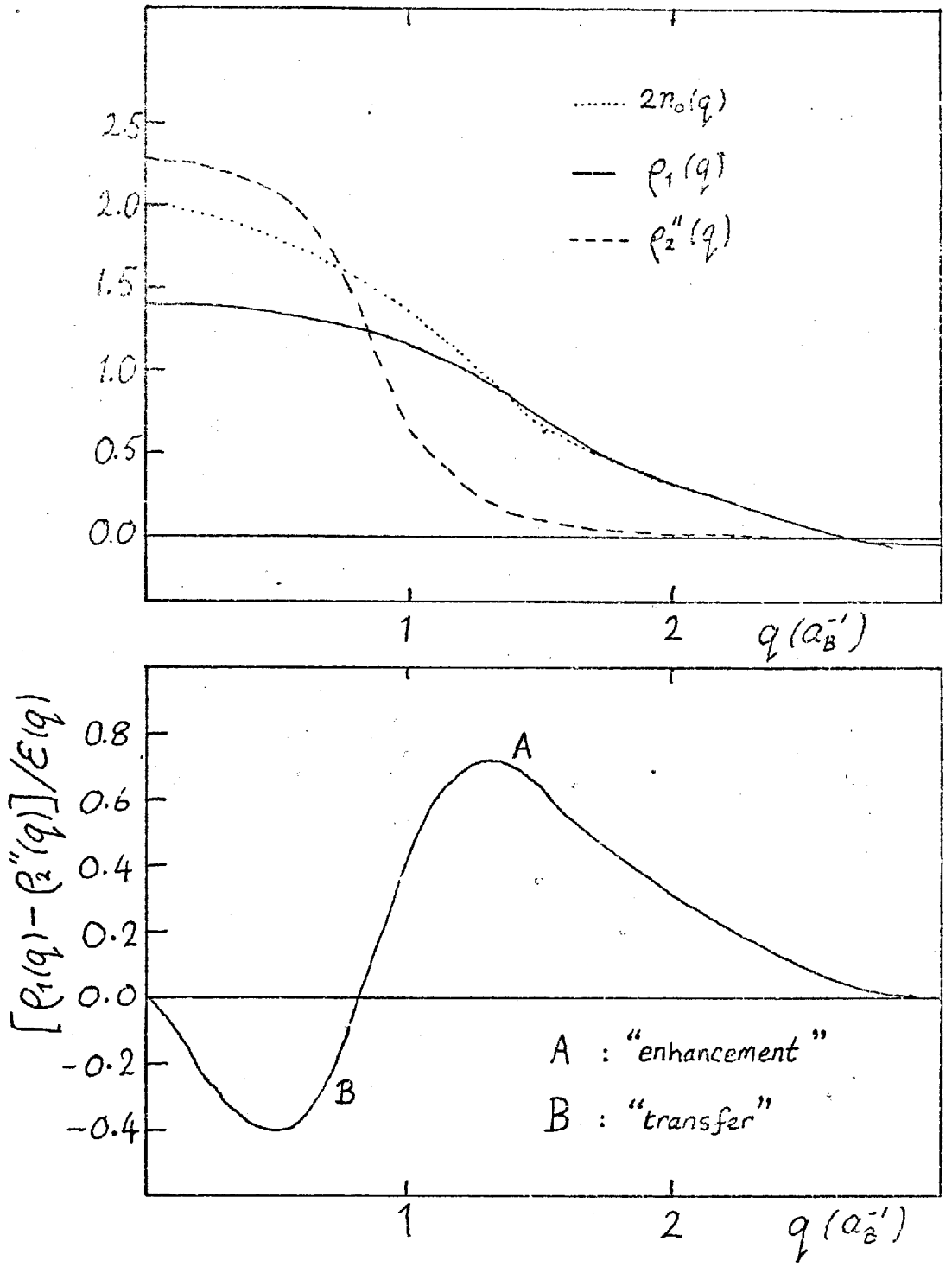

Figure 3.2 Some characteristic charge densities.
(Extracted from computations, taken to self-consistency, on the system Na P.)

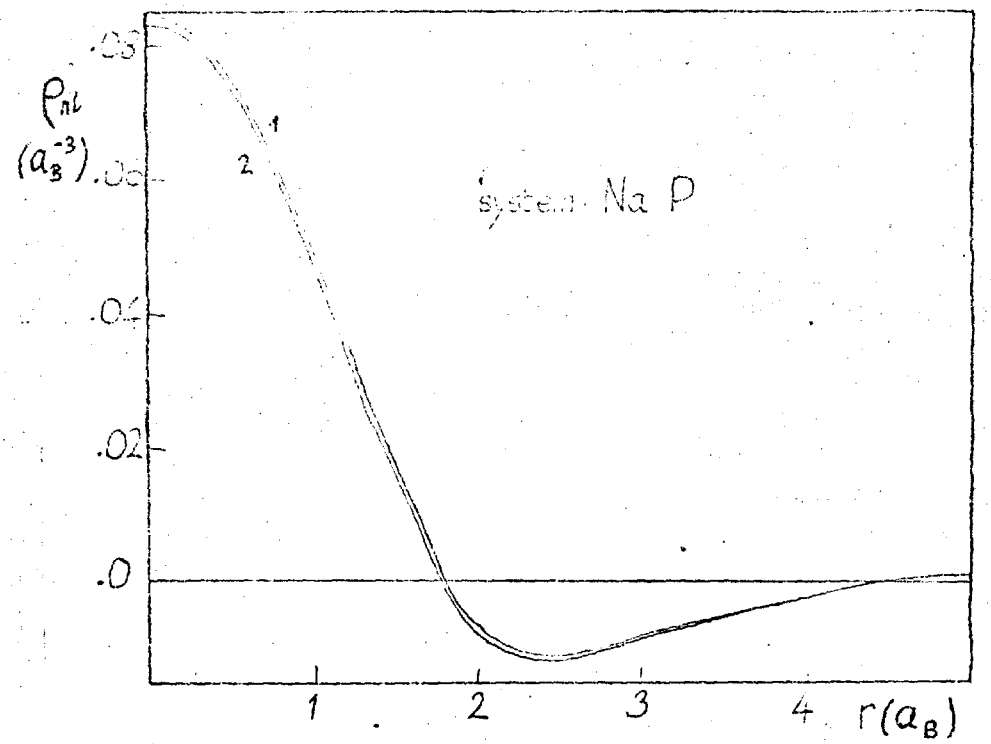

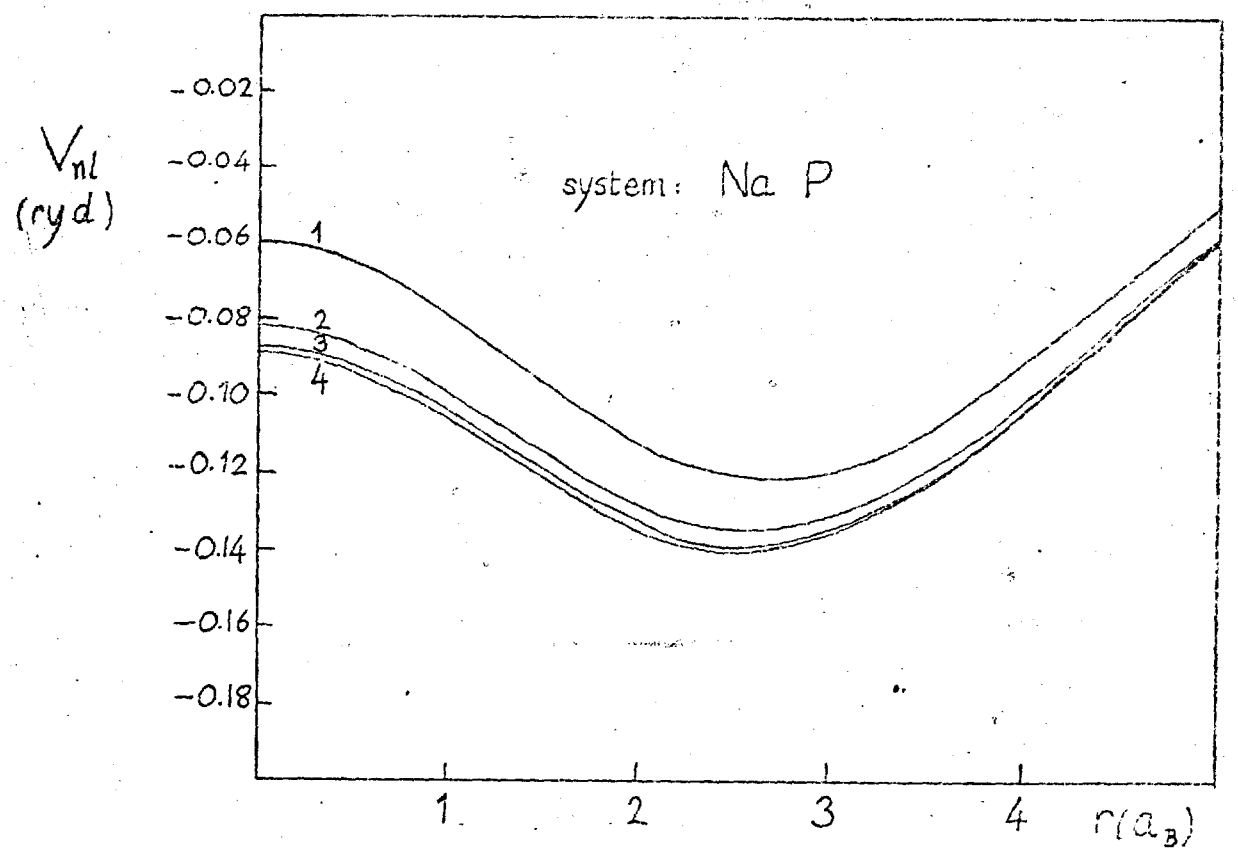

Figure 3.1 Approach to self-consistency of

(a) ρ_{nl}

(b) V_{nl}

in the iterative scheme (3.6), (3.7).

Curves 1,2,3... give the results of

successive iterations.

becomes more attractive, both density enhancement on the impurity and transfer of charge from the impurity cell become stronger. Because of the effect of G(q), the charge transfer has the greater effect on the screened potential. Thus $V_{n\ell}$ becomes more attractive still. We see that after 5 iterations, complete self-consistency has not been obtained. However, the iterative behaviour is then sufficiently well established for extrapolation to be reliable.

The self-consistent scheme has been applied to the systems listed in Table 3.1. This list has been compiled so as to include systems which should be modelled well by the scheme (e.g. Mg Si) as well as systems which will indicate the behaviour of the scheme as the model parameters are varied.

We are now in a position to confirm our assertion in §2.2 that $\mathcal{V}_2$ is not a weak potential for band electrons. We compare $V^s(k_F)$ as computed in our scheme with $\langle k_F|\mathcal{V}_1|k_F\rangle$ (where $\mathcal{V}$ is just V^s) in Table 3.2. It follows from these numbers, that while $\mathcal{V}_2$ is weaker than V^s for Fermi surface electrons, it cannot be regarded as negligibly small.

Table 3.1

Model parameters of the systems studied.

Host	Impurity	Z^i-Z^o	A_o	R_M	r_s
Na	P	4	-5.67	2	3.93
Na	Aℓ	2	-2.57	2	3.93
Mg	Aℓ	1	-1.41	2	2.65
Mg	Si	2	-2.84	2	2.65

Table 3.2

System	$V^s(k_F)$	$\langle k_F \mid \mathcal{V}_i \mid k_F \rangle$
Na P	280	106
Na Al	141	64
Mg Al	45	11
Mg Si	89	46

CHAPTER 4

RESULTS AND FURTHER DEVELOPMENTS

§4.1 Screening Charge

The screening charge densities computed in the present scheme for the systems listed in Table 3.7 are given in Fig. 4.1.

The form of $\rho_{\ell in}(r)$ first requires some comment. Since our model U(q) (3.20) has a shorter range than the Coulomb potential with the corresponding large r behaviour, $\rho_{\ell in}(r)$ has a longer range than the charge density induced by the corresponding Coulomb potential. No attempt has been made to compute the long range Friedel oscillations in $\rho_{\ell in}(r)$; instead we have concentrated on the charge density within the Wigner-Seitz cell of the impurity. Even with these restrictions, however, typically 99% of the charge contained $\rho_{\ell in}(r)$ is present in the region $r < 1.5\ r_s$.

For each system, $\rho_{n\ell}(r)$ is positive at the impurity and negative immediately outside the impurity core. The ratio $\rho_{n\ell}(r=0)/\rho_{\ell in}(r=0)$ is greatest for the largest values of $Z^i - Z^o$, and at constant $Z^i - Z^o$ is greater for the system with larger r_s. The negative region of $\rho_{n\ell}(r)$ is most substantial for large $Z^i - Z^o$ and small r_s.

We also compare the total screening charge density $\rho_{\ell in} + \rho_{n\ell}$ with n_o, the charge density of an electron in the bound state of the self-consistently screened potential V^s.

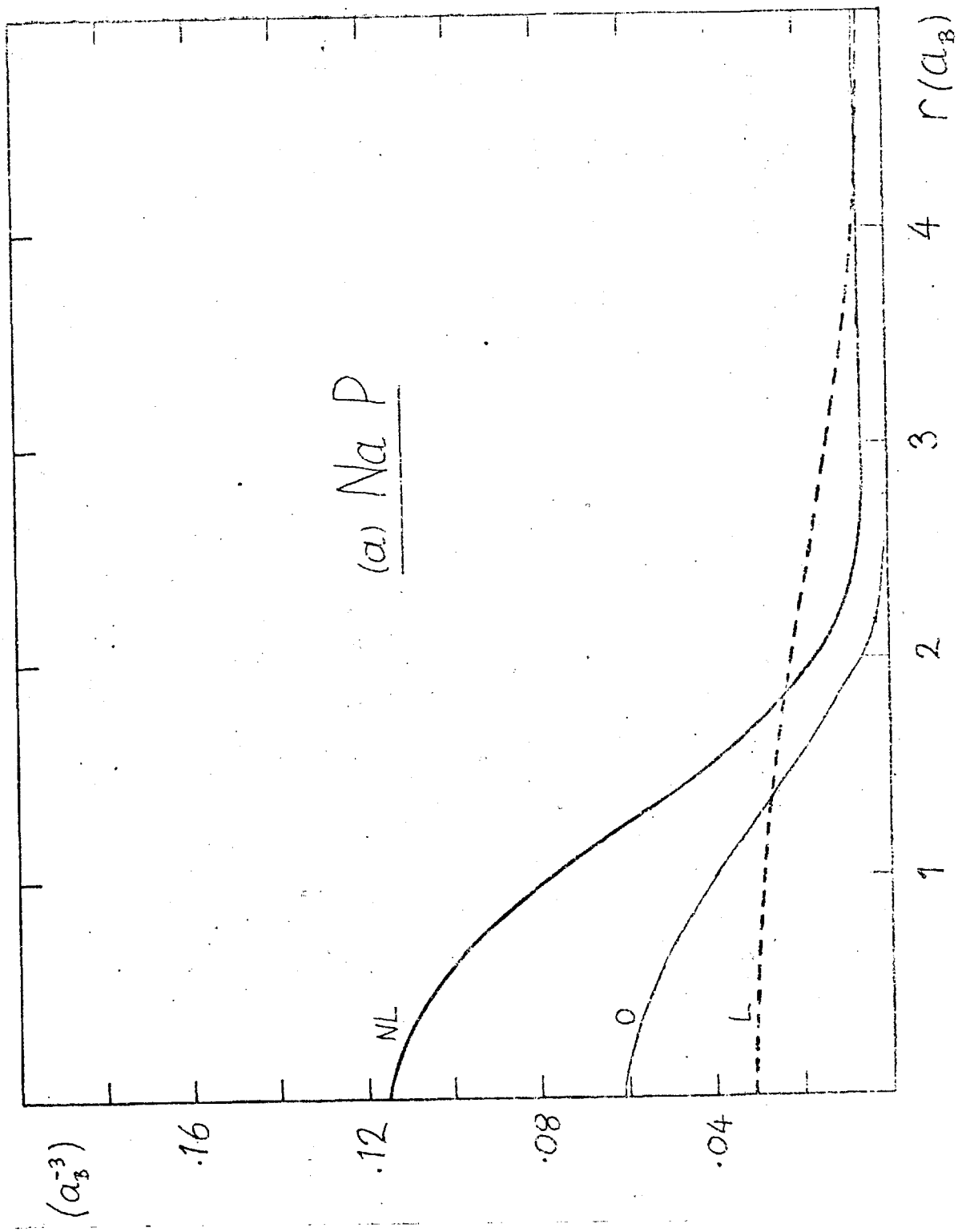

Figure 4.1 (a)-(d) Electron densities in linear and non-linear screening theory.

Curve L : $\rho_0 + \rho_{lin}$

Curve NL : $\rho_0 + \rho_{lin} + \rho_{nl}$

Curve 0 : n_0

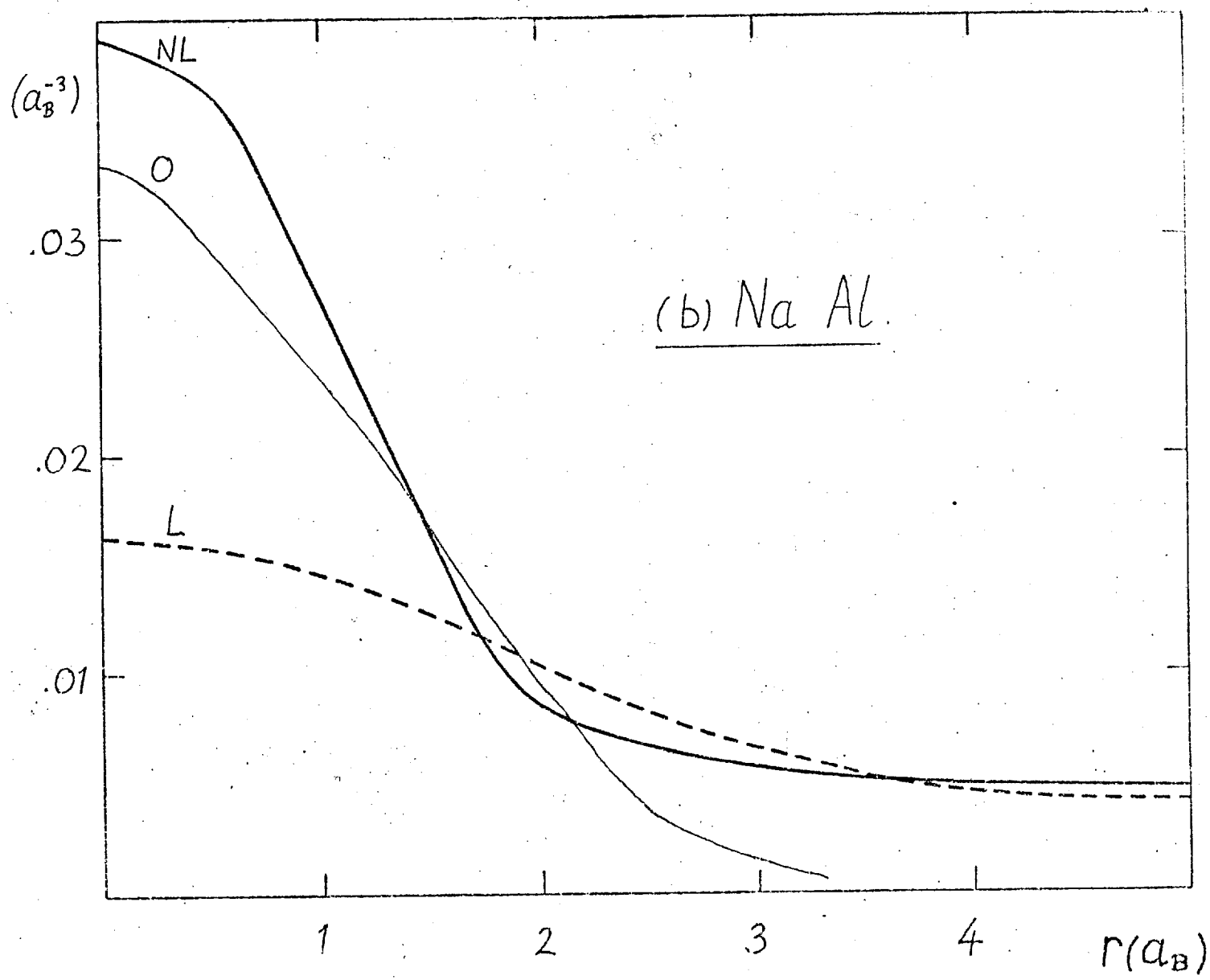
NL
O
L
(a_B^{-3})
.03
.02
.01
1
2
3
4
$r(a_B)$
(b) Na Al.

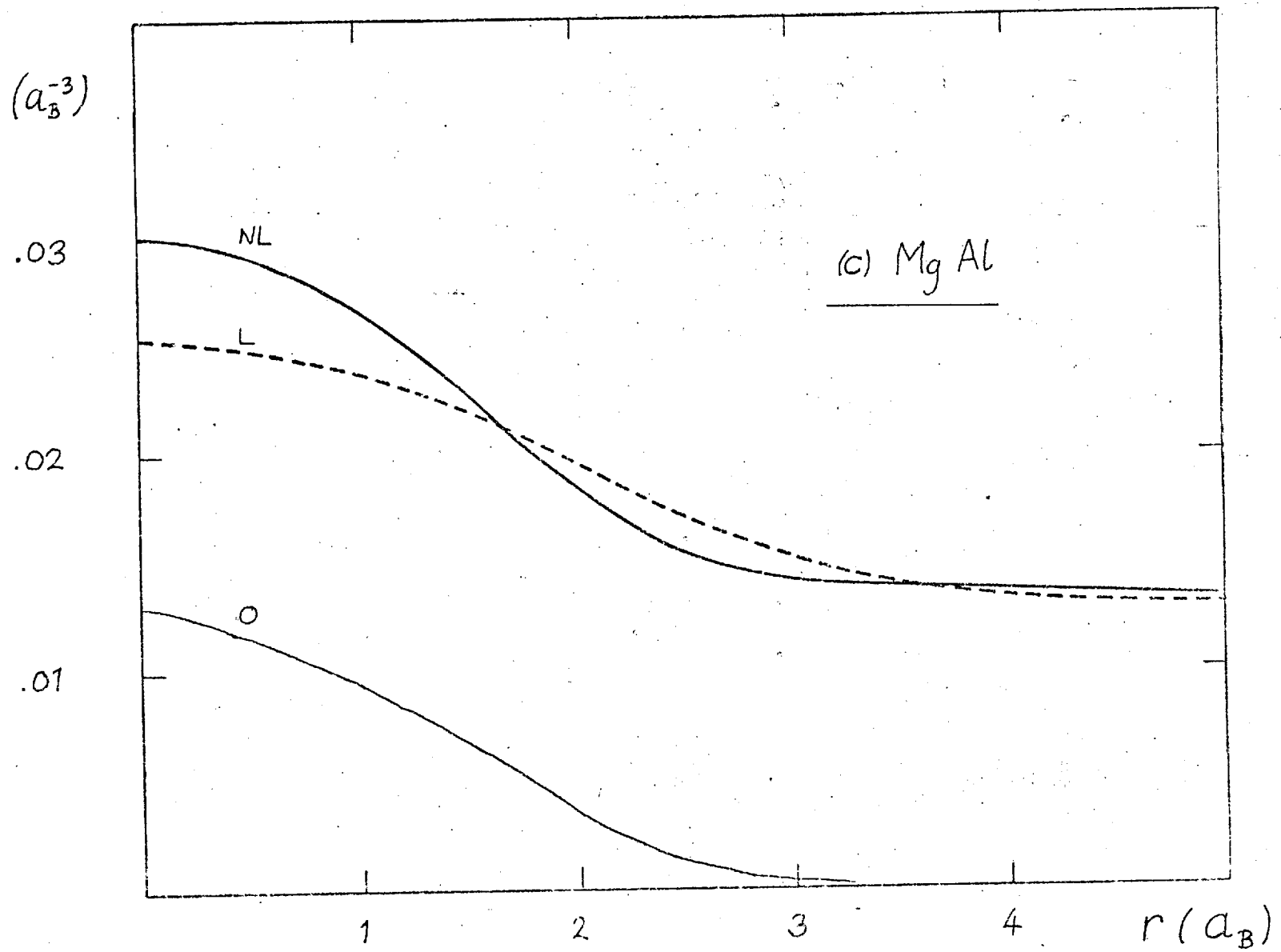
(a_B^{-3})
.03
.02
.01
NL
L
O
(c) Mg Al
1
2
3
4
$r(a_B)$

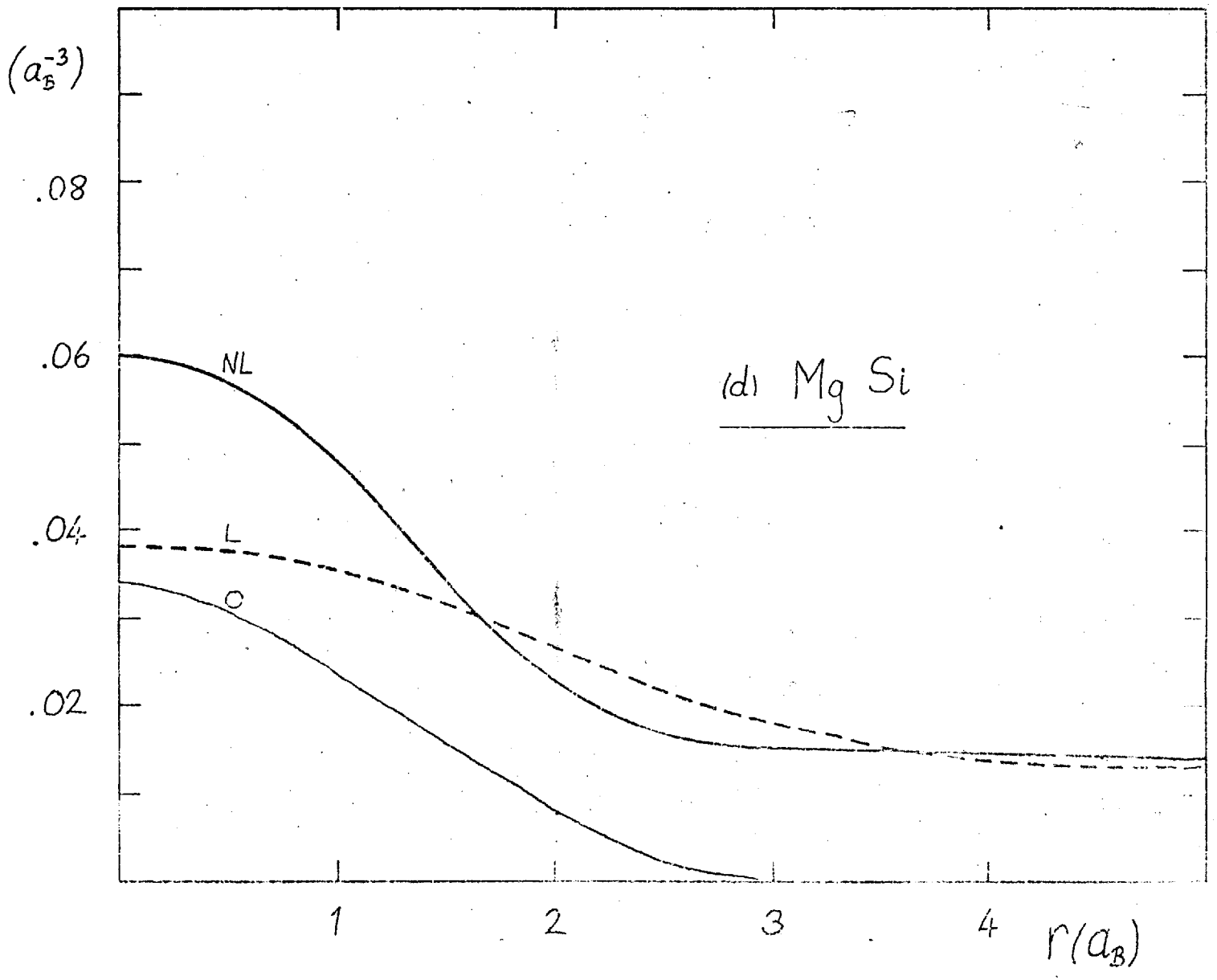
(a_B^{-3})
.08
.06
.04
.02
NL
L
C
(d) Mg Si
1
2
3
4
$r(a_B)$

Within the core region, $\rho_{\ell in} + \rho_{n\ell}$ does not exceed $2n_o$ even in the extreme hypothetical case of the system Na P. Furthermore, the range of n_o corresponds approximately to that of that of the short range peak in $\rho_{\ell in} + \rho_{n\ell}$. Thus, the numerical results are in accord with our hypothesis of a doubly-degenerate bound state making a substantial contribution to the screening charge density, and our discovery that this bound state has the effect of repelling electrons which are not bound.

In the system Mg Aℓ, which has the weakest impurity potential of those we have studied, the non-linear correction $\rho_{n\ell}$ is weakest. This prompts us to ask whether a system which has no bound state will have an appreciable non-linear correction to the charge density. A negative answer seems likely, but in §4.5 a method of calculation, similar to the present one, is proposed for such a system.

Another vital point in the interpretation of $\rho_{n\ell}(r)$ is to recall that it is calculated from a pseudopotential. Consequently, the wavefunction $\langle r|\psi\rangle$ which enters our discussion has none of the nodes which the actual bound state wavefunction (say, a 4s state) would have in an impurity system. $\rho_{n\ell}$ therefore lacks structure in the core region. Such structure may have an appreciable effect in a real system, probably giving rise to less charge in the core region than our model predicts.

The overall structure of our non-linear charge density is similar to that obtained in the non-linear theory of

Sjölander and Stott[14] in that $\rho_{n\ell}$ represents an accumulation of screening charge on the impurity. However, unlike their scheme, which behaves very strangely when applied to attractive impurity potentials, our scheme behaves in a comprehensible way even for the extremely attractive potential of P in Na.

§4.2 Charge Transfer

The problem of charge transfer in alloys is one of wide interest. We have therefore presented the effect of our non-linear correction on charge transfer in Table 4.1, where the number Q of electrons outside the Wigner-Seitz sphere of the impurity is given for each of the systems we have studied, both with and without the non-linear correction $\rho_{n\ell}$. These numbers have been obtained by integrating $\rho_{\ell in}(r)$ and $\rho_{n\ell}(r)$ outwards from the origin.

Table 4.1

Charge Transfers Q in the linear and non-linear theories.

System	Q_{linear}	$Q_{non-linear}$
Na P	1.19	2.11
Na Al	0.66	1.01
Mg Al	0.25	0.37
Mg Si	0.52	1.14

As we noted in §4.1, our model potential gives rise to a long range in $\rho_{\ell in}(r)$ and so Q is large even in linear screening theory. The non-linear correction leads to a still larger Q, the increase being most marked for large $Z^i - Z^o$

and small r_s. However, these results are critically dependent on the fine balance between the positive and negative regions of $\rho_{n\ell}(r)$, so that one cannot put too much reliance on the precise numerical values of Q. Nevertheless, $Q_{\text{non-linear}}$ does indicate an important physical effect- the repulsion of band electrons from an impurity arising from the formation of a bound state.

We have here a partial resolution of paradox. A theory of alloys which is based on linearly-screened ionic potentials leads to very small charge transfers[13], whereas a theory which constructs the alloy from renormalized atomic states[3] predicts substantially larger charge transfers. The latter theory seems to be confirmed by experiment. We suggest that the discrepancy is due to the failure of linear screening theory to treat the poles in the impurity-electron interaction, and the consequent inadequacy of a description of screening in terms of a simple RPA screening length.

§4.3 Screened Potentials and Bound States

The screened potentials and binding energies of the deepest s-states in these potentials are given in Fig. 4.2 for each of the systems in Table 3.1.

Since $\rho_{n\ell}$ only represents a redistribution of charge, $V_{n\ell}$ is weak. $V_{n\ell}$ is attractive throughout the impurity cell, and this is consistent with the transfer of charge out of the impurity cell represented by $\rho_{n\ell}$. We have already mentioned that the absence of structure in $V_{n\ell}(r)$ for small r is due to

the cut-off in k-space imposed by $(1-C(k))$. This effect should be most marked for small k_F, but because of the great range of the size of the structure in $\rho_{n\ell}(k)$, it has not proved possible to confirm this trend.

In all the systems we have studied $V_{n\ell}$ is much weaker than V^s throughout the core region of the impurity cell. Consequently, provided the binding energy of the bound state in the linearly screened potential U/ε is sufficiently large, this binding energy is not appreciably modified by $V_{n\ell}$. If, however, the binding energy in U/ε is small, the effect on the binding energy of $V_{n\ell}$ may be appreciable.

An important conclusion to be drawn from the present work is that, in metallic alloys, bound states, split off from the valence band, are likely. This is in accord with the self-consistent Hartree computations of Sjölander and Stott[14] who find bound states associated with a single point charge embedded in an electron gas with $r_s > 2$. However, the presence of states split off from the valence band is difficult to establish by experiment. Such states are often far removed from the Fermi energy and have little effect on transport and thermodynamic measurements. Only in optical experiments will they play a significant rôle, soft-X-ray emission spectra, for instance[30].

Soft-X-ray emission spectra arise from electronic transitions from valence states to core levels. In alloys, the transitions to core states on different types of site may be distinguished. The intensity of the spectrum reflects the

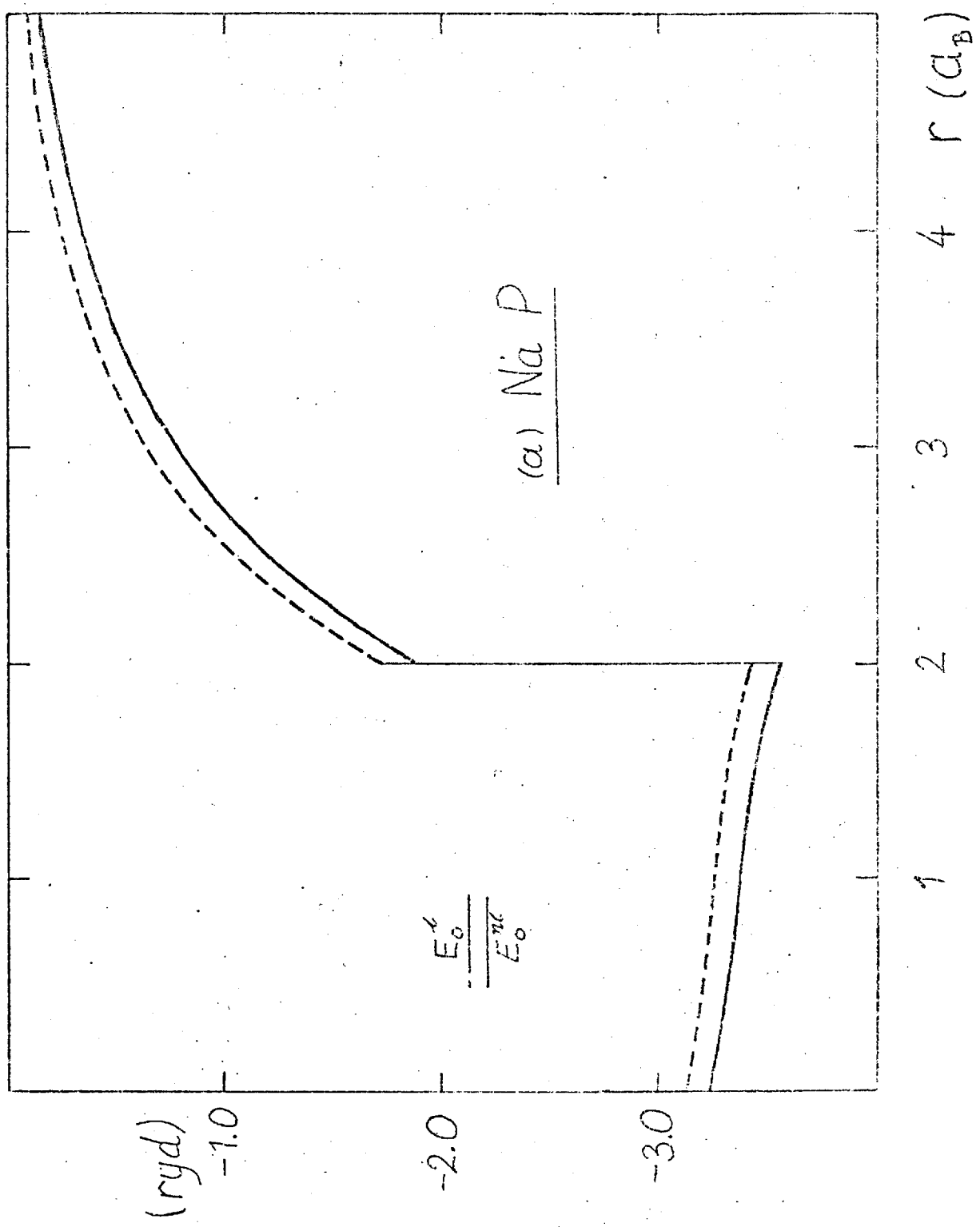

Figure 4.2 (a)-(d) Screened impurity potentials.

Dashed curve : $U + V_{lin}$ (linear screening theory).

Solid curve : $V = U + V_{lin} + V_{nl}$ (non-linear screening),

E_o' and E_o^{nl} are the energies of the deepest s-states in these two potentials respectively.

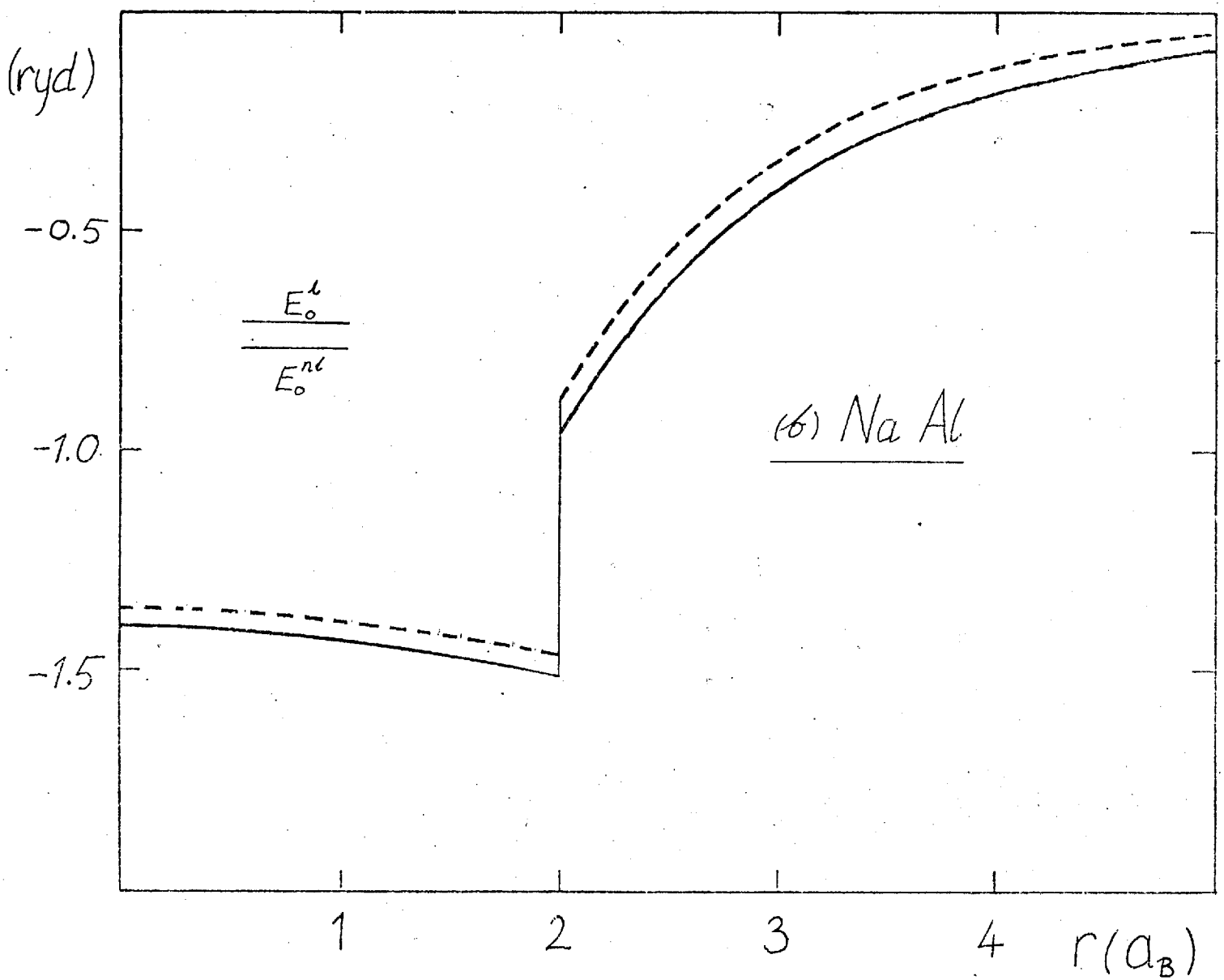
(ryd)
-0.5
-1.0
-1.5
$\frac{E_o^{\ell}}{E_o^{n\ell}}$
(6) Na Al
1
2
3
4
r(a_B)

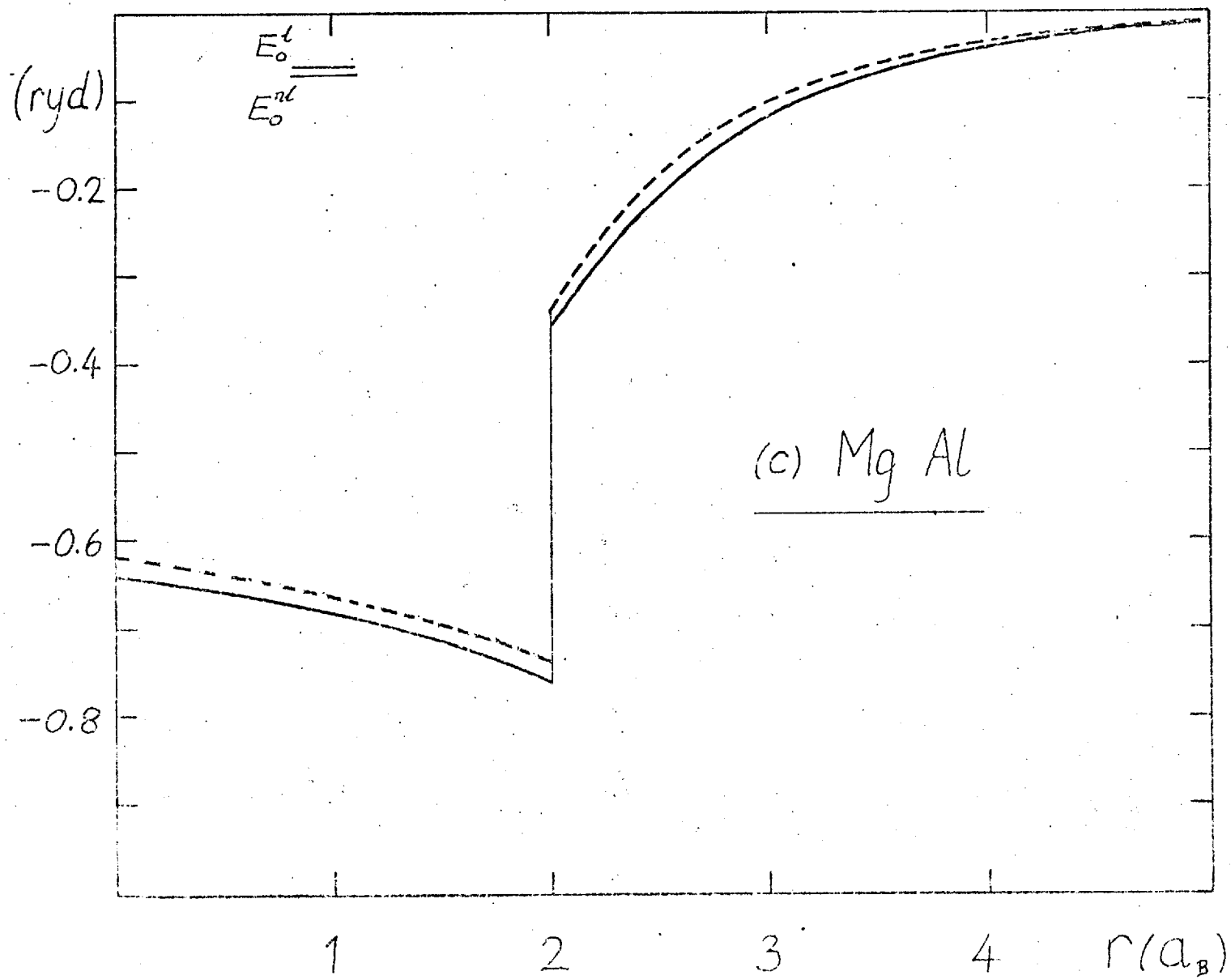
E_o^{ℓ}
$E_o^{n\ell}$
(ryd)
-0.2
-0.4
-0.6
-0.8
(c) Mg Al
1
2
3
4
r(a_B)

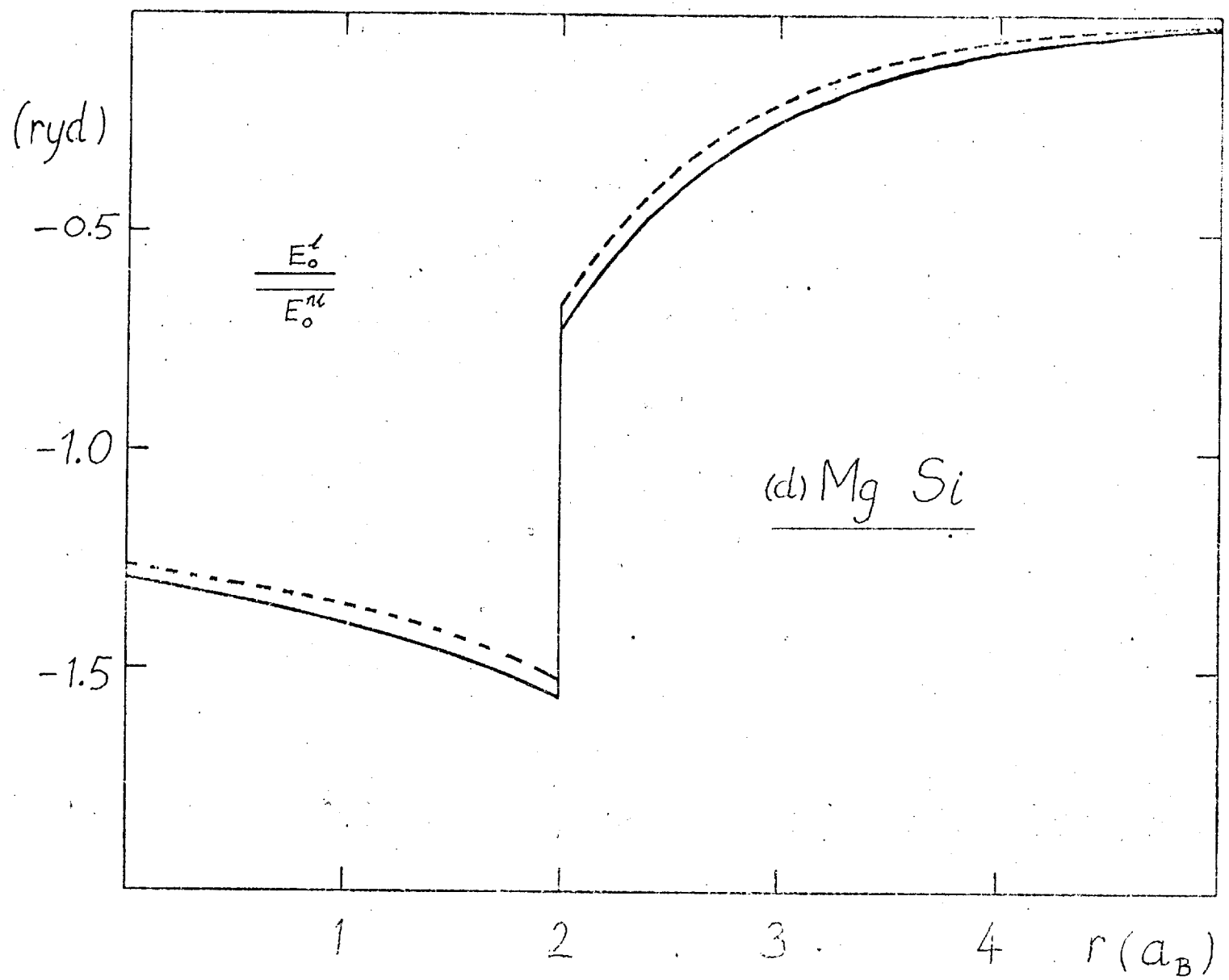
(ryd)
-0.5
-1.0
-1.5
$\frac{E_o^{\ell}}{E_o^{nl}}$
(d) Mg Si
1
2
3
4
r (a_B)

local density of valence states of the system at a particular type of site, modified by factors such as matrix elements coupling core and valence states. If a localized state below the valence band is present in a system, one therefore expects a peak in the spectrum below the peak due to the valence band itself.

Experiments on dilute alloys are difficult because the solvent spectrum is modified little by the solute, whereas the spectrum on solute sites is very weak. Experiments on concentrated alloys have been performed, and in these there is evidence of bound states below the valence band: the spectrum on the sites of higher valence has a split-off peak. An example is given in Fig. 4.3.

To interpret such spectra, we make the following assumptions:

(1) The peak at the lower end of the solute spectrum is due to a bound state, the broadening being due to matrix element effects etc.

(2) The upper part of the spectrum is due to the free-electron band of the solvent valence electrons.

(3) The top of the spectrum corresponds to the Fermi level.

We can now estimate the binding energies of the supposed bound states. For a Mg Al alloy[31] we obtain $E_o \approx -0.5$ev and, for Mg Si[32], $E_o \approx -3$ev. These numbers are not inconsistent with our self-consistent calculations, since non-linear screening is likely to be modified in concentrated alloys.

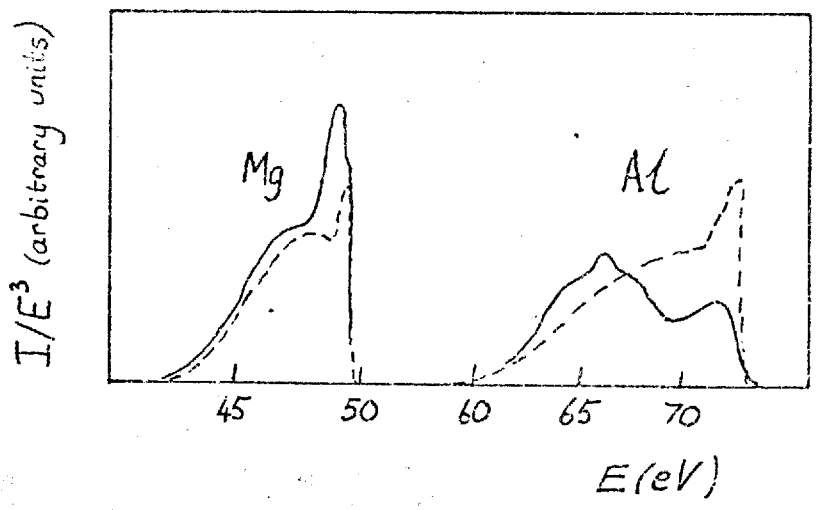

Figure 4.3 $L_{2,3}$-emission spectra on magnesium and aluminium in the pure metals (solid curve) and in the alloy $Al_{12}Mg_{17}$ (dashed curve). (Data taken from reference 31.)

Perhaps better accord with experiment might be obtained via Jacobs's[33] calculations of soft-X-ray spectra of Aℓ alloys, which are in good agreement with the spectra of Appleton and Curry[31]. Jacobs models the alloys by arrays of square wells of different depths, so that by choosing appropriate well depths on the basis of our calculations, it should be possible to investigate the effect on soft-X-ray spectra of our non-linear screening corrections.

Finally, we remark that it may be possible to infer the presence of corrections such as $V_{n\ell}$ via calculations involving the use of screened pseudopotentials, calculations of cohesive energies, for example. However, all experimental checks of the present theory rely on the precise form of the pseudopotential, so a more sophisticated choice of pseudopotential than that employed here would be necessary.

§4.4 Diagrammatic Arguments

In the theory we have described, we have used perturbation theory to calculate charge densities and then completed the solution to the problem by a self-consistent field argument. It is instructive to see which of the terms of the correct many-body perturbation series this procedure generates. This will give us some idea of the deficiencies of our theory and suggest some remedies.

We make two initial assumptions about our scheme (3.5).

1. That the treatment of electron correlations in the absence of the impurity is exact.

2. That our approximate t-matrix, calculated using U_1 is also exact.

(3.6) and (3.7) then generate the diagrammatic terms shown in Fig. 4.4 which uses the notation of Chapter 1. We call this series for V^s, Series A. The complete many-body perturbation theory treatment which was introduced in Chapter 1 gives a well-known series for V^s which we call Series B.

We begin by noting that B includes diagrams which do not appear in A. For example, A only includes "tree-diagrams", that is diagrams which can be split up by cutting a single renormalized interaction γ. Thus (a) of Fig. 4.5 is excluded. Also excluded from A are diagrams (b) and (c) of Fig. 4.5. We may regard all these excluded diagrams as being corrections due to exchange and correlation of the series shown in Fig. 4.6. Since the latter series represents the contribution of a bound state to a screening charge density, we conclude that the excluded terms are a consequence of neglecting exchange and correlation between bound electrons. In principle, this could be remedied by using a more sophisticated separable potential (2.10) in which the positions of the poles were determined by a treatment which included exchange (the atomic Hartree-Fock method, for example). In the light of the remarks following (2.10), this would be very difficult in practice.

The next point to note is that Series A does not include any diagram of Series B more than once, i.e. Series A

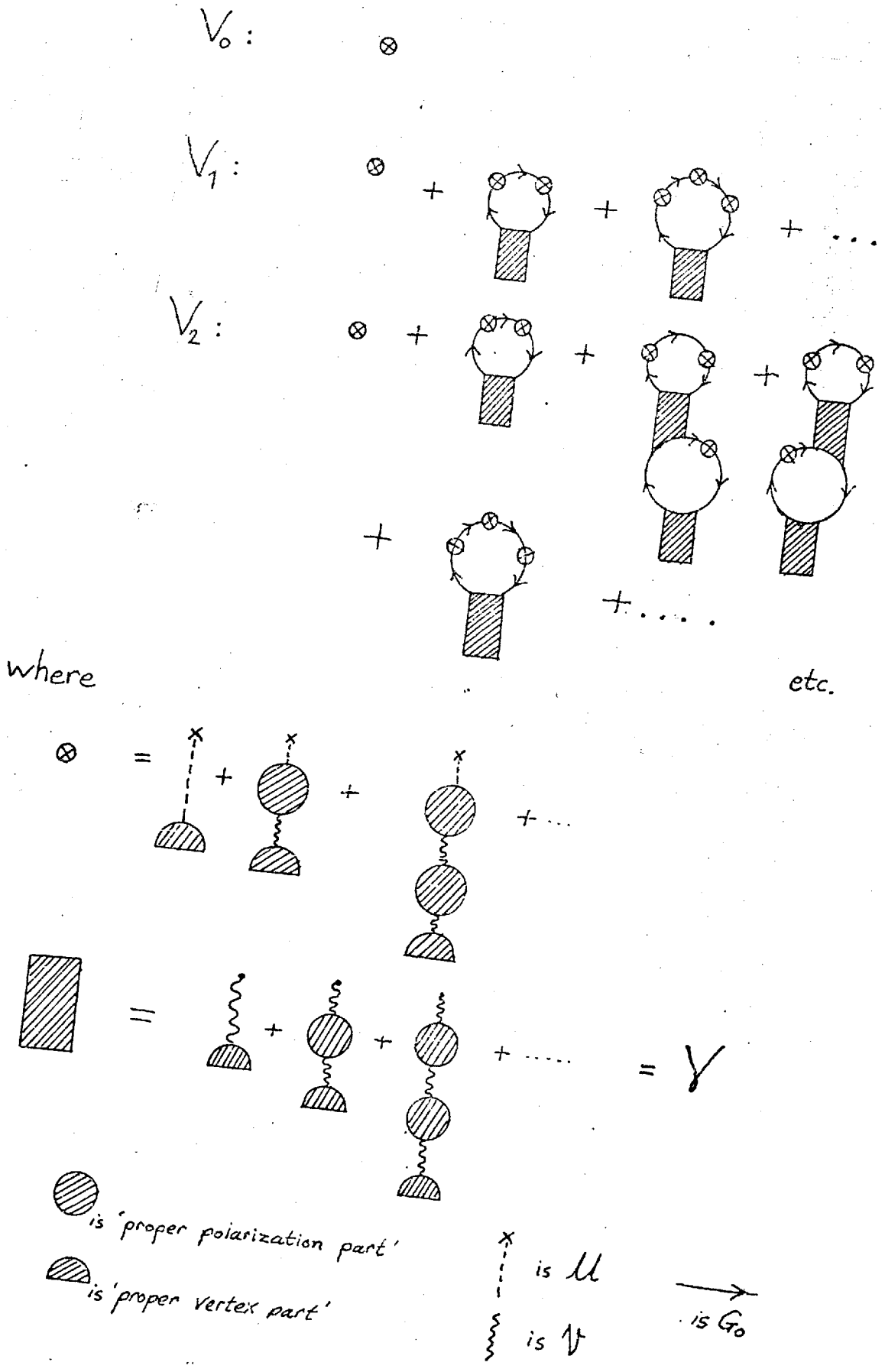

Figure 4.4 Generation of Series A for V.

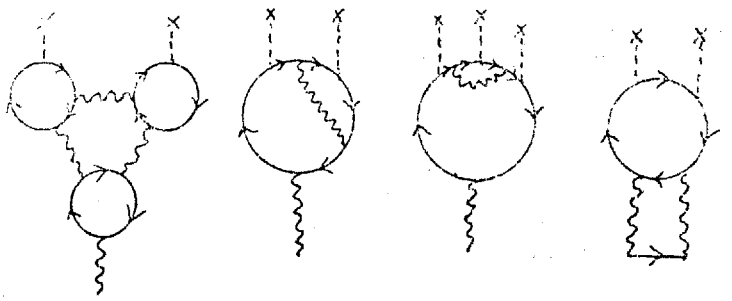

Figure 4.5 Some terms of Series B which Series A does not reproduce.

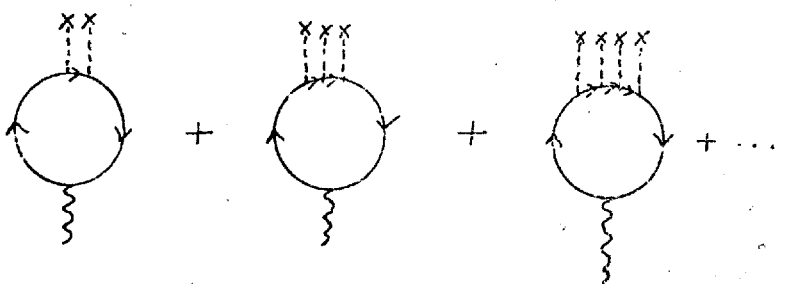

Figure 4.6

does not "overcount". This is consequence of Series A only including "tree diagrams", because of the iterative way it is generated.

Finally, we comment on the two assumptions we made at the start of this discussion. The assumption that γ has been calculated exactly is satisfactory when it couples free electrons since the theory of Singwi *et al.*[13] is well tested. However, in Series A, γ may couple states of free character with bound states, a situation which the theory of Singwi *et al.* was not set up to handle. The assumption may only be justified if a more sophisticated scheme, such as (2.58), is employed. The assumption that the t-matrix of U_1 is exactly the t-matrix of U is also not really justifiable. This defect of the theory may be remedied by using the more sophisticated separable potential (2.10), but we have seen that such a remedy involves considerable difficulty.

§4.5 Other Potentials

Although the theory we have presented so far is applicable only to impurity potentials which have a self-consistent bound state, it is readily modified to take account, not only of weaker attractive potentials, but also of repulsive potentials. We outline here how this may be accomplished.

Given a weak attractive impurity potential or a repulsive impurity potential U, we define a constant β such that the potential βU has at least one bound state $|\psi(\beta)\rangle$ with energy $E_o(\beta)$.

$$(H_0 + \beta U)|\psi(\beta)\rangle = E_0(\beta)|\psi(\beta)\rangle. \tag{4.1}$$

For a weak attractive potential $\beta > 1$, whilst for a repulsive potential $\beta < 0$. The fictitious state $|\psi(\beta)\rangle$ permits a separation of U analogous to (2.3).

$$\begin{aligned} U &= U_1 + U_2 \\ U_1 &= \frac{U|\psi(\beta)\rangle\langle\psi(\beta)|U}{\langle\psi(\beta)|U|\psi(\beta)\rangle} \\ U_2 &= U - U_1 \end{aligned} \tag{4.2}$$

U_1 and U_2 have similar properties to U_1 and U_2 of Chapter 2, and we treat them in a similar way, using a theory which is linear in U_2, but summing the t-matrix perturbation series for U_1 thus:

$$T_1 = \frac{U|\psi(\beta)\rangle\langle\psi(\beta)|U}{\langle\psi(\beta)|U|\psi(\beta)\rangle - \langle\psi(\beta)|UG_0U|\psi(\beta)\rangle} \tag{4.3}$$

Using an identity analogous to (2.20), the denominator of (4.3) reduces to

$$\frac{1}{\beta}\langle\psi(\beta)|UG_0|\psi(\beta)\rangle\left\{E - E_0(\beta) + (\beta-1)\frac{\langle\psi(\beta)|U|\psi(\beta)\rangle}{\langle\psi(\beta)|UG_0|\psi(\beta)\rangle}\right\}$$

(4.4)

Since U has no bound state, we expect $T_1(E)$ to have no pole

for $E < 0$, although this may only be true for certain values of β. We also know from our previous analysis that $\langle\psi(\beta)|U\,G_o|\psi(\beta)\rangle$ will have a finite imaginary part in the band region $E > 0$. Consequently, $T_1(E)$ has no poles on the real E axis, where it may be written

$$T_1(E) = U|\psi(\beta)\rangle\langle\psi(\beta)|U\;\tilde{T}(E) \qquad (4.5)$$

$\tilde{T}(E)$ is a complex function of E, non-singular for real E and which may be computed in practice just as $D_r(E)$ and $D_\ell(E)$ of Chapter 2. In place of (2.37) we now have a corresponding expression with the factor in curly braces replaced by

$$\frac{\tilde{T}_+(\varepsilon_{\underline{k}})f(\varepsilon_{\underline{k}}) - \tilde{T}_+(\varepsilon_{\underline{k}+\underline{q}})f(\varepsilon_{\underline{k}+\underline{q}})}{\varepsilon_{\underline{k}} - \varepsilon_{\underline{k}+\underline{q}}}$$

$$+ \frac{1}{\pi}\int_{-\infty}^{E_F} dE\;\tilde{T}_i(E)(E-\varepsilon_{\underline{k}})^{-1}(E-\varepsilon_{\underline{k}+\underline{q}})^{-1} \qquad (4.6)$$

The second term of (4.6) can be written

$$\frac{1}{\pi}\;\frac{\tilde{\mathcal{S}}(\varepsilon_{\underline{k}}) - \tilde{\mathcal{S}}(\varepsilon_{\underline{k}+\underline{q}})}{\varepsilon_{\underline{k}} - \varepsilon_{\underline{k}+\underline{q}}} \qquad (4.7)$$

where $$\tilde{\mathcal{S}}(\epsilon) = \mathcal{P}\int_{-\infty}^{E_F} \frac{\tilde{T}_i(E)}{E-\epsilon}\,dE\,.$$

Consequently, the integrals to be performed in order to obtain $\rho_1(q)$ take exactly the same form as integrals which we have evaluated in Chapter 3. The numerical complexity of

such a calculation would be comparable with that of Chapter 3, but there would be the added complication of confirming that the results were essentially independent of the precise value of β chosen.

§4.6 Summary

We have assessed the effects on impurity screening in metals of the possible formation of bound states. To achieve this, multiple scattering of electrons from the impurity has been studied. Simple models of the impurity potential and the metallic electron gas have been employed, and we have found that, compared with a corresponding theory which neglects these effects:

1. There is a large enhancement of charge density on the impurity.
2. The charge transferred out of the impurity Wigner-Seitz cell is increased.
3. The screened potential is more attractive throughout the impurity cell.

The effect differs from one system to another only in a quantitative way.

Whilst the computations necessary for the self-consistent scheme are tedious, the scheme is applicable to more realistic models and to other systems with little increase in difficulty. The scheme provides a link between the screened pseudopotential and atomic-state viewpoints of the electronic structure of alloys.

CHAPTER 5

ZERO-GAP SEMICONDUCTORS

§5.1 Introduction

A number of materials which crystallize in the diamond or zinc-blende structures have transport and optical properties which are best explained by a model of the band structure which was first proposed by Groves and Paul[34] for grey tin, α-Sn. The model, which has since been applied to Hg Te, Hg S, Hg Se, $Cd_3 As_2$ as well as a number of ternary alloys[35], is characterized by having valence and conduction bands which are degenerate at the Fermi level and in the centre of the Brillouin zone. The two valence and two conduction band states at the zone centre all belong to the same irreducible representation of the group of the wavevector (Γ_8^+ for diamond and Γ_8 for the zinc-blende structure). The degeneracy is thus a direct consequence of the crystal symmetry and these materials are referred to as "symmetry-induced zero-gap semiconductors".

This degeneracy may be lifted only by breaking the crystalline symmetry (by applying a magnetic field or uniaxial stress for example). Such symmetry breaking is also expected in the transition to the excitonic insulator phase, first proposed by Mott[35] and examined in some detail by Sherrington and Kohn[37] with reference to zero-gap semiconductors. However, the conclusions which we reach in Chapter 6 on the effect of screening on the formation of donor levels in zero-gap semi-

conductors, suggest that the formation of excitons in these materials is unlikely. Indeed, no symmetry-breaking electronic transitions have been observed. The exciton problem is a difficult self-consistent one: the symmetry-breaking lifts the degeneracy, this modifies the dielectric function, and this in turn has an influence on exciton formation and the possibility of the excitonic phase. We shall therefore adopt the ideal zero-gap band structure in our discussions.

The band structure close to Γ_8^+ degeneracy of α-Sn is shown schematically in Fig. 5.1. For comparison, the corresponding part of the band structure of a typical diamond structure semiconductor, Si is given in Fig. 5.2. We see that the gapless nature of the α-Sn band structure is a consequence of the re-ordering of the Γ_7^- and Γ_8^+ levels in Si. The fact that the degeneracy in α-Sn lies exactly at the Fermi level for the pure material is also a consequence of this re-ordering.

Perhaps the most interesting consequence of the band structure of zero-gap materials is the distinctive dielectric and screening behaviour to which it leads, intermediate between that of a metal and asemiconductor. However, before discussing this behaviour in more detail, it is necessary to know the precise form of the band structure as well some properties of the states in the band. We shall present this information in the next section.

However, we first note another interesting property of these systems in which the band structure plays an important rôle: the formation of impurity states. Such states have

been inferred from recent magneto-transmission and magneto-resistance measurements[38]. In Hg Te, for example, acceptor states with activation energies of 2.2 meV and 0.7 meV have been detected via both types of experiment, but no donor states appear to be present. Because the acceptor states must be degenerate with band states, we can expect them to have a finite resonant width. Since the states are easily detected, the resonant widths must be small, but they have not been measured. It is the nature of these impurity states, the apparent absence of donor states, the activation energies and resonant widths, and the influence on all of these of screening which will concern us in Chapter 6.

§5.2 The Band Structure

In order to perform calculations on the screening properties of zero-gap semiconductors, it is necessary to specify some of the band structure and band states in a rather precise way. We introduce the band structure via the effective-mass formalism of Luttinger and Kohn[39] which we shall require for the study of impurity states in Chapter 6.

The effective-mass formalism is a method of studying the electronic states in a crystal to which a perturbing potential U is applied: it is particularly appropriate, therefore, to calculations on screening and impurity states. The aim of the method is to discover a representation in terms of states $|n,\underline{k})$, where n labels a band and $\underline{k}$ is a reduced wavevector, such that two conditions are satisfied for small

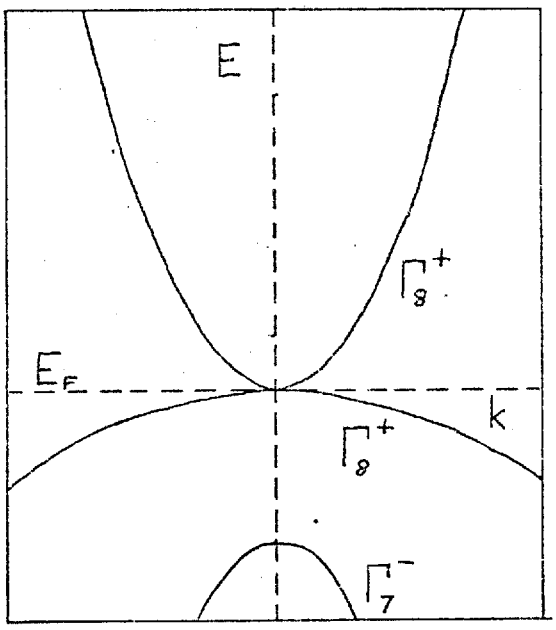

Figure 5.1 Schematic band structure of α-Sn close to the Fermi level E_F and the zone centre.

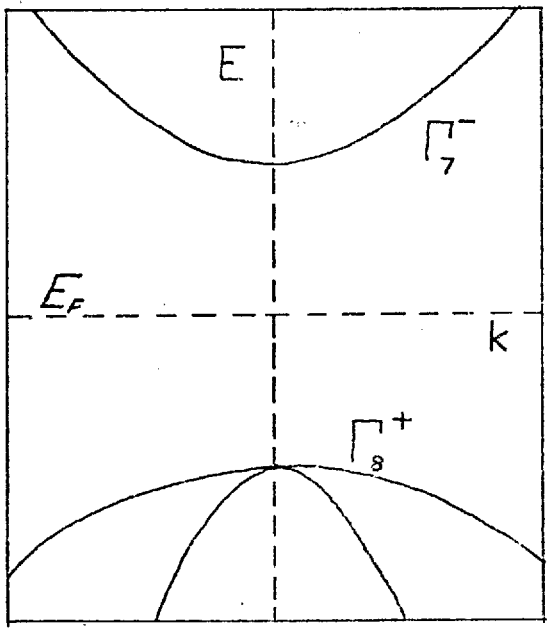

Figure 5.2 Schematic band structure of Si close to the Fermi level E_F and the zone centre.

$|k|$:

(a) U does not couple states in different bands; and

(b) the part H_o of the Hamiltonian describing the pure crystal is represented by

$$(n\underline{k}|H_o|n'\underline{k}') = \sum_{i,j} D_{ij}^{nn'} k_i k_j \qquad (5.1)$$

where k_i and k_j are Cartesian components of $\underline{k}$. $D_{ij}^{nn'}$ is known as the effective-mass tensor of the system and is obtained by using the $\underline{k}.\underline{p}$ perturbation method to second order in k.

In order to obtain a representation satisfying (a) and (b) several approximations are necessary. First, if $U(\underline{k})$ is a Fourier component of U, $\underline{k}$ is close to the centre of the Brillouin Zone and $\underline{K}$ is a reciprocal lattice vector, we require

$$U(\underline{k}+\underline{K}) \ll U(\underline{k}) \qquad (5.2)$$

Equivalently, U must be slowly varying in real space on the scale of the atomic cell size. This is a good approximation for an impurity potential except in the impurity cell itself. For this reason, considerable effort has been expended in studying the "central cell" corrections[2] which are particularly important for impurity s-states. However, we shall see that in zero-gap semiconductors the spatial extent of the impurity states is very large, so that the influence of

the impurity cell is small. The second major approximation involves dropping terms of order a^2/a_i^2, where a is the lattice spacing and a_i the spatial extent of the impurity state. Again this is an excellent approximation for a zero-gap semiconductor.

We now write down the matrix

$$D^{nn'} = \sum_{ij} D_{ij}^{nn'} k_i k_j' \tag{5.3}$$

describing the four $\Gamma_8^+(\Gamma_8)$ bands of a crystal of the diamond (zinc-blende) structure in the presence of spin-orbit interactions. The symmetry of the system implies that $D^{nn'}$ takes the form

$$D(\underline{k}) = \begin{bmatrix} \frac{1}{2}P & 0 & R & S \\ 0 & \frac{1}{2}P & -S^* & R^* \\ R^* & -S & \frac{1}{6}P+\frac{2}{3}Q & 0 \\ S^* & R & 0 & \frac{1}{6}P+\frac{2}{3}Q \end{bmatrix} \tag{5.4}$$

where

$$\begin{aligned} P &= 2Ak^2 + B(k_x^2 + k_y^2 - 2k_z^2) \\ Q &= Ak^2 - B(k_x^2 + k_y^2 - 2k_z^2) \\ R &= -\frac{N}{\sqrt{3}}(k_x - ik_y)k_z \\ S &= \frac{1}{2\sqrt{3}}\left[3B(k_x^2 - k_y^2) - 2iNk_xk_y\right] \end{aligned} \tag{5.5}$$

Thus, the band structure for small k is defined in terms of just three effective mass parameters A, B and N. In the absence of impurities, the band structure $E = E(\underline{k})$ is obtained

from the roots of

$$\det \left| D(\underline{k}) - E \right| = 0 \tag{5.6}$$

which gives us

$$\left\{ (Ak^2 - E)^2 - B^2 k^4 + C^2 (k_x^2 k_y^2 + k_y^2 k_z^2 + k_z^2 k_x^2) \right\}^2 = 0 \tag{5.7}$$

where $C^2 = 3B^2 - {}^1/_3 N^2$.

Now in α-Sn and other zero-gap semiconductors, the Γ_8^+ bands are almost exactly parabolic for small k. We therefore use the parabolic approximation

$$C^2 = 0 \tag{5.8}$$

in all that follows. We then have the two doubly-degenerate bands

$$E(\underline{k}) = (A \pm B) k^2 \tag{5.9}$$

It is convenient to define the alternative notation in terms of the effective masses m_c and m_v

$$m_c = \frac{\hbar^2}{2(A+B)}$$

$$m_v = \frac{\hbar^2}{2(B-A)} \tag{5.10}$$

It should be noted that alternative expressions to (5.4) in the approximation (5.8) exist in terms of the 4 x 4 angular momentum matrix for $J = {}^3/_2$ [40,41] and in terms of the 4 x 4

Dirac γ-matrices of spinor theory[42]. Whilst these are elegant and convenient for certain algebraic manipulations, (5.8) will prove quite adequate for our purposes.

Lastly we note the magnitudes of the effective-mass parameters in α-Sn:

$$A \approx 18.9 \frac{\hbar^2}{2m} \qquad m_c \approx m/40$$
$$B \approx 22.7 \frac{\hbar^2}{2m} \qquad m_v \approx m/4 \tag{5.11}$$

where m is the free-electron mass. These parameters have been obtained by many workers[43] from both optical and transport measurements. Some discrepancies exist between interband and intraband determinations of effective masses in zero-gap semiconductors[44], but the differences are too small to have any appreciable effect on the conclusions we reach here.

In α-Sn, as in all the zero-gap systems we have mentioned, m_v is much greater than m_c. In fact, the band structures of all these systems have a close quantitative similarity with each other, and all conclusions we reach regarding α-Sn apply at least qualitatively to the other systems.

§5.3 Dielectric Behaviour

The distinctive band structure of zero-gap semiconductors leads to many distinctive features in the dielectric function. These features have been reviewed by Broerman[45]. Here we shall mention some of the more important conclusions, and present numerical computations of one feature of the dielectric function which has not previously been published.

Almost all calculations of dielectric functions in zero-gap semiconductors have used the RPA. This is not a very good approximation when applied to an electron gas of very low density (see Chapter 1). In a zero-gap semiconductor, since the number of electrons close to the Fermi level and available for screening is small, we may expect the RPA to be deficient too. Some study of the corrections to RPA has been carried out[46] and it seems that the RPA results should be enhanced somewhat. However, these calculations are complicated and not definitive: we shall use the RPA throughout, assuming it to give the essential behaviour.

The dielectric function $\varepsilon(\underline{q},\omega)$ for a many band system with eigenstates $|n\underline{k}\rangle$ and eigenenergies $\varepsilon_{n\underline{k}}$ (n labels the band and $\underline{k}$ is the reduced wavevector) is given in the RPA[47] by the simple analogue of (1.6).

$$\mathcal{E}(\underline{q},\omega) = 1 - \lim_{\alpha\to 0} \frac{4\pi e^2}{\Omega q^2} \sum_{nn'\underline{k}} |\langle n\underline{k}|e^{-i\underline{q}\cdot\underline{r}}|n'\underline{k}+\underline{q}\rangle|^2 \frac{f(\mathcal{E}_{n'\underline{k}+\underline{q}}) - f(\mathcal{E}_{n\underline{k}})}{\mathcal{E}_{n'\underline{k}+\underline{q}} - \mathcal{E}_{n\underline{k}} - \hbar\omega - i\alpha} \qquad (5.12)$$

In the presence of deflects, (5.12) is modified by the replacement

$$\alpha \to \hbar \tau_{nn'}^{-1} \qquad (5.13)$$

where $\tau_{nn'}$ is the scattering lifetime between bands n and n'.

For a zero-gap semiconductor it proves convenient to split $\varepsilon(\underline{q},\omega)$ into four terms:

$$\mathcal{E} = 1 + \mathcal{E}_{intra} + \mathcal{E}_{inter} + \mathcal{E}_{inter}^{\Gamma_8} \qquad (5.14)$$

$\varepsilon_{inter}^{\Gamma_8}$ includes only interband terms ($n \neq n'$) involving the Γ_8 or Γ_8^+ states, ε_{inter} includes the remaining interband terms and ε_{intra} contains the remainder of ε, in particular the intraband terms ($n = n'$).

Now ε_{intra} vanishes at $T = 0$ in the pure material. At finite temperatures and in impure samples, ε_{intra} has the same type of behaviour as the intraband contribution to the dielectric function of an ordinary semiconductor. Similarly, ε_{inter} has no distinctive properties, being independent of q and ω for small q and ω. The interesting part is $\varepsilon_{inter}^{\Gamma_8}$:

$$\mathcal{E}_{inter}^{\Gamma_8} = \frac{-e^2}{\pi^2 q^2} \int d^3k \left| \langle v\underline{k} | e^{-i\underline{q}\cdot\underline{r}} | c\underline{k}+\underline{q} \rangle \right|^2 \frac{f(\mathcal{E}_{c\underline{k}+\underline{q}}) - f(\mathcal{E}_{v\underline{k}})}{\mathcal{E}_{c\underline{k}+\underline{q}} - \mathcal{E}_{v\underline{k}} - \hbar\omega - i\alpha}$$

$$+ \text{ conjugate expression with } v \rightleftarrows c \qquad (5.15)$$

where v and c refer to the valence and conduction bands. The states $|v\underline{k}\rangle$ and $|c\underline{k}\rangle$ are obtained as eigenvectors of the matrix (5.4), and in the parabolic approximation (5.8) the equality

$$\left| \langle v\underline{k} | e^{-i\underline{q}\cdot\underline{r}} | c\underline{k}+\underline{q} \rangle \right|^2 = \frac{3}{4k^2} \frac{|\underline{k}\times\underline{q}|^2}{|\underline{k}+\underline{q}|^2} \qquad (5.16)$$

is established[42].

Using this matrix element, the static T = 0, RPA dielectric function was computed by Liu and Brust[42]. For small q, this takes the form

$$\mathcal{E}(q) = \mathcal{E}_0\left(1 + \frac{\lambda}{q}\right) \tag{5.17}$$

This behaviour is intermediate between that of a typical semiconductor

$$\mathcal{E}(q) = \text{constant} \qquad (q \to 0) \tag{5.18}$$

and of a metal

$$\mathcal{E}(q) = \text{constant} + \frac{\kappa^2}{q^2} \qquad (q \to 0) \tag{5.19}$$

In other words, the screening of a potential in a zero-gap semiconductor is weaker than that in a metal: the singularity of the Coulomb potential at q = 0 remains when it is screened by (5.17). The screened Coulomb potential $v^s(\underline{r})$ then takes the form

$$v^s(\underline{r}) = -\frac{e^2}{\mathcal{E}_0 r} F(\lambda r) \tag{5.20}$$

where

$$F(x) = \cos x\left[1 - \frac{2}{\pi} Si(x)\right] + \frac{2}{\pi} \sin x\, Ci(x) \tag{5.21}$$

and Si(x) and Ci(x) are the sine and cosine integral functions.

In α-Sn, for example, the effect of the function F(x) is to halve the strength of the Coulomb potential at r = 150Å[42]. Because of this fact, it has been suggested that the function F(x) has little effect on the problem of impurity binding, but this is not so for our model calculations on impurity states in Chapter 6.

The work of Liu and Brust has been extended most notably by Broerman. He has shown[48] that the parabolic approximation (5.8) is not really justified, but that little modification of the result is required because of a fortuitous cancellation of the errors in (5.9) and (5.16). In addition, he has shown that at finite impurity concentrations and finite temperatures (when the chemical potential is moved away from the Γ_8 degeneracy), the singularity in $\varepsilon(q)$ (5.17) at $q = 0$ is removed[49]. In particular, he has calculated $\varepsilon_{inter}^{\Gamma_8}(q = 0)$ for finite temperatures at various doping and compensation levels. This is achieved by reducing (5.15) to a one dimensional integral. $\varepsilon_{inter}^{\Gamma_8}(q = 0)$ is finite at all finite temperatures, but peaks strongly when the chemical potential falls close to the degenerate Γ_8 levels.

In order to gain an understanding of the temperature dependence of screening and the formation of localized states, a finite temperature calculation of $\varepsilon_{inter}^{\Gamma_8}$ for $q \neq 0$ is required, again in the static limit. This calculation has been performed numerically in order to facilitate the discussion in Chapter 6. (5.15) is reduced to the two-dimensional integral:

$$\mathcal{E}_{inter}^{\Gamma_8}(q) = -\frac{3}{2\pi} e^2 q \alpha \xi(\alpha), \qquad (5.22)$$

where

$$\zeta(\alpha) = \int_0^\infty d\gamma \int_{-1}^{1} d\mu \; \frac{\gamma^2(1-\mu^2)}{\gamma^2+1+2\gamma\mu} \; \frac{\left[e^{(\gamma^2+1+2\gamma\mu)\frac{1}{\alpha}-x_0}+1\right]^{-1} - \left[e^{\gamma^2/\alpha - x_0}+1\right]}{(\gamma^2+1+2\gamma\mu)\frac{1}{\alpha} - \gamma^2/\alpha} ,$$

$$\tau = \frac{m_c}{m_v} , \qquad \alpha = \frac{2m_c k_B T}{\hbar^2 q^2} ,$$

$$\gamma = \frac{k}{q} , \qquad \cos\mu = \frac{\underline{k}\cdot\underline{q}}{kq} ,$$

$$x_0 = \frac{\mu_0(T)}{k_B T} \tag{5.23}$$

and $\mu_o(T)$ is the chemical potential. The approximate linear dependence of $\mu_o(T)$ on T which Broerman has established[49]

$$x_0 = -0.75 \ln \frac{m_c}{m_v} \tag{5.24}$$

has been employed, and the band parameters of α-Sn in the parabolic approximation have been used. The integration presents no numerical difficulties because the integrand is non-singular at finite temperatures. For the region $\gamma > \gamma'$ where

$$\gamma' \gg 1 , \tag{5.25}$$

we have the contribution

$$\int_{\gamma_1}^{\infty} d\gamma \int_{-1}^{1} d\mu \, (1-\mu^2) \frac{1}{\frac{\gamma^2}{\alpha}(\gamma-1)} \qquad (5.26)$$

to $\xi(\alpha)$.

Thus, in the region defined by (5.25), the integral may be performed exactly, thus avoiding the difficulty of the infinite range of the integral over γ.

The numerical results appear in Fig. 5.3. We find that $\varepsilon^{\Gamma_8}_{\text{inter}}(q)$ differs appreciably from the T = 0 result

$$\varepsilon^{\Gamma_8}_{\text{inter}}(q) = \varepsilon_0 \lambda q^{-1} \qquad (5.27)$$

only for

$$(m_c^{-1} + m_v^{-1}) \frac{\hbar^2 q^2}{2} \lesssim k_B T \,. \qquad (5.28)$$

The $q \to 0$ limit computed by Broerman[49] is reproduced in this calculation.

The effect on $\varepsilon(q)$ of magnetic fields and uniaxial stress has been studied extensively by Liu[50]: again the dielectric singularity (5.27) is removed. However, the shifts in energy levels induced by typical magnetic fields arfe small by comparison with $k_B T$ in a typical experiment. Consequently, finite temperatures and finite doping levels are likely to be the dominant effects removing the dielectric singularity in most real systems.

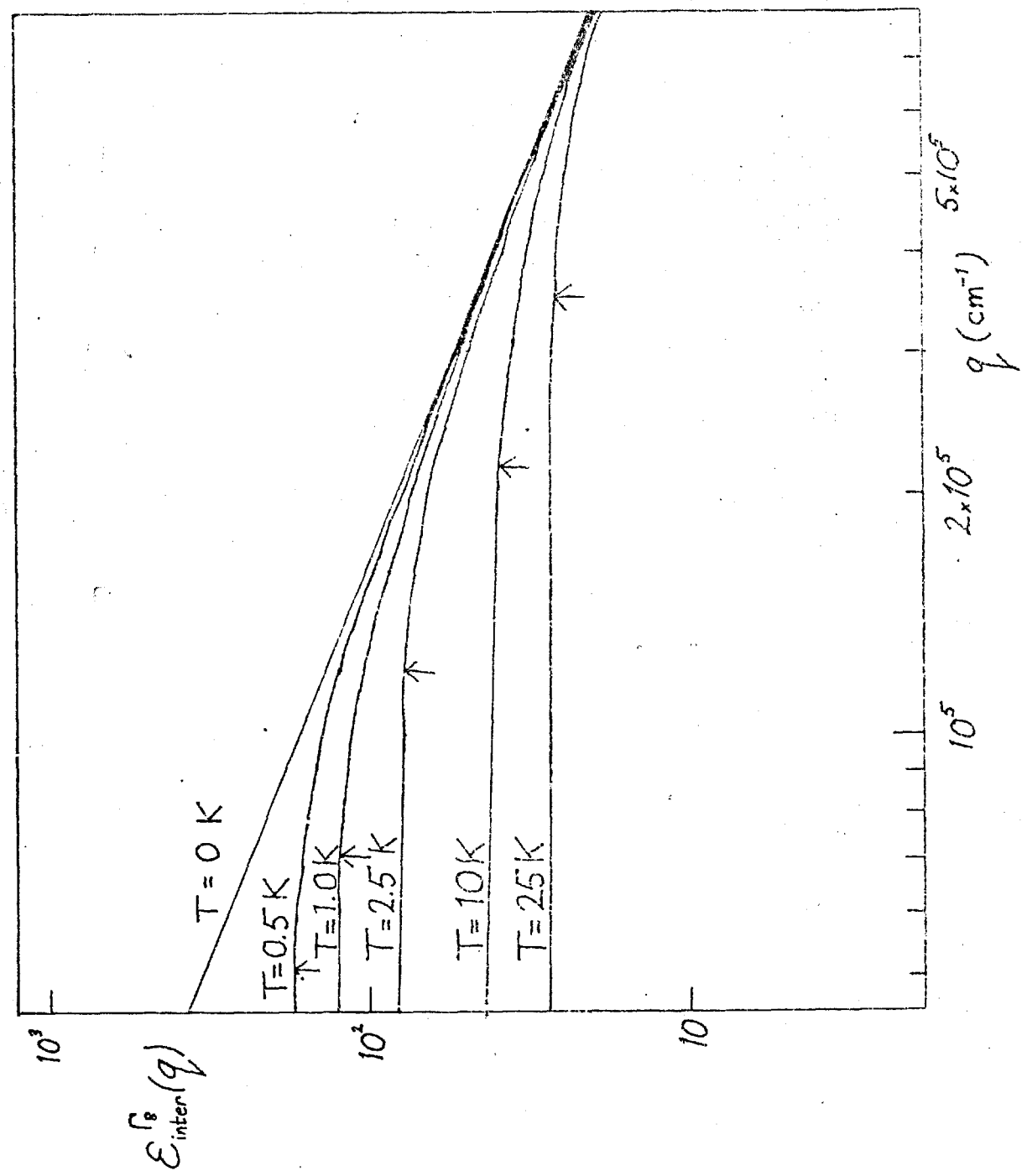

Figure 5.3 Finite temperature static interband dielectric function $\mathcal{E}^{\Gamma_8}_{inter}(q)$ calculated from (5.22). The T=0 limit is obtained from (5.27), and the ticks separate the regions defined by (5.28).

We also note that, at finite temperatures, a singularity of the form q^{-2} appears in the static dielectric function. This arises from the intraband term ε_{intra}.

Corresponding anomalies exist in the finite-frequency, zero-momentum-transfer dielectric function. The calculations of Sherrington and Kohn[51] have been extended to finite temperatures by Grynberg and others[52], and the results fitted to infrared reflectance spectra of Hg Te. This gives a relatively simple confirmation of the calculations. Unfortunately, no such simple test of the finite-momentum-transfer calculations is possible: whilst the dielectric singularities must affect the mobility of electrons[53], in practice the interpretation of experiments is complicated by non-parabolic effects and scattering from defects[48].

CHAPTER 6

IMPURITY STATES IN ZERO-GAP SEMICONDUCTORS

§6.1 Introduction

The discussion of impurity states in zero-gap semiconductors is difficult by virtue both of the characteristic band structure and the consequent characteristic screening behaviour. We begin, therefore, with a qualitative discussion which will illuminate our choice of model to describe such states.

If we introduce into a material with the band structure of Fig. 5.7 an impurity which is attractive to electrons, we expect a bound donor state to be formed beneath the conduction band. However, the general theory of impurity states[54] tells us that because the density of states of the system is finite in this region, the donor state will only be a quasi-localized resonant state with a finite resonant width. Similar arguments indicate that there are resonant acceptor states in the presence of appropriate impurities. A schematic density of states for a zero-gap semiconductor with both donor and acceptor states is shown in Fig. 6.1.

Supposing the donor states to be approximately Hydrogen-atom-like orbitals constructed from conduction band states, then the Bohr radius of the ground state is

$$r_0^{donor} = \frac{\mathcal{E}\hbar^2}{e^2 m_c} \qquad (6.1)$$

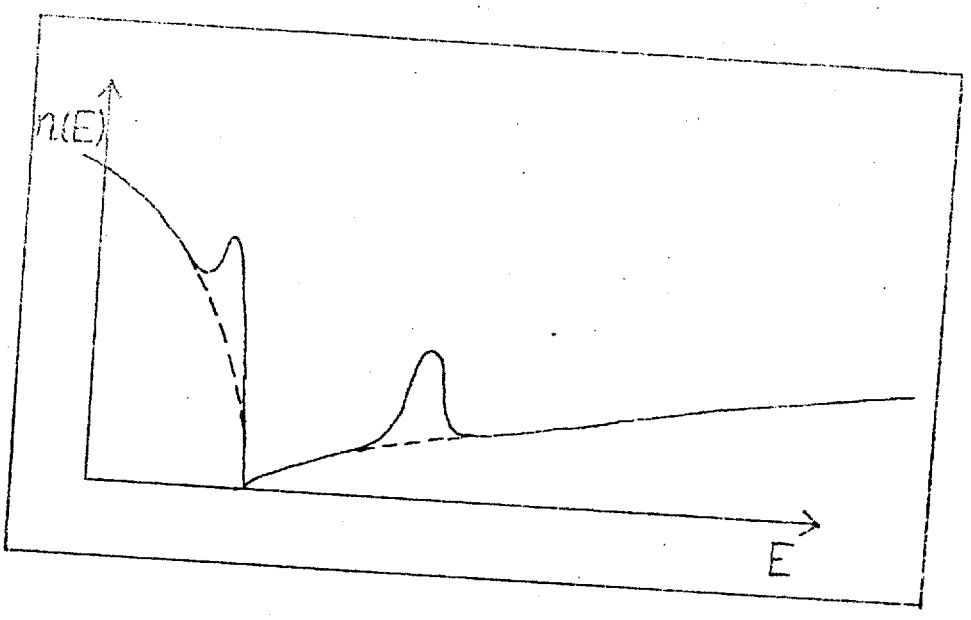

Figure 6.1 Schematic density of states n(E) in a zero-gap semiconductor doped dilutely with both p- and n-type impurities.

where ϵ is the dielectric function. For α-Sn, $r_o^{donor} \approx 5 \times 10^{-4}$ cms and, similarly, $r_o^{acceptor} \approx 5 \times 10^{-5}$ cms. Now the screening length of α-Sn is about 5×10^{-5} cms. We therefore expect screening to exert some influence, particularly on donor states. We also note that the large spatial extent of these states (over 10^9 and 10^6 atomic cells respectively) suggests that central cell corrections will not be significant.

The impurity problem in α-Sn was first tackled by Liu and Brust[55]. Their theory, whilst treating the band structure carefully, concentrated on the effects of the central cell part of the potential, ignoring the long-range screening arising from the dielectric singularity completely. Gelmont and others[41] were able to decouple the four coupled Schrödinger equations arising from the four-band model of the impurity problem using a Coulomb potential. Activation energies E_o and widths Γ of resonant states were obtained via a phase-shift analysis of these equations. In their model, $E_o^{acceptor}$ depends on both m_c and m_v,

$$\frac{\Gamma^{acceptor}}{E_o^{acceptor}} \propto \left(\frac{m_c}{m_v}\right)^{3/2}, \qquad (6.2)$$

whilst no resonant donor states are possible. The importance of screening was recognised by Gelmont and his co-workers, but could not be included in their rigorous calculations.

Recently, Bastard and others[38] have reported calculations based on a similar principle to the calculations of

this chapter, but using a model potential which, whilst being non-local, is essentially of very short range. They find both acceptor and donor states for appropriate strengths of the impurity potential.

As well as reproducing (6.2), they find

$$\frac{\Gamma^{donor}}{|E_o^{donor}|} \propto \left(\frac{m_v}{m_c}\right)^{3/2} \qquad (6.3)$$

It is our aim in this chapter to steer a middle course between the theories of Gelmont et al. and Bastard et al., employing neither the infinite ranged Coulomb potential nor a very short ranged potential, but something of intermediate range, more appropriate to a Coulomb potential screened in the characteristic manner of a zero-gap semiconductor. In this way, we intend to discuss the effects of screening in a systematic way. The four-band model is used in the parabolic approximation and the central cell correction is ignored. The Coulombic nature of the unscreened potential is sacrificed, but the separable model potential has many desirable properties. The model potential is screened in a variety of ways, and the dependence of resonant state formation on screening is discussed.

§6.2 The Model Potential

We saw in Chapter 2 (2.21), how the Dyson equation is easily solved for electrons responding to a separable potential. In this chapter, we wish to calculate a density of

states via a Green's function. In order to be able to calculate the Green's function simply from a Dyson equation, we employ a model impurity potential which is separable, that is with a momentum-space representation of the form

$$V_{\underline{k}\underline{k}'} = W_{\underline{k}} W_{\underline{k}'} . \tag{6.4}$$

Bastard et al.[38] have used

$$W_{\underline{k}} = V^{1/2} u_{\underline{k}} \tag{6.5}$$

where V is a constant and $u_{\underline{k}}$ is an isotropic function, equal to one for small k, and vanishing for some large value of k. We shall use the more sophisticated choice

$$W_{\underline{k}} = [U(\underline{k})]^{1/2} \tag{6.6}$$

where $U(\underline{k})$ is the momentum representation of the potential to be modelled.

The choice (6.6) in (6.4) can in no way be regarded as an approximation to the potential U. However, if we take the concrete example of U being a Coulomb potential, then (6.6) gives a potential which has singularities and an infinite range in real space, just as U does. Furthermore, there are many situations where our choice yields results which differ from those of using U only by a numerical factor of order unity. For example, the exchange energy per unit volume E_{ex} of completely uncorrelated electrons interacting via the Coulomb potential U is

$$E_{ex} = -\frac{1}{\Omega}\sum_{\underline{k}}\sum_{\underline{k}'\neq\underline{k}} \mathcal{U}(\underline{k}-\underline{k}') = -\frac{e^2 k_F^4}{4\pi^3} \qquad (6.7)$$

If E_{ex} is calculated using the model potential defined in (6.6), we obtain

$$E_{ex} = -\frac{1}{\Omega}\sum_{\underline{k}}\sum_{\underline{k}'\neq\underline{k}} W_{\underline{k}} W_{\underline{k}'} = \frac{e^2 k_F^4}{16\pi^3} \qquad (6.8)$$

Thus, the model potential yields one quarter of the energy obtained via the true potential and gives the correct dependence on physical parameters. In §6.3, we shall see that (6.6) yields a ground state energy of the Hydrogen atom which is four times the true energy.

We shall make the choice (6.6) for all potentials U, but one must bear in mind that energies computed via (6.6) will only be approximately correct.

§6.3 The Density of States

We begin by writing down the momentum-space Dyson equation for the one-electron Green's function $G(\underline{k},\underline{k}'; E)$ in a crystal containing single impurity represented by a one-electron potential $U_{\underline{k}\underline{k}'}$.

$$G(\underline{k},\underline{k}';E) = G_0(\underline{k},E)\,\delta_{\underline{k}\underline{k}'} + \sum_{\underline{k}_1} G_0(\underline{k},E)\,\mathcal{U}_{\underline{k}\underline{k}_1}\,G(\underline{k}_1,\underline{k}';E) \qquad (6.9)$$

Here,

$$G_0(\underline{k},E) = \left[E - H_0(\underline{k})\right]^{-1} \qquad (6.9)$$

where $H_o(k)$ is the effective mass Hamiltonian of the crystal and

$$\delta_{\underline{k},\underline{k}'} = \begin{cases} 1 & \underline{k} = \underline{k}' \\ 0 & \text{otherwise} \end{cases} \qquad (6.10)$$

If H_o refers to an n-band system, then all the functions in (6.9) are n x n matrix functions: δ is, of course, diagonal, and $U_{\underline{k}\underline{k}'}$ is a diagonal n x n matrix by virute of the effective mass representation used in H_o.

We now replace $U_{\underline{k}\underline{k}'}$ with the model separable potential of (6.4) and (6.6). (6.9) may then be re-arranged to give

$$G(\underline{k},\underline{k}';E) = G_o(\underline{k},E)\delta_{\underline{k}\underline{k}'} + G_o(\underline{k},E)W_{\underline{k}}\left[1 - \sum_{\underline{k}''} W_{\underline{k}''}G_o(\underline{k}'',E)W_{\underline{k}''}\right] W_{\underline{k}'}G_o(\underline{k}',E)$$

$$= G_o(\underline{k},E)\delta_{\underline{k}\underline{k}'} + G_{imp}(\underline{k},\underline{k}';E) \qquad (6.11)$$

The density of states of the system is easily written

$$n(E) = \lim_{\delta\to 0} \frac{1}{\pi} \mathrm{tr} \sum_{\underline{k}} \mathrm{Im}\, G(\underline{k},\underline{k};E-i\delta)$$

$$= n_o(E) + n_{imp}(E) \qquad (6.12)$$

Here n_o and n_{imp} correspond to the parts G_o and G_{imp} of G, and the trace is taken over the n x n matrix for G.

The hydrogen atom

As a test of our model potential, we now apply (6.12) to a free-electron system in the presence of a Coulomb poten-

tial to obtain an estimate of the ground state energy of the hydrogen atom. We have

$$H_o(k) = \frac{\hbar^2 k^2}{2m}$$

$$W_{\underline{k}} = \left(-\frac{4\pi e^2}{\Omega k^2} \right)^{1/2} \qquad (6.13)$$

Now we expect $n_{imp}(E)$ to peak at the binding energy E_o of the system, and (6.12) tells us that such a peak will occur where (6.11) indicates that $G_{imp}(E)$ has a pole in the complex E plane. Thus E_o is given by the solution to

$$1 - \sum_{\underline{k}} W_{\underline{k}}^2 \frac{1}{E_o - \frac{\hbar^2 k^2}{2m}} = 0 \qquad (6.14)$$

The sum in (6.14) is replaced by a principal part integral and

$$E_o = -\frac{2me^4}{\hbar^2} \qquad (6.15)$$

is obtained. This is exactly four times the ground state energy of the hydrogen atom as we anticipated in §6.2.

Zero-gap semiconductor

We now apply (6.11) to the case where H_o is the effective mass Hamiltonian of a zero-gap semiconductor in the parabolic approximation, $W_{\underline{k}}$ being as yet unspecified. We begin by inverting the matrix $E - H_o(\underline{k})$ to give

$$G_o(\underline{k},E) = \frac{1}{[E-(A+B)k^2][E-(A-B)k^2]} \begin{bmatrix} E-\frac{1}{6}P-\frac{2}{3}Q & 0 & R & S \\ 0 & E-\frac{1}{6}P-\frac{2}{3}Q & -S^* & R^* \\ R^* & -S & E-\frac{1}{2}P & 0 \\ S^* & R & 0 & E-\frac{1}{2}P \end{bmatrix} \qquad (6.16)$$

Next, we examine the elements of the matrix

$$\sum_{\underline{k}} W_{\underline{k}} \, G_0(\underline{k}, E) \, W_{\underline{k}} \quad , \tag{6.17}$$

and consider, for example,

$$\sum_{\underline{k}} W_{\underline{k}} \frac{E - \frac{1}{2}P}{\left[E-(A+B)k^2\right]\left[E-(A-B)k^2\right]} W_{\underline{k}} \, . \tag{6.18}$$

We replace the sum in (6.18) by an integral and utilise the fact that $W_{\underline{k}}$ is a function of k only. The angular part of the integral is readily performed and we prove that (6.18) is equal to

$$\sum_{\underline{k}} W_{\underline{k}}^2 \frac{E - Ak^2}{\left[E-(A+B)k^2\right]\left[E-(A-B)k^2\right]} = \frac{1}{2}\sum_{\underline{k}} W_{\underline{k}}^2 \left[\frac{1}{E-(A+B)k^2} + \frac{1}{E-(A-B)k^2}\right]. \tag{6.19}$$

The other elements of (6.17) can also be simplified in this way: the diagonal terms are all equal and the remaining elements vanish.

We also have

$$Tr \, G_0(\underline{k}, E) G_0(\underline{k}, E) = \frac{4\left\{(E-Ak^2)^2 + B^2k^4\right\}}{\left\{\left[E-(A+B)k^2\right]\left[E-(A-B)k^2\right]\right\}^2}. \tag{6.20}$$

Thus, (6.19) and (6.20) permit the following explicit expression for n_o and n_{imp} to be written:

$$n_0(E) = \lim_{\delta \to 0} \frac{4}{\pi} Im \sum_{\underline{k}} \frac{E - Ak^2 - i\delta}{\left[E-(A+B)k^2 - i\delta\right]\left[E-(A-B)k^2 - i\delta\right]} \tag{6.21}$$

$$n_{imp}(E) = \lim_{\delta\to 0} \frac{2}{\pi} \mathrm{Im} \sum_{\underline{k}} \frac{(E - Ak^2 - i\delta)^2 + B^2k^4}{[E-(A+B)k^2 - i\delta]^2 [E-(A-B)k^2 - i\delta]^2}$$

$$W_{\underline{k}}^2 \left[1 - \sum_{\underline{k}''} W_{\underline{k}''} \frac{E - Ak''^2 - i\delta}{[E-(A+B)k''^2][E-(A-B)k''^2]} \right]$$

(6.22)

Density of band states

We now confirm that (6.21) generates the density of band states of a zero-gap semiconductor. We apply the identity

$$\lim_{\delta\to 0} \frac{1}{x - i\delta} = \mathcal{P}\frac{1}{x} + i\pi\delta(x)$$

to give

$$n_0(E) = \frac{4}{\pi} \mathcal{P} \sum_{\underline{k}} \frac{E - Ak^2}{E-(A+B)k^2} \pi\delta(E-(A-B)k^2)$$

$$+ \frac{4}{\pi} \mathcal{P} \sum_{\underline{k}} \frac{E - Ak^2}{E-(A-B)k^2} \pi\delta(E-(A+B)k^2).$$

(6.23)

We first consider the case E > 0. Since (A-B) < 0, A+B > 0 and k > 0, it is possible to make the replacements

$$\delta(E-(A+B)k^2) \longrightarrow \frac{1}{\sqrt{(E(A+B))}} \delta\left(k - \sqrt{\frac{E}{A+B}}\right)$$

$$\delta(E-(A-B)k^2) \longrightarrow 0 \quad . \qquad (6.24)$$

in (6.23). Therefore,

$$n_0(E) = \frac{\Omega}{2\pi^2}(A+B)^{-3/2} E^{1/2}. \qquad (6.25)$$

Similarly for $E < 0$, we have

$$n_0(E) = \frac{\Omega}{2\pi^2}(B-A)^{-3/2}(-E)^{1/2}. \qquad (6.26)$$

(6.25) and (6.26) are just the charge densities we expect for doubly degenerate bands with effective masses m_c and m_v.

Density of impurity states

The density of impurity states $n_{imp}(E)$ cannot be directly evaluated from (6.22) since the second order poles in the complex E plane which appear in the summand, lead to an apparently divergent result. However, if we write

$$1 - \sum_{\underline{k}} W_{\underline{k}}^2 \frac{E - Ak^2 - i\delta}{[E-(A+B)k^2 - i\delta][E-(A-B)k^2 - i\delta]} = 1 - X(E,\delta) - iY(E,\delta) \qquad (6.27)$$

where $X(E,\delta)$ and $Y(E,\delta)$ are both real, we can confirm by simple differentiation that

$$n_{imp}(E) = \frac{2}{\pi} Im \frac{d}{dE} \ln[1 - X(E) - iY(E)] \qquad (6.28)$$

where $X(E)$ and $Y(E)$ are the limits as $\delta \to 0$ of $X(E,\delta)$ and $Y(E,\delta)$. For any complex number Z

$$Im \ln Z = \arg Z + n\pi \qquad (6.29)$$

where n is an integer. (6.28) therefore becomes

$$n_{imp}(E) = \frac{2}{\pi} \frac{d}{dE} \tan^{-1} \frac{1-X(E)}{Y(E)}$$

$$= \frac{2}{\pi} \frac{(1-X)Y' - YX'}{(1-X)^2 + Y^2} \qquad (6.30)$$

where primes denote differentiation with respect to E.

By comparison with the free-electron result (6.14), we expect $n_{imp}(E)$ to peak strongly around $E = E_o$ where

$$X(E_o) = 1 \qquad (6.31)$$

We therefore expand X(E) about $E = E_o$

$$X(E) = 1 + (E-E_o)X'|_{E_o} + O([E-E_o]^2) \qquad (6.32)$$

and define

$$\Gamma(E) = \frac{-Y}{X'} \qquad (6.33)$$

Then, provided $E - E_o$ is sufficiently small to use only the first two terms on the right hand side of (6.32), to put X(E) = 1 in the numerator of (6.30) and that Γ is approximately constant over this restricted range of E, we get

$$n_{imp}(E) = \frac{2}{\pi} \frac{\Gamma(E_o)}{(E-E_o)^2 + \Gamma(E_o)^2} \qquad (6.34)$$

Thus, $n_{imp}(E)$ is, subject to these restrictions, a Lorentzian peak of width $\Gamma(E_o)$. The fulfillment of these restrictions, together with the condition

$$\Gamma(E_o) \ll E_o \tag{6.35}$$

will be taken in what follows as evidence for the existence of a well defined, quasi-localized resonant impurity state. $|E_o|$ will then be interpreted as the activation energy of that state, and $\Gamma(E_o)$ its resonant width.

We note that

$$\int_{-\infty}^{\infty} n_{imp}(E)\, dE = 2 \tag{6.36}$$

so that $n_{imp}(E)$ represents a doubly-degenerate impurity state.

§6.4 Impurity Levels: Activation Energies and Widths

6.4.1 Coulomb Potential

We now examine the density of impurity states corresponding to the model impurity potential (6.6) arising from different types of screened potential. We begin with the case where the static dielectric function is independent of wavevector. The potential is then

$$W_{\underline{k}}^2 = \begin{cases} \dfrac{4\pi e^2}{\Omega \varepsilon_o k^2} & \text{for a singly-charged acceptor} \\ -\dfrac{4\pi e^2}{\Omega \varepsilon_o k^2} & \text{for a singly-charged donor} \end{cases} \tag{6.37}$$

where ε_o is the dielectric constant.

For a singly-charged acceptor impurity, we begin by calculating X(E) in the range E > 0. Replacing the sum in the definition of X by an integral gives

$$X(E) = \frac{e^2}{\pi\varepsilon_0}\,\mathcal{P}\int_0^\infty dk\left[\frac{1}{(B-A)k^2+E} - \frac{1}{(A+B)k^2-E}\right]$$

$$= \frac{e^2}{2\varepsilon_0}\,\frac{1}{\sqrt{E(B-A)}} \qquad (6.38)$$

For E < 0

$$X(E) = \frac{e^2}{2\varepsilon_0}\,\frac{-1}{\sqrt{-E(A+B)}} \qquad (6.39)$$

For a donor impurity, the sign of X(E) is reversed, and the solutions to (6.31) are obtained:

$$E_0 = \frac{e^4}{4\varepsilon_0^2}\,\frac{1}{B-A} \qquad \text{(acceptor)} \qquad (6.40a)$$

$$E_0 = -\frac{e^4}{4\varepsilon_0^2}\,\frac{1}{B+A} \qquad \text{(donor)} \qquad (6.40b)$$

These are exactly the ground state energies of hydrogen-like systems whose effective masses are those of the hole and electron in our zero-gap material. We note, however, that as a result of using the separable model (6.6), the acceptor binding energy is independent of m_c whilst the donor binding energy in independent of m_v. In the light of reference[41], this is an unrealistic feature of the model, but when screened

potentials are modelled, both binding energies do depend on both m_v and m_c.

To calculate $\Gamma(E_o)$ from (6.33), we first note that, from (6.38)

$$X'(E)\Big|_{E_o} = -\frac{1}{2}E_o^{-1} \qquad \text{(donor or acceptor)} \tag{6.41}$$

To calculate Y(E), the same technique as was used to derive (6.25) is employed.

$$Y(E_o) = \begin{cases} \frac{2}{\pi}\ \frac{e^2}{4\varepsilon_o}\left[E_o(A+B)\right]^{-1} & \text{(acceptor)} \\ -\frac{2}{\pi}\ \frac{e^2}{4\varepsilon_o}\left[E_o(A-B)\right] & \text{(donor)} \end{cases} \tag{6.42}$$

Then (6.33) gives

$$\frac{\Gamma(E_o)}{|E_o|} = \begin{cases} \frac{2}{\pi}\left(\frac{B-A}{B+A}\right)^{1/2} & \text{(acceptor)} \\ \frac{2}{\pi}\left(\frac{B+A}{B-A}\right)^{1/2} & \text{(donor)} \end{cases} \tag{6.43}$$

Since all zero-gap semiconductors have B+A >> B-A, (6.34) is not a good approximation to the density of impurity states associated with a donor impurity over any meaningful range of energies. We do not expect well defined resonant donor

states in any zero-gap semiconductor, no matter how strong the impurity potential. Resonant acceptor states, on the other hand, are well defined. Thus our conclusion parallels that of Gelmont et al.[41], even though the energies (6.40) differ from theirs, and the power law in (6.43) differs from theirs in (6.2).

Numerical estimates are bound to be rough in the present model. For reference, we obtain $E_o^{acceptor} \sim 6meV$ and $\Gamma/E_o^{acceptor} \sim 0.2$.

6.4.2 Zero-Gap Screening

We now examine the effect on these model calculations of the introduction of the dielectric function (5.17) applicable at small $|\underline{k}|$ to a pure zero-gap semiconductor at T = 0. For an acceptor impurity, (6.38) becomes

$$\chi(E) = \frac{2e^2}{\pi\varepsilon_0}\mathcal{P}\int_0^\infty dk\ \frac{\frac{1}{2}k^2}{k+\lambda}\left\{\frac{1}{(B-A)k^2+E} - \frac{1}{(B+A)k^2-E}\right\} \qquad (6.44)$$

$$= \frac{e^2}{\pi\varepsilon_0}\left\{\frac{\lambda}{(A+B)\lambda^2-E}\ln\left|\frac{E}{(A+B)\lambda^2}\right|\right.$$

$$\left. + \frac{\lambda}{(B-A)\lambda^2+E}\left[\ln\left|\frac{(B-A)\lambda^2}{E}\right| + \frac{\pi}{2}\left|\frac{E}{(B-A)\lambda^2}\right|\right]\right\}$$

(6.31) cannot now be solved analytically, except for very small λ: what we choose to do is make a numerical solution, valid for all λ, but restricted to the typical situation

$$\frac{B+A}{B-A} = 10 \qquad (6.45)$$

We can then rewrite (6.31) as

$$\frac{t}{x} = [f(x)]^2, \quad f(x) > 0. \tag{6.46}$$

Here $t = (B-A)\lambda^2/\bar{E}_o$,

$x = (B-A)\lambda^2/E_o$,

$$f(x) = \frac{1}{1+x} + \frac{1}{\pi}\frac{\sqrt{x}\ln x}{1+x} \cdot \frac{1}{\pi}\frac{\sqrt{x}}{10x-1}\ln 10x$$

and $\bar{E}_o$ is the $\lambda \to 0$ limit of E_o.

We note the limit

$$\lim_{x\to\infty} f(x) = \frac{1}{\pi}\frac{\ln x}{x}. \tag{6.47}$$

(6.46) is solved graphically in Fig. 6.2. Since $f(x)^2$ approaches zero for large x more slowly than $1/x$, solutions exist for all r and hence for all λ. However, as r becomes large, the ratio $E_o/\bar{E}_o$ becomes very small. This effect is illustrated in Table 6.1.

Table 6.1

Reduction of E_o due to screening. E_o, $\bar{E}_o$ and r are defined in the text.

r	$E_o/\bar{E}_o$
10^{-2}	0.55
2.10^{-2}	0.44
5.10^{-2}	0.34
10^{-1}	0.26
2.10^{-1}	0.18
5.10^{-1}	0.069
1	0.040
2	0.025

For α-Sn, taking the approximate values $E_o \sim 6$ meV and $\lambda \sim 5 \times 10^5$ cm^{-1}, we obtain $E_o/\bar{E}_o \sim 0.25$: the reduction in binding energy is substantial.

We now examine the effect of screening on $\Gamma(E_o)$. We see from Fig. 6.2 that, close to $E = E_o$, $f(x)$ is slowly varying function of x. This permits us to write, for α-Sn, close to $E = E_o$,

$$X(E) \approx 0.45\, \bar{X}(E) \tag{6.48}$$

where $\bar{X}$ is the $\lambda \to 0$ limit of X. It follows that $X'(E_o)$ is 1.6 times its value in the abs ence of screening. $Y(E_o)$ is evaluated in the usual manner and is ~0.67 times its value in the absence of screening. Finally, the width of the state is reduced by ~0.42, giving

$$\frac{\Gamma}{E_o} \approx 0.3 \tag{6.49}$$

We conclude that well-defined acceptor states are still possible in the presence of screening, but that the binding energies are reduced, and the relative widths of the states are increased somewhat.

We now turn our attention to donor states. The same analysis as for acceptor states is possible, and the activation energies are obtained by solving, subject to (6.45),

$$\frac{s}{y} = [g(y)]^2, \quad g(y) > 0 \tag{6.50}$$

where

$$s = \frac{(A+B)\lambda^2}{|\bar{E}_o|}, \quad y = \frac{(A+B)\lambda^2}{|E_o|},$$

$$g(y) = \frac{1}{1+y} + \frac{1}{\pi}\frac{\sqrt{y}}{1+y}\ln y - \frac{1}{\pi}\frac{\sqrt{y}}{\frac{1}{10}y-1}\ln\frac{y}{10}$$

This is carried out in Fig. 6.3. Now, however, g(y) becomes negative for $y \gtrsim 0.2$, and no solutions are possible for $s \gtrsim 0.23$. Using the parameters of α-Sn which were employed earlier, we obtain $s \sim 10$. Consequently, even taking account of the considerable quantitative defficiencies of the model potential, it seems certain that the screening in pure α-Sn is sufficient to prevent the formation of even weak donor resonances.

6.4.3 Metallic Screening

In a crystal of α-Sn, dilutely-doped with p-type impurities, we have seen that quasi-localised acceptor states are expected. However, we have neglected effects arising from more than one impurity. The treatment of the effects high impurity concentrations is beyond the scope of the present technique, but one important many-impurity effect can be mentioned. This arises from the metallic-like screening which arises because the Fermi level is shifted from the Γ_8^+ degeneracy.

We therefore study the effects of using the model potential

$$W_{\underline{k}}^2 = \frac{4\pi e^2}{\Omega k^2 \varepsilon_0} \frac{1}{1+\frac{K^2}{k^2}} \qquad (6.51)$$

To examine the acceptor activation energy E_0, we solve the analogue of (6.44)

$$1 = \frac{e^2}{\bar{E}_0}\left\{\frac{\sqrt{\frac{E_0}{B-A}} - K}{E_0 - (B-A)K^2} - \frac{K}{E_0 + (B+A)K^2}\right\}. \quad (6.52)$$

In the approximation (6.45), (6.52) reduces to

$$\frac{t}{z} = [h(z)]^2, \quad h(z) > 0 \quad (6.53)$$

where

$$t = \frac{(B-A)K^2}{\bar{E}_0},$$

$$z = \frac{(B-A)K^2}{E_0},$$

$$h(z) = \left\{1 - \frac{\sqrt{z} - z}{1-z} - \frac{\sqrt{z}}{1+10z}\right\}.$$

As a consequence of the limit

$$\lim_{z\to\infty}[h(z)]^2 = \frac{0.81}{z}, \quad (6.54)$$

no solutions to (6.53) exist for large t. From Fig. 6.4 we obtain the limiting value $t_{crit} \approx 0.48$, and we conclude that no quasi-bound acceptor states may be formed if the screening parameter K is greater than about 10^6 cm^{-1}. The dependence of $E_0/\bar{E}_0$ upon t is given in Table 6.2.

Table 6.2

Reduction of binding energies due to metallic screening. E_o, $\bar{E}_o$ and t are defined in the text.

t	$E_o/\bar{E}_o$
5.10^{-3}	0.70
10^{-2}	0.56
2.10^{-2}	0.45
5.10^{-2}	0.35
10^{-1}	0.25
2.10^{-1}	0.14
$4.8.10^{-1}$	0.00

Now in the Fermi-Thomas approximation, K is related to the number density n_o of charge carriers and the Fermi energy E_F by

$$K^2 = \frac{6\pi n_o e^2}{E_f} \qquad (6.55)$$

Consequently the critical concentration is reached at a concentration of about 10^{13} holes cm^{-3} or 10^{16} electrons cm^{-3} in α-Sn. However, since

$$n_o \propto K^6 \qquad (6.56)$$

we cannot place too much reliance on these critical concentrations.

At low temperatures, we know that holes are quasi-localised in acceptor states, so that the total hole concen-

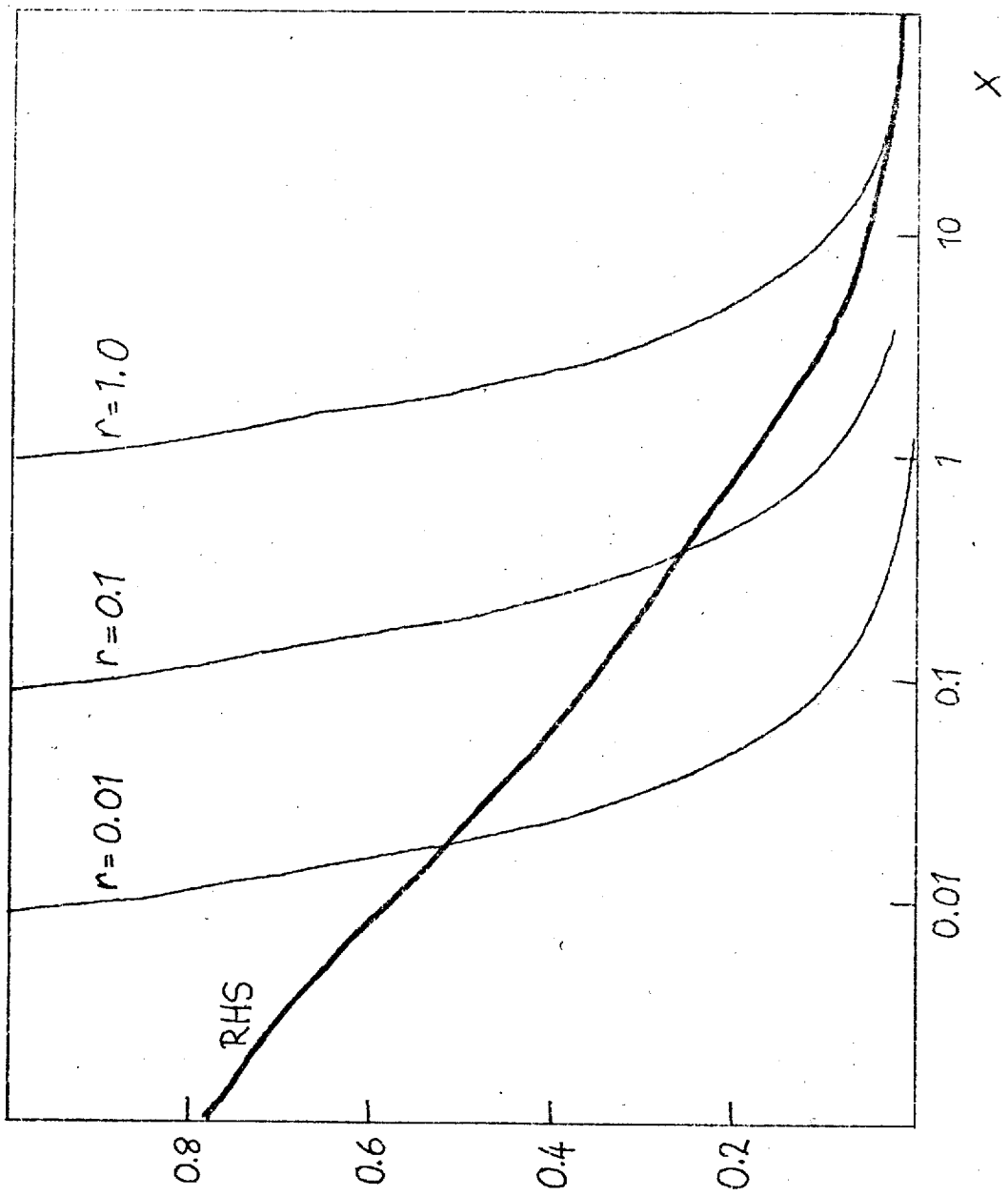

Figure 6.2 Graphical Solution of Equation (6.46). The LHS and RHS are plotted against x, the former for several values of r. For each r, the solution is that value of x at which LHS and RHS intersect.

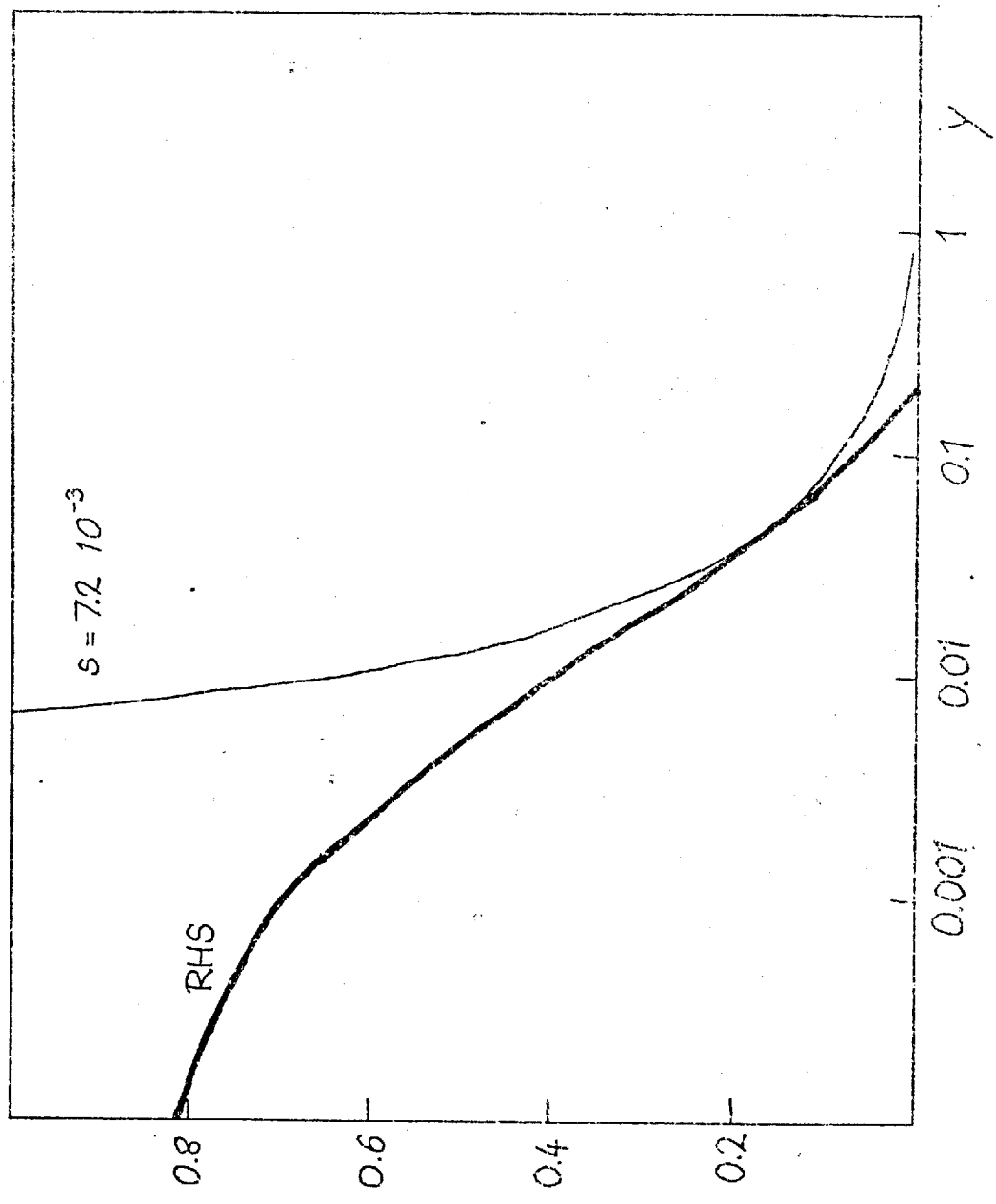

Figure 6.3 Graphical Solution of Equation (6.50). The LHS and RHS are plotted against y, the former for the maximum value of s for which a solution exists. That solution is the value of y at which LHS and RHS touch.

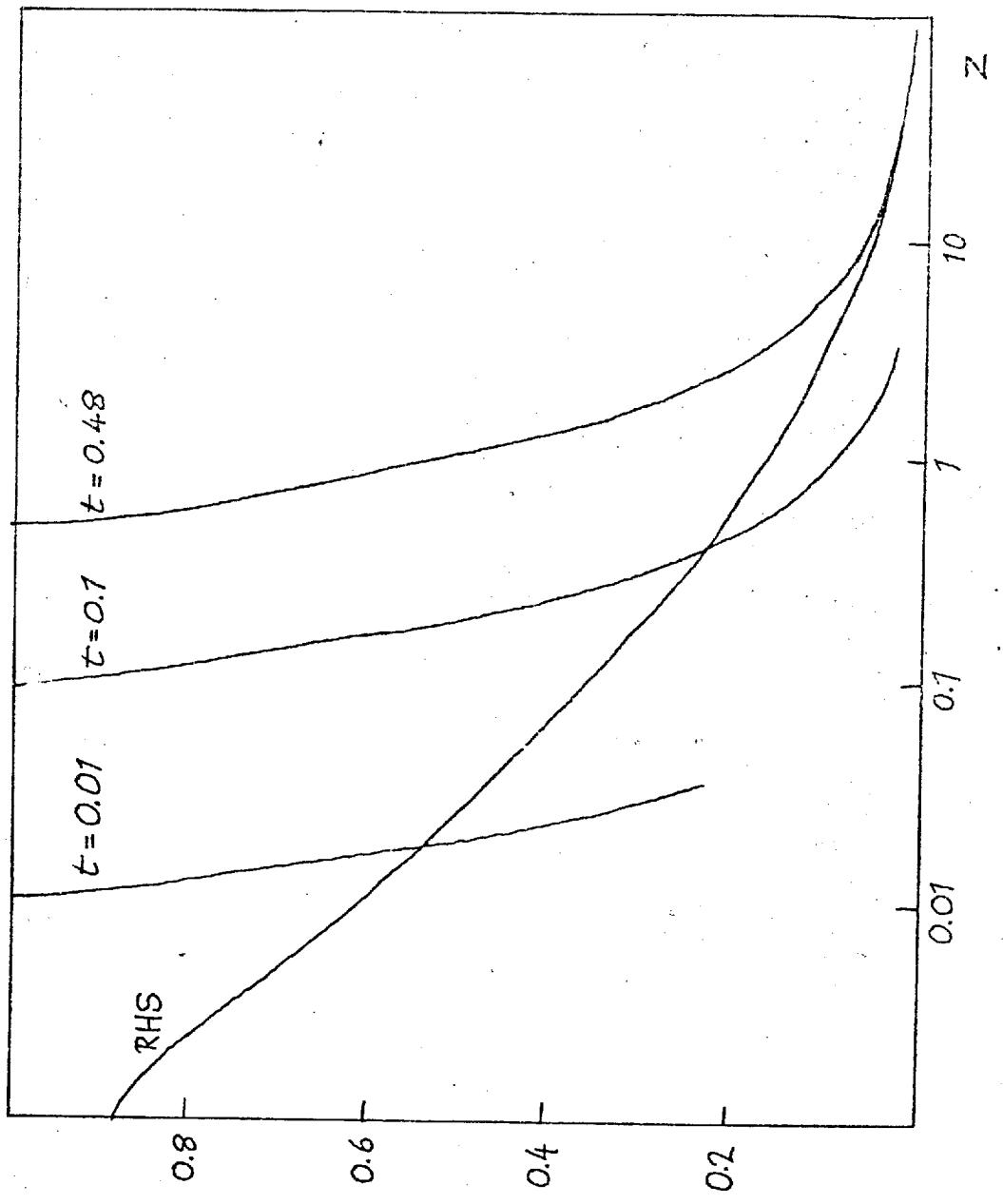

Figure 6.4 Graphical Solution of Equation (6.53). The LHS and RHS are plotted against z, the former for several values of t. For each t, the solution is that value of z at which LHS and RHS intersect.

tration should not be used in (6.55). We may nevertheless be sure that at sufficiently high concentrations of acceptors, the concentration of holes of a free character will be sufficiently high to prevent (self-consistently) quasi-localization of acceptor states.

n-type impurities are not expected to have bound impurity states at low temperatures. Consequently, impurity electrons are freely available for screening. This suggests that acceptor localization is less likely in compensated samples than in samples containing p-type impurities only.

§6.5 Conclusions

We begin by discussing the effects of temperature on the calculations of this chapter. We have seen the dielectric singularity used in §6.4.2 is removed at finite temperatures, but that departures from singular behaviour are important only for

$$k_B T \gtrsim \frac{\hbar^2 q^2}{2}\left(\frac{1}{m_c} + \frac{1}{m_v}\right)$$

Consequently, at temperatures ($k_B T \lesssim E_o$) where the effects of bound states are most easily detected, the finite temperature modification becomes appreciable only for

$$\frac{\hbar^2 q^2}{2}\left(\frac{1}{m_c} + \frac{1}{m_v}\right) \lesssim E_o \qquad (6.57)$$

The small range of q over which this applies has only a small effect on the integrals X(E) and Y(E) and our conclusions are

not significantly modified.

By far the most important effect of finite temperatures is the introduction of a singularity in the intraband part of the dielectric function, and the consequent metallic screening as in §6.4.3. A temperature of $1^{o}K$ is sufficient to introduce the same degree of screening as about 10^{16} conduction band electrons per cm^{3}. We may therefore expect a dependence on temperature of the acceptor activation energy. Such dependence has not been observed, presumably because of the low temperatures at which acceptor activation energies have been measured.

Finally we summarise the results contained in this chapter. The presence or absence of quasi-localized impurity states in a zero-gap semiconductor is found to be critically dependent on the type of screening in the system and the masses of the touching $\Gamma_8^+(\Gamma_8)$ bands. Acceptor states are expected in dilutely doped samples at low temperatures, whilst donor states will be absent. The metallic screening at finite temperatures and at higher doping levels (especially in compensated samples) may inhibit the presence of even quasi-localized acceptor states.

APPENDIX - UNITS

In accordance with standard usage, two types of units are used in this thesis.

In Chapters 1 - 4, atomic units are used with energy measured in rydbergs, and length measured in terms of a_B, the Bohr radius. This system is produced by putting the fundamental physical constants

$$m_e = 4\pi\varepsilon_o = \tfrac{1}{2}$$

$$\hbar = c = e = 1$$

Chapters 5 and 6 employ the c.g.s. system.

REFERENCES

1. See, for example, D. Pines, 'The Many Body Problem', Benjamin (New York), 1961.

2. For a recent review, see F. Bassani, G. Iadonisi and B. Preziosi, Rep. Prog. in Phys., 37, 1099, 1974.

3. C.H. Hodges and M.J. Stott, Phil. Mag. 26, 375, 1972.

4. Recent information on these systems appears in Proceedings of the International Conference on Semimetals and Narrow Gap Semiconductors, Nice, 1973.

5. D. Bohm and D. Pines, Phys. Rev. 92, 626, 1953.

6. See, for example, A.A. Abrikosov, L.P. Gorkov, I. Ye. Dzyloshinsky, 'Quantum Field Theoretical Methods in Statistical Physics', Pergamon (London) 1955.

7. D. Bohm and D. Pines, Il Nuovo Cimento (X) 9, 470, 1958.

8. J. Lindhard, Kgl. Danske Mat. Fys. Medd. 28, 8, 1954.

9. R.D. Mattuck and A. Theumann, Advances in Physics 20, 721, 1971.

10. H. Ehrenreich and M. Cohen, Phys. Rev. 115, 786, 1959.

11. J. Hubbard, Proc. Roy. Soc. A243, 336, 1957.

12. T.P. Fishlock and J. Pendry, J. Phys. C6, 1909, 1973.

13. K.S. Singwi, M.P. Tosi, R.H. Land and A. Sjölander, Phys. Rev. 176, 589, 1968.
K.S. Singwi, A. Sjölander, M.P. Tosi and R.H. Land, Phys. Rev. B1, 1044, 1970.

14. A. Sjölander and M.J. Stott, Phys. Rev. B5, 2109, 1972.
Z.D. Popovich and M.J. Stott, Phys. Rev. Letters 33, 1164, 1974.

15. W.A. Harrison, 'Pseudopotentials in the Theory of Metals', Benjamin (New York) 1966.

V. Heine, Solid State Physics 23, 1, 1970.

16. V. Heine and I.V. Abarenkov, Phil. Mag. 9, 451, 1965.

17. J.M. Ziman, Advances in Physics 13, 89, 1964;

Proc. Phys. Soc. 91, 701, 1967.

18. L. Dagens, J. Phys. C5, 2333, 1972.

19. For example,

A. Meyer, G.M. Stocks and W.H. Young, J. Phys. F3, 1381, 1973.

20. J.C. Stoddart, A.M. Beattie and N.H. March, Int. J. of Quantum Chemistry 4, 35, 1971.

21. W. Kohn and L.J. Sham, Phys. Rev. 140, A1133, 1965.

22. N.H. March and N.G. Murray, Proc. Roy. Soc. A266, 559, 1962.

23. L.C.R. Alfred, Phys. Letters A46, 65, 1973.

24. L.C.R. Alfred and N.H. March, Phil. Mag. 46, 759, 1955.

N.G. Murray and N.H. March, Proc. Roy. Soc. A256, 400, 1960.

25. J. Weinberg, Phys. Rev. 130, 776, 1963;

Phys. Rev. 131, 440, 1963.

26. J. Pendry, J. Phys. C3, 1711, 1970.

27. A.O.E. Animalu, Phil. Mag. 11, 379, 1965.

28. T. Loucks, 'The Augmented Plane Wave Method', Benjamin (New York) 1965.

29. A. Abramowitz and M. Stegun, 'Handbook of Mathematical Functions', p. 232, Dover (New York) 1964.

30. For general information on this technique, see 'Soft-X-Ray Band Spectra' (ed. Fabian), Acad. Press (London) 1968).

31. A. Appleton and C. Curry, Phil. Mag. 12, 245, 1965.

32. C. Curry, p. 173 of reference 30.

33. R.L. Jacobs, J. Phys. F3, L166, 1973.

34. S.H. Groves and W. Paul, Phys. Rev. Letters 11, 194, 1963.

35. C.R. Whitsett, Phys. Rev. 138. A829, 1965.

J.G. Broerman, Phys. Rev. 183, 754, 1969.

S.H. Groves, R.N. Brown and C.R. Pigeon, Phys. Rev. 161, 779, 1967.

R. Zallen and M.L. Slade, Solid State Comm. 8, 1291, 1970.

R.J. Wagner, E.D. Palik and E.M. Swiggard, J. Phys. Chem. Solids 32, Suppl. 1, 471, 1971.

36. N.F. Mott, Phil. Mag. 6, 287, 1961.

37. D. Sherrington and W. Kohn, Rev. Mod. Phys. 40, 767, 1968.

38. G. Bastard, Y. Guldner, A. Mycielski, P. Nozières and C. Rigaux, Int. Conf. on the Physics of Semiconductors, Stuttgart, 1974.

39. J.M. Luttinger and W. Kohn, Phys. Rev. 97, 869, 1955.

See also

G. Dresselhaus, A.F. Kip and C. Kittel, Phys. Rev. 98, 368, 1955.

E.O. Kane, J. Phys. Chem. Solids 1, 82, 1956.

40. J.M. Luttinger, Phys. Rev. 102, 1030, 1956.

41. B.L. Gel'mont and M.I.D. D'Yakonov,

Sov. Phys. - Semiconductors 5, 1905, 1972;

Sov. Phys. - JETP 35, 377, 1972.

42. L. Liu and D. Brust, Phys. Rev. 173, 777, 1968.

43. E.D. Hinkley and A.W. Ewald, Phys. Rev. 134, A1261, 1964.
R.J. Wagner and A.W. Ewald, Bull. Am. Phys. Soc. 11, 629, 1966.

44. L.M. Blick in reference 4.

45. J.C. Broerman, Int. Conf. on the Physics of Semiconductors, Warsaw, 1972.

46. J. Kübler, J. Phys. Chem. Solids 32, Suppl. 1, 209, 1971; Phys. Rev. 183, 702, 1969.
L.J. Sham and T.V. Ramakrishnan, J. Phys. Chem. Solids 32, Suppl. 1, 219, 1971.

47. H. Ehrenreich and M.H. Cohen, Phys. Rev. 115, 786, 1959.
P. Nozières and D. Pines, Phys. Rev. 109, 762, 1958.

48. J.G. Broerman, Phys. Rev. B1, 4568, 1970.

49. J.G. Broerman, Phys. Rev. Letters 25, 1658, 1970.

50. L. Liu in reference 4.

51. D. Sherrington and W. Kohn, Phys. Rev. Letters 21, 153, 1968.

52. M. Grynberg and R. Letoullec, Int. Conf. on the Physics of Semiconductors, Warsaw, 1972.

53. E.D. Hinkley and E.W. Ewald, Phys. Rev. 134, A1260, 1964.

54. I. Izyumov, Advances in Physics 14, 569, 1965.

55. L. Liu and D. Brust, Phys. Rev. 157, 627, 1967.